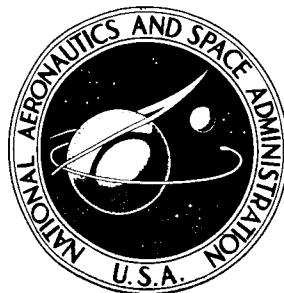


**NASA CONTRACTOR  
REPORT**



18 X  
**NASA CR-2408**

**NASA CR-2408**

**VEHICLE DESIGN CONSIDERATIONS  
FOR ACTIVE CONTROL APPLICATION  
TO SUBSONIC TRANSPORT AIRCRAFT**

*by L. Gregor Hofmann and Warren F. Clement*

*Prepared by*

**SYSTEMS TECHNOLOGY, INC.**

Hawthorne, Calif. 90250

*under subcontract with*

**MCDONNELL DOUGLAS AERONAUTICS COMPANY WEST**

Huntington Beach, Calif. 92647

*for Langley Research Center*

**TECHNICAL LIBRARY**

NAVAL TRAINING EQUIPMENT CENTER  
ORLANDO, FLORIDA 32813



**NATIONAL AERONAUTICS AND SPACE ADMINISTRATION • WASHINGTON, D. C. • AUGUST 1974**

1. Report No. NASA CR-2408		2. Government Accession No.		3. Recipient's Catalog No.	
4. Title and Subtitle VEHICLE DESIGN CONSIDERATIONS FOR ACTIVE CONTROL APPLICATION TO SUBSONIC TRANSPORT AIRCRAFT				5. Report Date August 1974	
				6. Performing Organization Code	
7. Author(s) L. Gregor Hofmann and Warren F. Clement				8. Performing Organization Report No. T.R. No. 2037-1	
				10. Work Unit No. 502-22-10-02	
9. Performing Organization Name and Address Systems Technology, Inc. Hawthorne, California 90250				11. Contract or Grant No. NAS1-12436	
				13. Type of Report and Period Covered Contractor Report	
12. Sponsoring Agency Name and Address National Aeronautics and Space Administration Washington, D.C. 20546				14. Sponsoring Agency Code	
15. Supplementary Notes Report prepared under Subcontract No. L.S.-2975-A3 with McDonnell Douglas Astronautics Co.-West  Final Report					
16. Abstract <p>This report summarizes the consensus of a panel of aircraft industry experts convened by NASA to assess the state of the art in active control technology, and to consider how current design criteria and airworthiness regulations might restrict application of this emerging technology to subsonic CTOL transports of the 1980's. Facets of active controls technology considered are: Augmentation of relaxed inherent stability, center-of-gravity control, ride quality control, load control, flutter control, envelope limiting, and pilot interface with the control system. A summary and appraisal of: the current state of the art, design criteria, and recommended practices, as well as a projection of the risk in applying each of these facets of active control technology is given. A summary of pertinent literature and technical expansions deemed appropriate by the authors are also presented.</p>					
17. Key Words (Suggested by Author(s)) Active Control technology; subsonic CTOL transport for 1980's; design criteria and airworthiness regulations affecting active controls.			18. Distribution Statement  Unclassified - Unlimited  STAR Category: 02		
19. Security Classif. (of this report) Unclassified		20. Security Classif. (of this page) Unclassified		21. No. of Pages 149	22. Price* \$4.75

## FOREWORD

This report was prepared by Systems Technology, Inc. (STI) under Subcontract No. L.S.-2975-A3 with McDonnell Douglas Astronautics Company-West (MDAC) under their Contract NAS1-12436 with the National Aeronautics and Space Administration, Langley Research Center, Hampton, Virginia. This work was administered under the direction of Mr. R. H. Christensen at MDAC with Mr. H. P. Adam serving as Task Manager. Mr. B. M. Hall of MDAC contributed considerably with his expertise as chairman of several working meetings.

Encouragement and assistance by Messrs. D. L. Keeton and F. R. Smith of MDAC is gratefully acknowledged. Participation by members of the Federal Aviation Administration (FAA) in making comments in both the initial planning stage and final manuscript review stage of this report is also gratefully acknowledged.

## CONTENTS

Section 1	INTRODUCTION AND SUMMARY	1
	1.1 Purpose and Scope	1
	1.2 Membership of the Panel	1
	1.3 Summary of the Panel Consensus	2
	1.4 Organization of the Report	3
Section 2	SUMMARY AND APPRAISAL OF THE CURRENT STATE OF THE ART IN ACTIVE CONTROL TECHNOLOGY	5
	2.1 Augmentation of Relaxed Inherent Stability	5
	2.2 Center-of-Gravity Control	10
	2.3 Ride Quality Control	11
	2.4 Load Control	13
	2.4.1 Maneuver Loading	13
	2.4.2 Gust Loading	13
	2.4.3 Cyclical Loading	14
	2.4.4 Other Loading Conditions	15
	2.5 Flutter Control	18
	2.6 Envelope Limiting	19
	2.7 Pilot Interface with ACT Systems	22
Section 3	DESIGN CONSIDERATIONS IN APPLYING ACT TO SUBSONIC CTOL TRANSPORT AIRCRAFT	25
	3.1 Projected Risk in Applying ACT Functions	25
	3.2 Potential Regulatory Limitations Upon ACT Applications	30
	3.2.1 Flight, Performance: Turbine Engine Powered Airplanes	30
	3.2.2 Flight, Controllability and Maneuver- ability Regulation	30
	3.2.3 Flight, Trim	32
	3.2.4 Flight, Stability	32
	3.2.5 Flight, Stalls	32
	3.2.6 Structure, General	33
	3.2.7 Structure, Flight Maneuver and Gust Conditions	33
	3.2.8 Structure, Control Surface and System Loads	34
	3.2.9 Structure, Ground Loads	34
	3.2.10 Structure, Fatigue Evaluation	34
	3.2.11 Design and Construction, General	34
	3.2.12 Design and Construction, Control Systems	34
	3.2.13 Equipment, General	35

3.3	Design Criteria	35
3.3.1	Structure Plus Control System	36
3.3.2	Flight Control System	37
3.3.3	Automatic Center-of-Gravity Control System	38
3.3.4	Ride Quality	38
3.3.5	Envelope Limiting	39
3.3.6	Flutter	40
Section 4	RECOMMENDED DESIGN PRACTICES	41
4.1	ACT Impact Upon the Configuration Cycle	41
4.2	Possible Weight and Drag Reduction with Relaxed Inherent Stability	42
4.3	Horizontal Tail Sizing Criteria	42
4.3.1	Trim Drag for Horizontal Tailless Designs	43
4.3.2	Trim Drag for Designs Having a Horizontal Tail	44
4.3.3	Trim at High Lift Coefficients	45
4.3.4	Short-Period Stability	50
4.3.5	Short-Period Frequency	51
4.3.6	Short-Period Damping	52
4.3.7	Control Authority Limitations	54
4.4	Vertical Tail Sizing Criteria	56
4.4.1	Directional Dynamic Stability	58
4.4.2	Control Authority Limitations	59
4.5	Center-of-Gravity Control	59
4.6	Ride Quality Control	60
4.7	Dynamic Load Analysis	63
4.8	Flutter Control	72
4.9	Envelope Limiting	72
Section 5	CRITICAL TECHNICAL AREAS AND FUTURE RESEARCH AND DEVELOPMENT	76
5.1	Improvement of Mathematical Models	76
5.2	Detail Design of ATT Aircraft	77
5.3	Iron-Bird Simulation Program	78
5.4	Control System Criteria Panel	79
5.5	Aeroelastic Techniques for ACT	79
Appendix A	HORIZONTAL TAIL SIZING CRITERIA AND PRACTICES WITH ANGLE OF ATTACK STABILITY AUGMENTATION VIA ACTIVE CONTROL	80
Appendix B	HORIZONTAL TAIL SIZING CRITERIA AND PRACTICES WITH PITCH ATTITUDE STABILITY AUGMENTATION VIA ACTIVE CONTROL	86
Appendix C	TRIM DRAG	99
Appendix D	COMPARISON OF RIDE AND TAIL LOAD RESPONSES FOR A SIMPLIFIED CASE OF A YAW DAMPER	108
Appendix E	APPROXIMATE TRANSFER FUNCTIONS FOR FLEXIBLE AIRFRAMES	110
Appendix F	LONGITUDINAL STABILITY DERIVATIVE DEFINITIONS	125
References		127

## FIGURES

1.	Horizontal Tail Sizing Criteria	8
2.	Model 954-108 and CCV KC-X Tanker Designs	9
3.	747 Wing Design Envelope	16
4.	A Form of Positive Automatic Load Factor Limiting	21
5.	An Alternate Form of Positive Automatic Load Factor Limiting	21
6.	Maneuvering Envelope	37
7.	Horizontal Tail Sizing Criteria	46
8.	Unaugmented Static Margin vs. Horizontal Tail Volume Coefficient as a Function of Wing-Body Aerodynamic Center Location	48
9.	Unaugmented Static Margin vs. Horizontal Tail Volume Coefficient as a Function of Relative Control Authority Required to Trim	49
10.	Effective Maneuver Margin With Pitch Attitude Stability Augmentation vs. Horizontal Tail Volume Coefficient as a Function of Pitch Attitude Feedback Control Gain	53
11.	Effective Pitch Damping With Pitch Rate Damping Augmentation vs. Horizontal Tail Volumetric Moment Coefficient as a Function of Pitch Rate Feedback Control Gain	55
12.	Vertical Tail Sizing Criteria	57
13.	A Possible Mechanization for Center of Gravity Control	61
14.	Illustrative Joint Probability Density Function and Strength Envelope	69
15.	Block Diagram Showing the Addition of an Automatic Limiting Feature to Basic Automatic Control System Loop Structure	74
A-1.	Effective Maneuver Margin With Angle-of-Attack Stability Augmentation vs. Horizontal Tail Volume Coefficient as a Function of Angle-of-Attack Feedback Control Gain	82

A-2. Effective Pitch Damping With Stability Augmentation vs. Horizontal Tail Volumetric Moment Coefficient as a Function of Rate Feedback Gain	84
E-1. Elastic Modes for Configuration 3	117

## TABLES

1.	Rapidity With Which System Is Compromised After Loss of an ACT Function	26
2.	Degraded Situation Severity and Means Available for Modifying Risks Presented by Failures	27
3.	ACT Function Application Experience	29
B-1.	Some Average Temporal Properties of a Gaussian Random Process Computed From the Power Spectral Density (From ref. 56)	95
E-1.	Summary of Transfer Function Factored Forms	112
E-2.	Transfer Function Approximate Factors; Configuration 3; 3 Modes	113
E-3.	Transfer Function Approximate Factors; Configuration 3; 4 Modes	114
F-1.	Longitudinal Nondimensional Stability Derivatives	125
F-2.	Longitudinal Dimensional Stability Derivatives	126

## LIST OF ABBREVIATIONS AND ACRONYMS

ACT	Active Control Technology
AMSA	Advanced Manned Strategic Aircraft
ATT	Advanced Technology Transport
CAT	Clear Air Turbulence
CCV	Control Configured Vehicle
C.G.	Center of Gravity
CTOL	Conventional Takeoff and Landing
EAS	Equivalent Airspeed
FAR	Federal Aviation Regulation
GAG	Ground-Air-Ground
ILAF	Identical Location of Accelerometer and Force
LAMS	Load Alleviation and Modal Suppression
LDCS	Load Distribution Control System
NASA	National Aeronautics and Space Administration
RMS	Root Mean Square
RPA	Rational Probability Analysis
SAS	Stability Augmentation Systems
SAT	Storm Air Turbulence
SCW	Supercritical Wing
SST	Supersonic Transport
STOL	Short Takeoff and Landing
TAS	Tentative Airworthiness Standard
WRBM	Wing Root Bending Moment

LIST OF SYMBOLS

$a_x$	Longitudinal acceleration in body axes ( $m/s^2$ )
$A_w$	Root locus gain for $w/\delta$ transfer function ( $m/s^2$ )
$a_y'$	Lateral acceleration in body axes at the center of percussion for the rudder ( $m/s^2$ )
$a_z'$	Normal acceleration in body axes at the center of percussion for the elevator ( $m/s^2$ )
$A_\theta$	Root locus gain of $\theta_r/\delta$ transfer function ( $m/s^2$ )
$A_{\xi_r}$	Root locus gain of $\xi_r/\delta$ transfer function ( $m/s^2$ )
AR	Aspect ratio
$c$	Local chord (m)
$\bar{c}$	Mean aerodynamic chord (m)
c.g.	Center of gravity
$C(\cdot)$	Nondimensional stability derivative indicated by $(\cdot)_x$ . (Refer to Table F-2)
EI	Stiffness (Young's modulus times section moment of inertia) ( $Nm^2$ )
m	Meter
$F_{q\xi_r}$	Generalized force in $q^{th}$ mode per unit deflection in $r^{th}$ generalized coordinate (N/m)
$F_{q\dot{\xi}_r}$	Generalized force in $q^{th}$ mode per unit velocity in $r^{th}$ generalized coordinate (N/m/s)
$[F_\xi]$	Matrix of modal forces per unit deflections in $\{\xi\}$ (and unit velocities in $\{\dot{\xi}\}$ , etc.)
g	Gravitational acceleration constant ( $m/s^2$ )
h	Rigid-body displacement in altitude (positive up) (m)
i	Row index for a matrix; also an interval point index
$I_y$	Total pitch inertia of the system ( $kg/m^2$ )
j	Column index for a matrix

K, k	In general, gains
$k_y$	Pitching radius of gyration (m)
$K_i$	Active feedback control gain factor operating on the $i^{\text{th}}$ variable in the list of subscripts
L	Turbulence integral scale length (m)
$l_{x_i}$	Distance from the airframe center of gravity to the $i^{\text{th}}$ point on the longitudinal (fuselage) or x-axis, positive forward (m)
m	Total mass of the system (kg)
M	Rotational acceleration ( $\text{rad/s}^2$ )
$M_{\xi_k}$	Rotational acceleration per unit deflection of $k^{\text{th}}$ mode $\{(\text{rad/s}^2)/\text{m}\}$
$M_{\dot{\xi}_k}$	Rotational acceleration per unit velocity of $k^{\text{th}}$ ( $\text{rad/m-s}$ )
$N_w$	Numerator of $w/\delta$ transfer function
$N_\theta$	Numerator of $\theta/\delta$ transfer function
$N_{\xi_r}$	Numerator of $\xi_r/\delta$ transfer function
q	Dynamic pressure ( $\text{N/m}^2$ )
P	Index of performance, $\frac{V}{V_A}$ ( $\text{m}^2/\text{s}^2$ )
r	Yaw rate ( $\text{rad/s}$ )
rad	Radians
s	Laplace transform variable (1/s)
sec	Second(s)
S	Wing area ( $\text{m}^2$ )
T	Total thrust ( $\text{kg-m/s}^2$ )
t	Time (s)
$T(\cdot)$	Time constant designated by ( $\cdot$ ) (sec) also stable spectral factor of $\phi(\cdot)(\cdot)$
u	Rigid-body velocity perturbation measured parallel to instantaneous body reference line (m/s) , also called longitudinal velocity perturbation
$U_0$	Trimmed forward velocity of the vehicle (m/s)
$\bar{V}$	Horizontal tail volume coefficient, $S_H l_H / S \bar{c}$
$V_A$	Trimmed airspeed of the vehicle (m/s)

W	Aircraft gross weight ( $\text{kg-m/s}^2$ )
w	Rigid-body plunging velocity perturbation measured normal to instantaneous body reference line, positive down ( $\text{m/s}$ )
$w_i$	Plunging velocity of elastic vehicle at point i
WRBM	Wing root bending moment
x	Longitudinal position coordinate parallel to instantaneous body reference line, positive forward of the c.g. ( $\text{m}$ )
X	Longitudinal acceleration, along the x-axis ( $\text{m/s}^2$ )
y	Lateral position coordinate normal to rigid body plane of symmetry, positive right of the c.g. ( $\text{m}$ )
z	Normal (plunging) position coordinate with respect to the xy-plane, positive down with respect to the c.g. ( $\text{m}$ )
Z	Normal acceleration, along the z axis ( $\text{m/s}^2$ )
$Z_i$	Normal displacement of elastic vehicle at point i (positive down) ( $\text{m}$ )
$Z_q$	Normal acceleration per unit pitching velocity ( $\text{m/s}$ ) (See Table E-4)
$Z_u$	Normal acceleration per unit u ( $1/\text{s}$ ) (See Table E-4)
$Z_w$	Normal acceleration per unit w ( $1/\text{s}$ ) (See Table E-4)
$Z_\delta$	Normal acceleration per unit $\delta$ ( $\text{m/s}^2\text{-rad}$ ) (See Table E-4)
$Z_{\xi_k}$	Normal acceleration per unit deflection in $k^{\text{th}}$ mode ( $1/\text{sec}^2$ )
$Z_{\dot{\xi}_k}$	Normal acceleration per unit velocity in $k^{\text{th}}$ mode ( $1/\text{sec}$ )
$\alpha$	Angle of attack, $w/U_0$ (rad)
$\beta$	Angle of sideslip (rad)
$\gamma$	Longitudinal flight path angle (rad)
$\delta$	Control surface deflection (rad)
$\epsilon$	Downwash angle (rad)
$\Delta$	Transfer function denominator
$\zeta$	Damping ratio
$\zeta_{ke}$	Damping ratio of the $k^{\text{th}}$ coupled elastic mode
$\zeta_r$	Effective structural damping ratio of the $r^{\text{th}}$ mode
$\eta_H$	Dynamic pressure ratio at horizontal tail

$\theta$	Rigid-body rotation about the pitching axis (rad)
$\theta_i$	Rotation of elastic fuselage at point i about the pitching axis (rad)
$\iota_H$	Incidence of the horizontal tail (rad)
$\mu$	Mean value
$\mu_c$	Longitudinal relative density, $m/\rho S \bar{c}$
$\xi$	Thrust line inclination with respect to reference axis system (rad)
$\xi_r$	Generalized coordinate or displacement of the $r^{\text{th}}$ mode (m)
$\dot{\xi}_1$	Time rate of change of the generalized coordinate of the first mode, $w$ (m/s)
$\xi_2$	Generalized coordinate of the second mode, $\theta$ (rad)
$\rho$	Air density ( $\text{kg/m}^3$ )
$\sigma_{(\cdot)}$	Standard deviation of $(\cdot)$ (unit $(\cdot)$ )
$\tau$	Elevator effectiveness in rotating the zero-lift axis of the tailplane
$\phi_{(\cdot)}(\cdot)$	Power spectral density for the variable $(\cdot)$ (units $(\cdot)^2/\text{Hz}$ )
$\phi_{ir}$	Normalized translation of $i^{\text{th}}$ point in $r^{\text{th}}$ mode
$\phi'_{ir}$	Normalized rotation of surface at $i^{\text{th}}$ point in $r^{\text{th}}$ normal mode
$\phi_r$	Normalized shape of the $r^{\text{th}}$ normal mode
$\omega$	Frequency (rad/s)
$\omega_{ke}$	Frequency of the $k^{\text{th}}$ coupled elastic mode (rad/s)
$\omega_r$	Eignevalue of the $r^{\text{th}}$ normal mode (rad/s)
$\doteq$	Approximately equal to
$\equiv$	Is defined as
$\ll$	Much less than
$\gg$	Much greater than
$\sum$	Summation
$(\dot{\cdot})$	Dot over quantity denotes time derivative
[ ]	Matrix
{ }	Column matrix

( )' Prime denotes differentiation of normal mode shape with respect to the x-coordinate; also denotes redefinition of stability derivatives to include contributions from active feedback control of pitch rate and attitude

( )'' Double prime denotes redefinition of stability derivatives to include contributions from active feedback control of pitch attitude and angle of attack (or its dynamical equivalent)

$l_H$  Horizontal tail length (m)

$n_z$  Normal load factor,  $A_z/g$

$C_m/C_L$   $dC_m/dC_L$

### Subscripts

a Actuator

ac Aerodynamic center

COL Control column

c Command

cg Center of gravity

d Dutch roll

e Elevator

g Gust

H Horizontal tail

k Associated with  $k^{\text{th}}$  elastic mode

L Lower bound

limit Limit level value

max Maximum value

o Associated with null value

sp Short period

trim Trimmed value

U Upper bound

$w_k$   $k^{\text{th}}$  root of w transfer function numerator

WB Wing-body

x Longitudinal position coordinate parallel to instantaneous body reference line, positive forward of the c.g. (m)

y Lateral position coordinate normal to rigid body plane of symmetry, positive right of the c.g. (m)

z Normal (plunging) position coordinate with respect to xy-plane, positive down with respect to the c.g. (m)

$\alpha$	Angle of attack
$\theta$	Pitch attitude
$\dot{\theta}$	Pitch rate
$\theta_k$	$k^{\text{th}}$ root of $\theta$ transfer function numerator
$\xi_{rk}$	$k^{\text{th}}$ root of $\xi_r$ transfer function numerator
1/4	Designates the c.p. (ordinarily at 1/4 chord)
3/4	Three-quarter point of chord

---

Note: Transfer equations for accelerometer, rate-gyro, and angle-of-attack instrumentation; axes-system transfers of aerodynamic derivatives; and methods for measuring moments of inertia are summarized in NASA SP-3070.

Section 1  
INTRODUCTION AND SUMMARY

1.1 PURPOSE AND SCOPE

If the future subsonic transports described in reference 1 are to obtain full benefits from active control systems, they will have to satisfy design criteria and airworthiness standards which are somewhat different from those in current use. The achievement of full benefit from the active control systems requires that current design criteria and airworthiness standards be examined to determine in what manner they may overly restrict this emerging technology. On the other hand, active control systems may contain novel or unusual features which demand new design criteria or airworthiness standards. Accordingly, the National Aeronautics and Space Administration (NASA) convened a panel of aircraft industry experts to assess the state of the art in active control technology (ACT) and to consider the advantages and problems in applying it to the subsonic CTOL transport of the 1980s.

The panel was charged with the following tasks:

- Realistically assess the state of the art in ACT and the potential for the application of ACT to subsonic CTOL transports of the 1980s.
- Assess the risk of applying ACT and indicate areas in which existing design criteria and airworthiness standards may require modification or supplementation with new criteria and standards.
- Recommend design practices for the application of ACT.
- Recommend research programs needed to gain industry confidence for application of ACT to design of subsonic CTOL transports for the 1980s.

In the course of conducting their examination, panel members contributed written comments on personal and company experience with the topics under study. This provided the basis for extensive oral discussion of these topics during a three-day panel meeting. These written comments and the transcribed discussion have been edited to form a substantial portion of this report. Expansions on a number of subjects considered by the panel have been provided by the authors. At specific points in the text, the authors felt constrained to identify items contributed by the panel as a whole. This is accomplished by means of the phrase "experience cited for the panel."

1.2 MEMBERSHIP OF THE PANEL

The members of this panel are listed below.

Industry

Bert M. Hall	Task Advisor and Meeting Chairman McDonnell Douglas Astronautics Company
Fred C. Hall	Commercial Airplane Group The Boeing Company, Seattle

Robert B. Harris	Douglas Aircraft Company
L. Gregor Hofmann	Systems Technology, Inc.
Don L. Keeton	McDonnell Douglas Astronautics Company, Task Manager
Robert H. Parker	Engineering Department Transport and Military Flight Controls Sperry Flight Systems Division, Phoenix
John T. Rogers	Commercial Airplane Group The Boeing Company, Seattle
Warren A. Stauffer	Lockheed-Georgia Company, Marietta
Glenn O. Thompson	The Boeing Company, Wichita
John H. Watson	General Dynamics, Convair Aerospace Division Fort Worth Operations

NASA

Albert L. Braslow	NASA Langley Research Center
Ray V. Hood	NASA Langley Research Center
George W. Jones, Jr.	NASA Langley Research Center, Task Manager

### 1.3 SUMMARY OF THE PANEL CONSENSUS

The technical feasibility of all ACT functions except flutter control has been demonstrated individually, and the technology is adequate for application in commercial subsonic CTOL transport designs of the 1980s. The main deficiency in the current technology occurs with respect to the integrated application of ACT functions. This deficiency tends to obscure the true cost-benefit impact of ACT application, to result in unduly complex separate implementations of ACT functions, and to complicate and lengthen considerably the design cycle for aircraft which use ACT. In addition, reliability consistently arose in the panel discussion but is beyond the scope of this study.

Additional enveloping structural design criteria must be established which account for the presence of ACT functions. These criteria must have the ability to define with only modest conservatism that portion of structural strength which can be replaced by a given level and distribution of control authority without regard for the particular details of the required control laws. This implies that generic forms of control laws which are generally applicable\* for each (or perhaps all) of the ACT functions must be identified, and corresponding adjustments to existing structural design criteria affecting strength, fatigue, and flutter must be determined.

---

\*This must be accomplished in the spirit of the now classical generic solutions for various specific rigid-body dynamic deficiencies. Some of these generic control laws are pitch, roll, and yaw dampers, the sideslip stability augmentor, aileron-to-rudder crossfeeds, automatic throttles, Mach tuck compensators, elevator-to-throttle crossfeeds, turn-coordination systems. These generic solutions are used singly or in combination to correct for specific rigid body dynamic performance deficiencies. The ILAW (identical location of accelerometer and force) generic ACT control concept is representative of those required in the ACT area.

Existing airworthiness standards for transport category airplanes (ref. 2) do not generally legislate against ACT application. Certain requirements are restrictive, however, because of an earnest desire to ensure, through regulation, that all features essential to a high minimum level of acceptable safety are provided for, and because of practical considerations in demonstrating compliance with the regulations. The restrictive regulations do not appear to arise from fundamental technical limitations in any case. Rather, the nature of the restrictions involves the following factors:

- Interpretation of the fundamental intent of the regulation was not originally made in a context which included ACT.
- Practical considerations for demonstrating compliance have resulted in requiring arbitrary maneuvers or tests which have no counterpart in normal or probable degraded modes of operation. The result is untoward conservatism.
- Acceptable safe practice in the airworthiness standards tends to be consistent with the current or recent past state of the art and not projected state of the art of the many disciplines involved.

Tentative Airworthiness Standards for Supersonic Transports (ref. 3) and Special Conditions for the Concorde SST (ref. 4) provide only a small beginning to the revisions required to allow full application of ACT with the scope allowed by a high minimum level of acceptable safety.

In general, the panel felt that further research and experience are needed in the following areas:

- Improvement of mathematical models.
- Development of detailed designs of ATT aircraft.
- Iron-bird ACT system simulation
- Development of aeroelastic measurement techniques for ACT.

In addition, a panel of experts in aircraft design and analysis should be convened to review the state of the art in control technology for implementing ACT functions and identify active control system design criteria and recommended design practices.

#### 1.4 ORGANIZATION OF THE REPORT

In Section 2, the several ACT functions, such as ride quality control, are discussed separately. Each function is defined, the current state of its technology is described generally and in terms of recent applications, and its readiness for application in subsonic CTOL transports is assessed.

Section 3 assesses the risk in applying each ACT function from various points of view and identifies areas in current airworthiness standards which may need reinterpretation, revision, or additional regulation because of novel or unusual design features resulting from the application of ACT. The final part of Section 3 recommends changes in structural and structural-control system criteria. Section 4 recommends design practices which should accompany the application of ACT.

Section 5 outlines critical technical areas and future research and development programs needed to gain industry confidence for the application of ACT in a commercial environment.

A series of appendixes presents detailed technical developments of several design criteria and design practices summarized in the body of the report. The final appendix defines longitudinal stability derivatives.

## Section 2

### SUMMARY AND APPRAISAL OF THE CURRENT STATE OF THE ART IN ACTIVE CONTROL TECHNOLOGY

In this section, Active Control Technology\* (ACT) is discussed in six parts as follows:

- Augmentation of relaxed inherent stability
- Center of gravity control
- Ride quality control
- Load control (including maneuver load control, gust load control, and fatigue damage control)
- Flutter control
- Envelope limiting

The final section is devoted to a discussion of the pilot's interface with ACT systems.

These functions and considerations do not occur or apply independently of one another when implemented, but this classification is necessary for an orderly treatment. This classification scheme is also indicative of the somewhat topical approach which has led to the current state of the component technologies which together comprise ACT. Many of the component technologies have received extensive attention, but the combined application of several of the component technologies in an integrated way seems to have received much less attention. It is in this integration that ACT seems to offer the greatest potential because of a resultant synergistic effect. For example, the performance gains or gross weight reductions available from simultaneous application of maneuver and gust load control have been found to exceed significantly the sum of the gains available when these load control concepts are applied separately. For this reason, "Combined Application of ACT Functions" might be added to the above list, but there is little current art to summarize. Instead, this study will attempt to identify where synergistic interactions may be expected within the topics of the original list.

#### 2.1 AUGMENTATION OF RELAXED INHERENT STABILITY

Relaxed inherent stability is conventionally defined as a reduction in the stability of the short-period attitude modes of rigid-body aircraft motion. That is, reductions in inherent stability result with the reduction of

---

\*The scope of Active Control Technology in the context of advanced subsonic transports is established in the survey of reference 5.

aerodynamic restoring moment with respect to angle of attack or angle of sideslip or a reduction of aerodynamic damping moment with respect to pitch rate, yaw rate, or rate of change of attack or angle of sideslip for the unaugmented aircraft. In principle, relaxed inherent stability can also refer to reduction in stability for other modes of aircraft motion.

Longitudinal stability is classically explained in terms of the slope of the curve of pitching moment versus lift,  $dC_m/dC_L$  or  $C_{mC_L}$ , for the aircraft. Stability of the short-period attitude modes of the aircraft is more completely explained in terms of the approximate short-period and dutch roll undamped natural frequencies. The related equation for the short-period frequency is equation (A-1) of Appendix A. The role of  $C_{mC_L}$  in equation (A-1) is evident, but the pitch damping derivative,  $C_{mq}$  also plays a significant role, especially when the magnitude of  $C_{mC_L}$  is small. For stability of the longitudinal short-period mode, the square of the short-period undamped natural frequency,  $\omega_{sp}$ , must be positive. Similarly, stability of the dutch roll mode requires that the square of its undamped natural frequency,  $\omega_d$ , must be positive.

The stability requirement for short-period damping coefficient,  $2\zeta_{sp}\omega_{sp}$ , involves the stability derivatives  $C_{L\alpha}$ ,  $C_D$ ,  $C_{mq}$ , and  $C_{m\dot{\alpha}}$  as shown in equation (A-5) of Appendix A. For stability of the longitudinal short-period mode, its damping coefficient must be positive. Similarly, stability of the dutch roll mode requires that its damping coefficient be positive.

The equations cited above do not explicitly account for aeroelastic effects upon short-period frequency and damping. These effects can be significant and might be expected to be more so for an aircraft using ACT because of possible reduced structural stiffness. The effects of elastic modes usually are to reduce the short-period frequency and damping from values calculated for a rigid aircraft. Quantitative evaluations of the elastic effects are discussed in Appendix E and in references 6 to 8.

Desirability of relaxed inherent stability arises from the possibility that through operation with smaller tail volumes significant reductions in total aircraft drag and gross weight can be realized with invariant payload and mission. The deficiencies in inherent stability would, of course, be compensated for by augmenting  $C_{m\alpha}$ ,  $C_{mq}$ ,  $C_{n\beta}$ , and  $C_{nr}$  stability derivatives as necessary by means of an active control system having reliability consistent with its criticality for safe flight. The appropriate control laws for augmentation may feed back  $\theta$ ,  $\alpha$ ,  $\dot{\theta}$ ,  $\dot{\alpha}$ , or  $a_z$  to the elevator and  $\beta$ ,  $r$ ,  $\dot{\beta}$ , or  $a_y$  to the rudder. (Symbols are defined in the front matter.) In addition aileron-to-rudder crossfeed may also be used for dutch roll control.

However, there are concomitant difficulties for aircraft with relaxed inherent stability which do not have counterparts in more inherently stable aircraft. Among these difficulties are greater sensitivity of aircraft trim drag to c.g. location (which makes automatic c.g. control more of a necessity) and greater complexity of the augmentation (both from the point of view of reliability consistent with its flight-critical nature, and from the point of view of the integration of trim functions). Synchronization and interfacing with non-flight-critical automatic control functions, and virtual 100% authority for the flight-critical control functions pose further difficulties.

Experience cited for the committee in connection with the General Dynamics lightweight fighter studies contrasted the horizontal tail-sizing criteria for that aircraft with the horizontal tail-sizing criteria for a conventional aircraft. Horizontal tail area is normally set for a conventional design by the pitching moment required for the nose-gear unstick and the short-period frequency requirement in the absence of stability augmentation. For the relaxed stability design, horizontal tail area is set by the pitching moment required for nose-gear unstick and the pitching acceleration component required for control in the presence of gusts. These points are illustrated in figure 1. Furthermore, for subsonic missions static margins near zero tend to be optimum. Although these conclusions were reached for a specific fighter configuration, it is clear that they tend to apply in general.

An appreciation for the new dimensions in complexity attendant to flight-critical augmentation systems can be gained from Tomlinson's survey of the 2707 SST design effort (ref. 9). The discussion in this reference of trim function integration, interfacing of flight critical and non-flight critical automatic control functions and the design philosophy for reliability are notable for defining the limits of the state-of-the-art in flight critical augmentation systems. (However, the use of an inverse model of the desired pitch rate response in the feedback path of a high-gain flight critical augmentation loop cannot be recommended.)

Further examples of relaxed inherent stability cited for the committee are the Northrop flight demonstration more than two decades ago with the T-6 having a -13% static margin; the F-111, which has been flight-tested at negative maneuver margins; the Concorde SST, which can be statically unstable in landing approach and which becomes less stable with increasing load factor in cruise; and a number of paper designs--the 2707 SST previously cited, several Advanced Technology Transport (ATT) studies (one finding was that relaxed inherent stability plus automatic c.g. control offered the greatest payoff among the ACT function concepts), the General Dynamics lightweight fighter design previously cited, and two Boeing tanker designs using various combinations of other ACT functions with relaxed inherent stability. Comparison of the two tanker designs using ACT functions with a baseline aircraft designed to the same specification but not using ACT showed significant gross weight reductions. The design with relaxed inherent stability plus flutter control offered the largest reduction and produced an optimum configuration which had no horizontal tail. This design is shown as an overlay on the baseline configuration in figure 2.

In addition, a relaxed inherent stability system has been designed in connection with a project demonstrating the combined use of several ACT functions using the modified B-52 LAMS system and aircraft. This system was flight tested in mid-1973.

For relaxed inherent stability applications of ACT, the required theoretical understanding, control techniques, sensor technology, and certain aspects of reliability technology, (e.g., ref. 10) are in hand. Actual flight experience with relaxed inherent stability aircraft is not currently very extensive, but research programs such as those involving the NASA F-8 fly-by-wire aircraft,

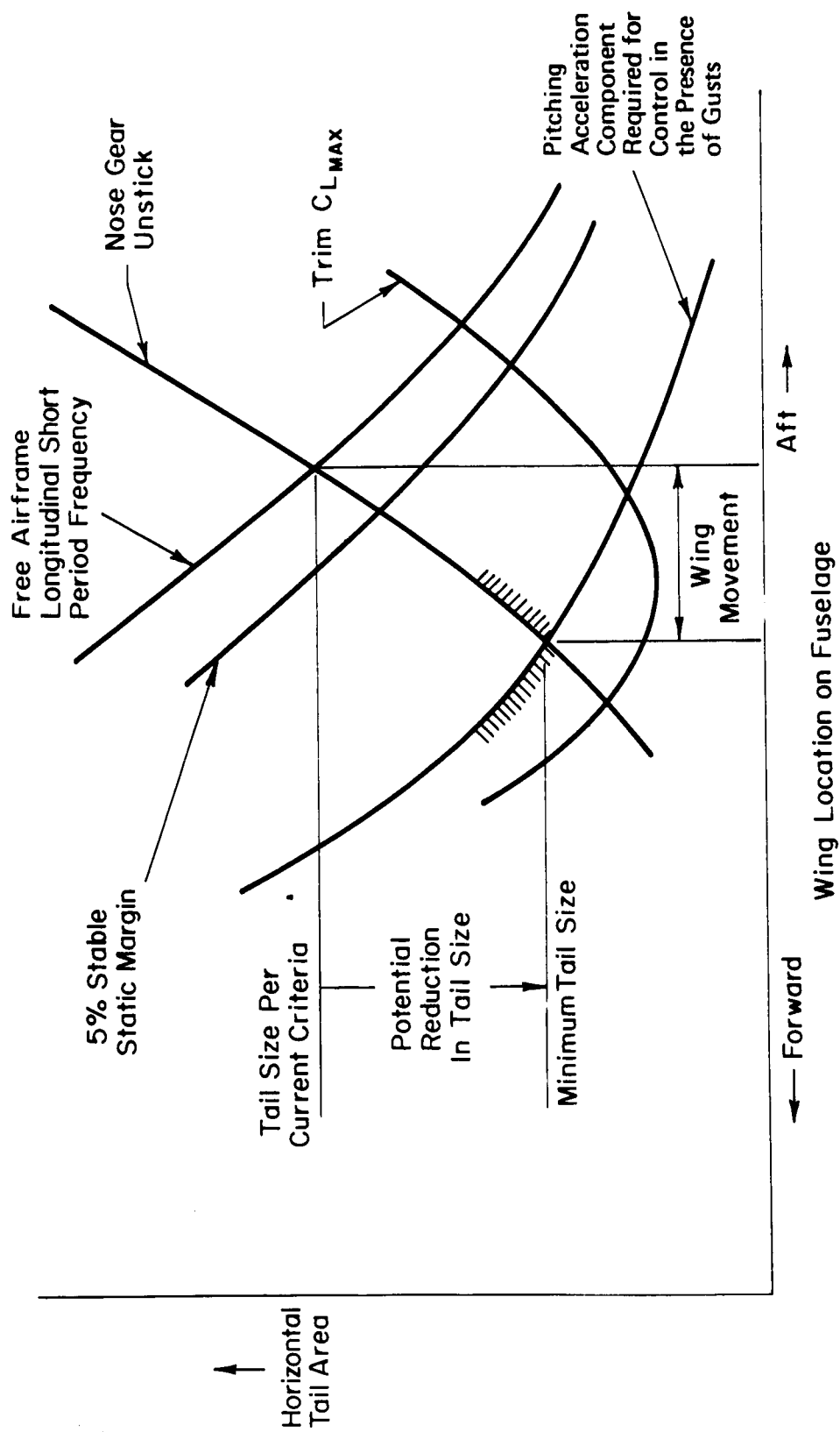


Figure 1. — Horizontal Tail Sizing Criteria

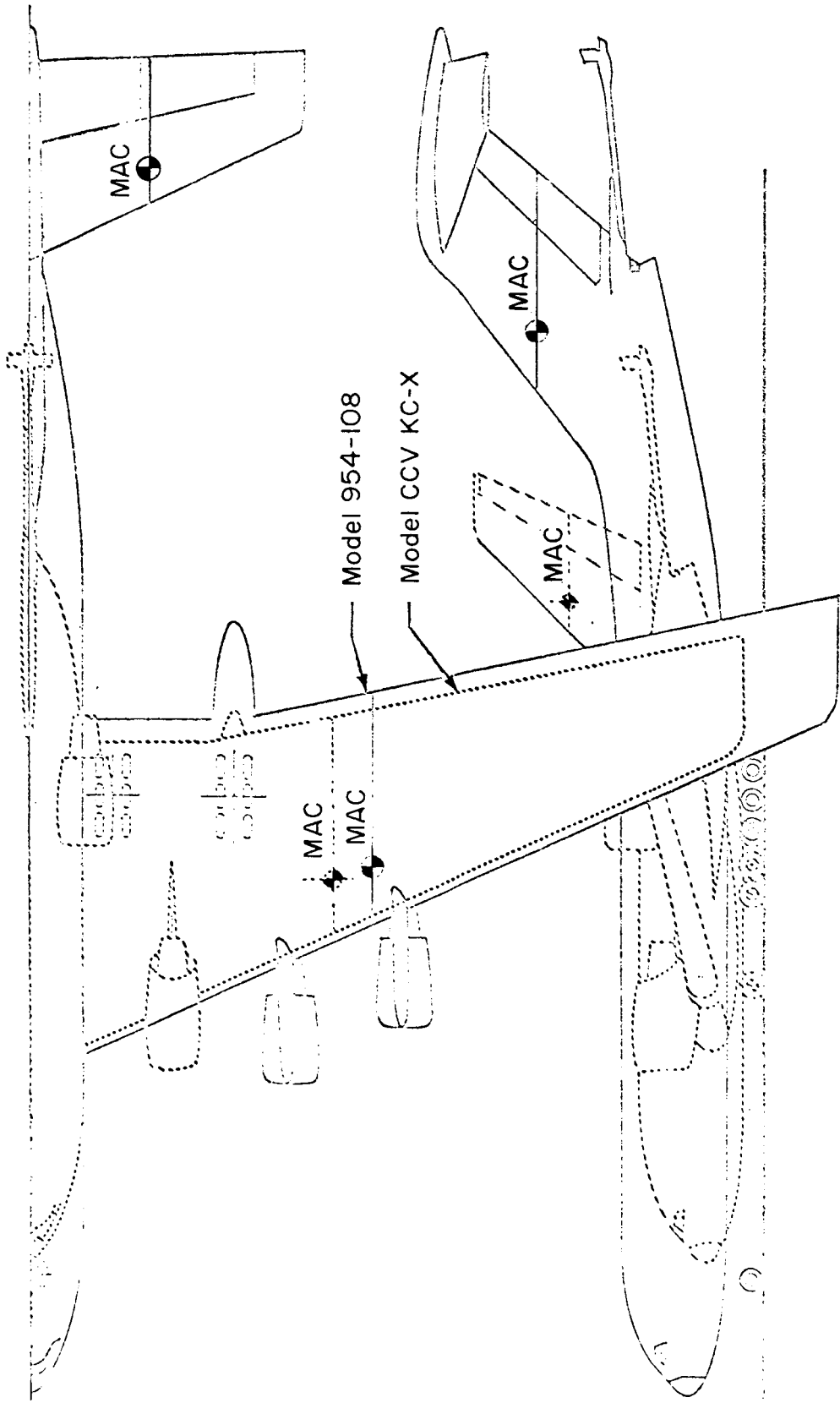


Figure 2. — Model 954-108 and CCV KC-X Tanker Designs

the B-52 control configured vehicle (formerly used in the LAMS program), and the F-4 control configured vehicle (CCV) will provide considerably more experience in the near future. The major need remaining to be satisfied is actual experience with the effect of relaxed inherent stability upon aircraft configuration. This experience is required to confirm that the drag and gross-weight reductions predicted by current methods are achievable in practice. .

The successful application of relaxed inherent stability design concepts will nevertheless require considerable broadening of design approaches, criteria for performance, and interpretation of regulations. The focus must be upon demonstration of acceptable safe practice. Novel design problems will involve provision of sufficient control authority with respect to extreme trim positions, resolution of the quality of response versus system complexity and reliability dilemma, and means for obtaining manageable behavior from full-authority flight-critical systems when authority limits are encountered. Some examples of the required design approaches are given in Section 3.4.

Another reason for both caution and optimism in connection with relaxed inherent stability applications of ACT concerns the introductory period for such systems. Early problems with fully powered controls were fairly numerous, but virtually all arose in connection with the details of the designs and their implementation rather than in connection with the basic concepts. The scenario may well be repeated for relaxed inherent stability applications of ACT. Therefore, progress would be best served if the early applications of relaxed inherent stability are only modestly ambitious.

## 2.2 CENTER-OF-GRAVITY CONTROL

Center-of-gravity control refers to the practice of shifting the aircraft c.g. location by means of redistributing fuel or payload mass within the aircraft. Automatic c.g. control is a state-of-the-art technique for which the theoretical principles are well understood and which has been implemented in production hardware for military use. Center-of-gravity management is a flight management task common to all aircraft. It is usually accomplished by appropriate distribution of the payload mass and by the selective loading and consumption of fuel. Precise c.g. control is not essential for conventional subsonic aircraft as long as the limits for c.g. location are not violated. For this reason, c.g. management is accomplished manually, perhaps with the aid of simple calculation devices or by groundbased computers prior to dispatch for aircraft having conventional inherent stability. Therefore, automatic c.g. control would not usually be cost effective for conventional subsonic aircraft although it might be cost effective or even essential for conventional aircraft which operate in the transonic and supersonic regions.

As noted in the previous subsection, sensitivity of aircraft trim drag to off-optimum c.g. location increases with decreasing inherent stability. Automatic c.g. control can considerably lessen, if not eliminate, this key disadvantage. The B-58 included a fuel management system for c.g. control for example. Automatic c.g. control also produces an advantage in that the automatic system can

function to maintain a constant maneuver margin\* as the aerodynamic center shifts rearward with increasing Mach number. Furthermore, manual takeover of fuel management under emergency conditions (a time when trim drag hardly matters) consists simply of transferring fuel forward or dumping the aft portion of the fuel load.

Boeing ATT studies show that augmented relaxed inherent stability combined with center-of-gravity control ACT functions offers the largest payoff for that aircraft in terms of gross weight reduction. This finding confirms the value of using these two ACT functions in combination.

### 2.3 RIDE QUALITY CONTROL

Ride quality control refers to automatic control system functions which reduce to acceptable levels the level of acceleration to which passengers and crew are subject. Ride quality involves components of acceleration at frequencies above those necessary for maneuvering the aircraft but below the lowest audible frequencies.

Factors such as low aircraft wing loading, aircraft structural flexibility, high turbulence levels, and high-speed, low-speed, low-altitude mission segments can produce an unacceptable ride singly or together. The level of acceleration exposure does not pose a direct safety hazard for passengers, because levels which are objectionable for reasons of personal comfort are reached long before pain or injury are inflicted. Adequate ride quality at crew stations in the cockpit can be essential to safety, since inadequate ride quality can result in increased fatigue and decreased proficiency in perception and control. In connection with control, vibration feedthrough can be important. Vibration feedthrough is a phenomenon wherein the pilot's body or limb acts as a bobweight in response to vibration. His contact with the controls results in inadvertent inputs which, if unfavorably phased, can further increase the amplitude of vibration.

The control techniques for improving ride quality are fairly well established both theoretically and operationally. Many commercial transports have some degree of ride quality control provided by means of conventional control surfaces.

The yaw damper systems of the DC-8, DC-9, DC-10, 727, 747, and L-1011 improve ride quality even though their fundamental purpose is to improve handling qualities. In these cases, it is principally the lateral acceleration level in the aft cabin which is reduced. Direct lift control in the prototype DC-10 also improved ride quality with respect to longitudinal acceleration as a side effect. However, direct lift control is not used in the production DC-10. In the USAF/Rockwell International B-1 strategic bomber, special dedicated control surfaces (small, forward-located, canted vanes) have been added for longitudinal ride quality control. The B-70 also uses ride quality control.

---

\*The maneuver margin is given in Appendix A as  $[-C_{mC_L} - C_{m_q}/4\mu_c]$ .

Additional paper studies of ride quality control systems cited for the panel were for the General Dynamics AMSA design, the Boeing SST design, and a Boeing low-wing loading commercial STOL design for which ride quality control was essential in the high-speed descent condition. The Lockheed SST design, L-2000, required ride quality improvement for the cockpit while taxiing as well as when airborne. An active system was proposed for airborne ride quality control, and passive landing gear modifications were proposed for the taxiing condition although active landing gear control was also considered.

The Boeing low-wing-loading commercial STOL design (ref. 11) is interesting in that simplicity of design for the basic airframe (there were no exotic high lift or propulsive lift devices employed) traded off very favorably with complexity added by the ride quality control system. Furthermore, the ride quality control system probably would require only fail-passive characteristics that would permit flight to safe landing within a reduced flight envelope. Typically, ride quality control functions do not require high reliability because loss of those functions does not have significant safety implications. For the same reason, ride quality control systems may well be inoperative and still allow aircraft dispatch. Indeed, this is similar to the philosophy for the B-1 ride quality control system (ref. 12).

Ride quality problems have tended to be secondary considerations with respect to resolution of structural load and flexibility problems. In fact, it was stated by two members of the panel that ride quality is not a major trade factor in design, because the criteria for ride quality in the commercial environment are:

- Ride must be merely acceptable to passengers
- Ride must be competitive with contemporary commercial aircraft

Satisfaction of these criteria tend to result in satisfactory ride in the cockpit as well as the passenger cabin.

Research is needed in ride control to establish reliable quantitative ride quality criteria. While working criteria exist for acceptable normal and lateral rms accelerations, other more sophisticated aspects of ride quality criteria are not yet quantified. For example:

- How do different levels of random vibrational accelerations in different axes combine in the perceived level of passenger ride quality?
- What are the effects of anxiety, noise, and other real-flight stress factors upon the level of passenger acceptable ride quality?
- What are the effects of duration of exposure upon the level of passenger-acceptable ride quality?
- How do random rotational inputs affect perceived ride quality?
- What are the effects of the spectral shape of vibrational accelerations upon the level of passenger-acceptable ride quality?

## 2.4 LOAD CONTROL

Load control refers to the use of passive or automatic control functions for the purpose of regulating the net load and distribution of load applied to the aircraft structure.

There are four main facets to load control. To some extent, all must be considered simultaneously to achieve a well-balanced design although some may receive considerably more emphasis than others. Three facets of load control which are specifically discussed in this subsection are maneuver load control, gust load control, and fatigue damage control. Flutter control might also be included as a fourth facet of load control because flutter is the result of a particular kind of loading. Flutter, however, tends to be disassociated from other types of loading for reasons which will be explained in the flutter control subsection which follows.

The first three facets of load control can be more fully appreciated in light of the following definitions for the types of loading to be controlled (e.g., refs. 13 to 17).

### 2.4.1 Maneuver Loading

Maneuver loading is that portion of forces acting on the airframe which results from accelerations required to maintain the aircraft on the intended flight path.

Maneuver loading is quasi-static in nature. That is, the power spectral density of maneuver loading in response to flight path commands has a half-power frequency which is small with respect to the short-period, roll-subsidence and dutch roll rigid-body attitude mode frequencies. Consequently, low-frequency approximations to the load response in these modes are adequate for maneuvering load evaluation. Similarly, low-frequency approximations to the load response in the aircraft flexibility modes are adequate for maneuvering load evaluation. The latter approximations being the so-called "static aeroelastic corrections".

To this point, the net maneuver loading on the aircraft (that is, the average load factor on the airframe) has been the focal point. However, the distribution of this loading over the airframe can have a powerful effect upon the shear forces and bending moments which must be transmitted at given points in the structure. The ability to tailor the distribution of maneuver loading over the airframe is maneuver load control. Maneuver load control can have a significant impact upon structural implementation and even upon configuration.

### 2.4.2 Gust Loading

Gust loading is that portion of forces acting on the airframe which results from atmospheric disturbances.

Gust loading is dynamic in nature, although only relatively low frequencies are involved. This is because the half-power frequencies for the gust power spectral densities\* are smaller than the rigid-body attitude mode frequencies. Therefore,

---

\*

$U_0/L$  is the half-power frequency for the longitudinal gust component power spectral density.  $U_0 / (\sqrt{3L})$  is the half-power frequency for the normal gust component and side gust component power spectral densities.  $U_0$  is the trimmed airspeed. The integral turbulence scale length,  $L$ , is 762 m (2500 ft) at altitudes above 762 m (2500ft).

the airplane responds in rigid-body modes and in modes having low frequencies. Both the net and distributed effects of gust loading are important. Gust-load control (e.g., refs. 18 to 21) is accomplished by the following means:

- Controlling the aircraft in such a way as to produce a net incremental load factor which tends to cancel the net gust-induced load factor. Because of aircraft inertia, this is best accomplished with direct lift control devices.
- Controlling the distribution of the incremental load factor which tends to cancel the gust-induced load factor in such a way that their distributions are similar.
- Augmenting damping for modes excited by gusts

The extent to which gust-load control is effective in performing all three listed functions can have a significant impact upon the structural strength and fatigue requirements. The extent to which gust-load control can be effective for the two latter functions is fundamentally limited by the degree of distribution of control capability over the airframe, that is, by the number of independent control surfaces.

Experience cited for the panel indicated that the impact of maneuver and gust-load control in terms of reduction of structural requirements tends to be significant only when both maneuver and gust-load control are practiced simultaneously. If only one of these load-control objectives is addressed, then the other source of loading becomes critical before any significant reduction in structural requirements is realized.

#### 2.4.3 Cyclical Loading

Cyclical loading is produced by forces applied to the airframe which result in stress-level oscillations in the structure. Fatigue damage results from accumulated stress cycles at given stress levels and at critical points in the airframe. Fatigue damage control is a technique for reducing the fatigue damage rate by using active controls to reduce the number of transient cycles at the higher stress levels to which the structure is subjected during operation (e.g., ref. 22). Fatigue damage is the result of cyclical loading.

The frequency range of damaging loads extends from once per 100 flights (e.g., from very "firm" landings) to the once per flight of the so-called ground-air-ground (GAG) cycle and to the characteristic frequency of the response to turbulence. The transition between the ground mean loading and the airborne mean loading of the GAG cycle accounts for as much as 80% of fatigue damage on the lower wing skin on some contemporary transport aircraft. Most of the remaining damage accrues from incremental loads in the 1/4- to 1/2-g range.

Fatigue damage control systems augment the damping of the rigid-body attitude and structural flexibility modes. The added damping reduces the initial load peak level in response to disturbances, and for modes having very small inherent damping, successive load peaks in the response are sharply reduced or eliminated.

The mean-to-mean fluctuation of the GAG cycle is not amenable to control by means other than fuel management. Even then, the gains may be small unless airborne fueling is practiced. Fatigue damage control with respect to longitudinal loads offers only potential improvement for the incremental load fluctuation about the mean levels of the GAG cycle. Larger potential for fatigue damage control with respect to lateral loads exists because there is no GAG cycle effect. Indeed, most existing fatigue damage control systems deal only with the lateral loads.

#### 2.4.4 Other Loading Conditions

Other, often critical, loading conditions for transport aircraft are encountered in connection with landing contact loads, ground loads during take-off, landing and taxi rolls (e.g., ref. 23), engine-out conditions, engine inlet shock wave expulsion, stall, buffet, vortex encounter, maximum rate roll at high speed, and so on. Most of these loadings are not presently amenable to control. The extent to which critical levels of various loads tend to lie one right behind the other in a well-balanced design may be appreciated from figure 3. This figure makes clear the need to consider virtually all types of loads simultaneously, for as soon as one critical loading boundary is pushed back by a small amount, another from a different source of loading is sure to become critical. Fortunately, however, it appears that present methods for load control tend to be effective in pushing back boundaries for more than one loading source at a time. This, in turn, tends to have a favorable effect upon the complexity of design trades, but will also have the unfavorable effect of possibly making critical previously unimportant loading sources and conditions which are not alleviated by load control.

The panel was asked to consider if mission segments involving collision avoidance, terminal area control, and automatic landing would likely produce any critical loading or structural criteria which would be unique in ACT applications. Simply stated, the panel consensus was that no unique critical loading or structural conditions are produced. The reasons for this consensus are elaborated below.

In connection with collision avoidance, all reasonable maneuvers will be accomplished within  $\pm 0.5$ -g load factor, which is the minimum maximum maneuvering load factor capability permitted by TAS 25.145(a) of reference 3. The necessity for angle of attack and load factor limiting in ACT applications arises, but the levels for these limits will be determined by other considerations. (Refer to the subsection on envelope limiting.) The considerations for maneuvering in response to terminal area control are the same except for the additional constraints imposed by passenger comfort considerations.

Automatic landing systems, if used for virtually every landing, offer the opportunity for reducing structural requirements set by landing touchdown loads. (Currently, a sink rate of 3.048 m/s (10 ft/s) at maximum landing weight is used to define limit load levels in landing {25.473(a)(1)(ii) of ref. 2}.) Mean touchdown sink rates for automatic landings cited for the committee were 0.762 m/s (2.5 ft/s) for the 747 and 0.2134 m/s (0.7 ft/s) for the L-1011. The standard deviation cited for the L-1011 sink rate was 0.06096 m/s (0.2 ft/s). However, it was pointed out to the panel that

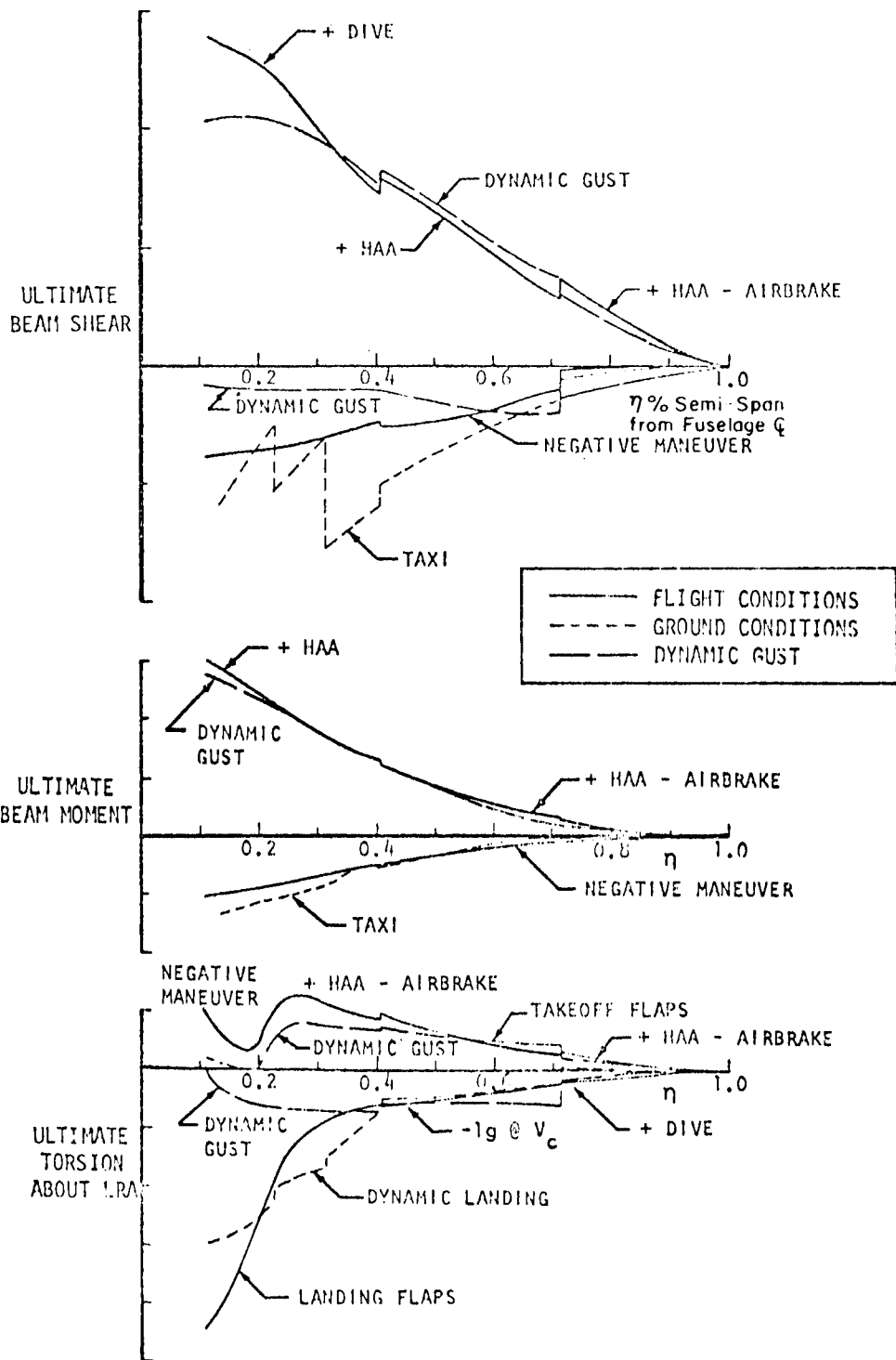


Figure 3. - 747 Wing Design Envelope

if structural design criteria were reduced to account for automatic landing system effectiveness, maximum-effort landing performance would be severely compromised. This is because the maximum effort landing demonstration frequently uses a sink rate at touchdown approaching that defining the limit load levels. If this sink-rate level is reduced significantly, then the maximum-effort landing performance deteriorates significantly also.

Load control experience cited for the panel is summarized in the following paragraphs.

Passive measures for load control cited were the spring-driven outboard aileron on the DC-8, flap blow-back feature on the DC-8, automatic flap retraction on the 747, programmed rudder limits on the DC-9 and 747, automatic dropping out of rudder segments with increasing airspeed on the L-1011, and fuel management, programmed aileron uprig, maximum gross weight revision, maximum positive g load restriction, and consideration of clipped wing tips for the C-5A.

Applications of maneuver load control have been flight tested in connection with the C-5A LDSC and the CCV B-52 programs. Flight tests are to be conducted with the CCV F-4. Study applications have been made for the KC-X advanced tanker, a refined C-5A LDSC, and the ATTT programs.

Examples wherein active control applications have reduced gust loads and the fatigue damage rate are quite numerous. They include a retrofitted pitch and yaw stability augmentation system for the B-52 G and H fleet; 727, 747, L-1011, and DC-10 yaw dampers; a longitudinal system for gust alleviation and structural dynamic stability augmentation for the B-70; B-1 longitudinal and lateral systems; the B-52 load alleviation and mode stabilization (LAMS) systems; and the C-5A load distribution control system (LDSC). The above examples range from systems in production to systems which have been flight tested over a considerable envelope.

There are, in addition, a number of studies, designs, and projects in which maneuver and gust load control have been applied: the L-2000 SST design; a refined version of the C-5A LDSC; a C-5A LAMS system; two advanced tanker (KC-X) designs; several ATTT (advanced technology transport) studies; and an integrated ACT function demonstration project using the modified B-52 LAMS system and aircraft.

Experience with passive load control measures and with active fatigue damage control systems is considerable. These may be regarded as definitely within the state-of-the-art. The general capabilities and limitations of passive load control measures are well established (e.g., ref. 24). The theoretical basis for their analysis is the same as that used for structural and aeroelastic analysis in their absence. Passive measures are so widely applied that they may be regarded as an essential part of the state-of-the-art. Fatigue damage control principles are well established both theoretically and in application (e.g., ref. 25). Maneuver and gust and gust load control experience has been largely the result of research and flight test (e.g., refs. 26 and 27). These may be regarded as state-of-the-art techniques since it appears that they are now sufficiently understood to warrant operational application.

## 2.5 FLUTTER CONTROL

Flutter control refers to the use of automatic control functions which alter the apparent structural mass or stiffness or aerodynamic damping.

Flutter is the result of a particular type of loading. Hence flutter control might logically be considered a type of load control. Indeed, if there is any reason at all to distinguish between flutter and other dynamic behavior of the airframe, it is on the basis of mathematical treatment of the unsteady aerodynamics. In the case of flutter, it is assumed at the outset that a state of harmonic motion exists. That is, flutter is regarded as a neutrally stable oscillation by definition. The result is that the unsteady aerodynamics are modeled in a somewhat different way than if the model were to represent convergent or divergent oscillations. The point of flutter analysis is to identify the airspeed-altitude conditions for which flutter is predicted and to determine the frequency and modes involved. If the airspeed-altitude conditions defining the flutter-condition envelope are too restrictive, it is conventional practice to change the airframe structure mass or stiffness distribution or possibly change the aerodynamic shape for increased aerodynamic damping in a way which will favorably affect the critical flutter mode. This is presently accomplished by strictly passive means such as engine location on wings, additions to mass distribution, increased structural stiffness, small changes in aerodynamic shape to affect lift growth, restricted operating envelope, and so on. Passive modifications to control surfaces such as mass balance and tailored linkage stiffness and slop are also used.

Active flutter control can be used to augment the inherent mass, stiffness, and damping without making physical changes to the airframe structural design. (This assumes that the necessary control surfaces for active flutter control are already part of the airframe design.) At present, the nature of the control law for achieving the required augmentation seems extremely sensitive to the unsteady aerodynamic forces and is also sensitive to the mass and stiffness distributions of the airframe. In the case of unsteady aerodynamics, the uncertainty of parameters in the model is difficult to estimate with confidence (refs. 28 to 30), contributing still further to difficulty in obtaining the appropriate control law. The state of development of generic control laws useful for flutter control is represented by references 31 and 32.

Active flutter control must be considered as a part of ACT even if it may not find commercial application in the near future. Flutter control is yet to be flight tested. A flutter control system designed for a single flight condition in connection with an integrated ACT function demonstration project using the modified B-52 LAMS system and aircraft has been analyzed and designed and was flight tested in mid-1973. In addition, a feasible means for flutter control was established for the 2707 SST design in order to increase the flutter placard speed. The concept was considered to present undue risk, however, and it was therefore abandoned in later design phases. Several ATT studies and a Boeing KC-X tanker study have considered flutter control. There is also an Aeroelastic Model Program in progress at NASA Langley which is exploring flutter control in connection with delta and swept wing aircraft. This program involves the combined use of analytical and model testing techniques with emphasis on the incorporation of active flutter controls.

The practical application of flutter control is beyond the state of the art and cannot be regarded as more than a promising area for research at the present time. This ACT function is not likely to be applied to subsonic CTOL transport designs of the 1980's. The present state of flutter control technology is such that basic research questions remain to be answered. Some of these research questions are:

- How should structure and aerodynamics be modeled in order to make control requirements clear?
- What are the control effectiveness characteristics of control surfaces which are practical for flutter control?
- How may the capability of given actuators and control surfaces for flutter control be assessed?
- How must control capability be distributed over the airframe for the purpose of flutter control?
- What are the generic forms of flutter control laws which display suitable insensitivity to flight condition and location on the aircraft?
- How should the trade-off of inherent structural properties for control augmentation be made?

While it is possible that flutter control may be demonstrated before these questions are answered, it is unlikely that significant, generally applicable knowledge will be obtained from such ad hoc solutions.

## 2.6 ENVELOPE LIMITING

Envelope limiting refers to those functions in an active control system that prevent or discourage operation of the aircraft outside its design envelope.

Envelope limiting is a technique for coping with the technical fact that all capabilities of an aircraft are not consistent at a given operating point. For example, in a fully powered elevator system, nose gear unstick at maximum take-off gross weight and forward center of gravity might set the elevator trailing-edge-up authority limit. However, at subsonic cruise, this same elevator authority (if not further limited by some means) would be more than adequate to allow the wings to be torn from the aircraft in the very literal sense if the elevator were to be suddenly driven to this trailing-edge-up limit. In this case, the inconsistencies in aircraft capability are between structural strength, load factor capability, stick force per g, and perhaps other factors. This classic illustration of the need for envelope limiting has a fairly standard solution in the artificial feel system. The artificial feel system provides "stick force per g," which means that the pilot must exert force on the stick or column which is proportional to the incremental load factor. The limitation is imposed in this case by pilot strength limitations: the pilot-applied forces required to reach high load factors are so high that they are not likely to be inadvertently applied.

There are more positive forms of load-factor limiting which are automatic system functions. Their mechanization might be equivalent to the form shown in figure 4.

One can see that if the sum ( $\delta_{COL} + kn_z$ ) exceeds the limit  $k(n_z)$  limit, the value of  $n_z$  is automatically commanded to  $(n_z)$  limit. An alternative, but less desirable, mechanization might be equivalent to the form shown in figure 5. The gain,  $k$ , tends to be larger in the latter case than in the former. High gain is required to negate the  $\delta_{COL}$  inputs if the threshold is exceeded. When  $k(n_z)$  limit is exceeded, a high gain feedback of  $n_z$  is applied to the elevator to reduce the load factor to  $(n_z)$  limit. The high gain causes undesirable suddenness in response and quite possibly large tail loads when the threshold is exceeded. Furthermore, if the mechanization is by means of a parallel servo wherein the pilot's column is driven by the feedback, a variety of pilot-induced oscillation\* can result if the pilot opposes the column motion.

Some examples of positive automatic envelope limiting cited for the panel were the B-58 g-limiting system, F-104 g-limiting system, the General Dynamics light-weight fighter g- and  $\alpha$ -limiting systems. Furthermore, virtually all automatic approach couplers have heading, bank angle, roll rate, and pitch attitude limiting.\*\* There also is a body of current opinion which holds that positive automatic limiting of angle of attack, pitch rate, airspeed, and longitudinal acceleration in some combination could be used to prevent overspeed conditions in connection with upsets.

Implementation of envelope limiting by means of artificial feel forces has greater versatility than positive automatic limiting. This arises because the pilot, by means of extreme effort, can induce loads beyond the ultimate when extreme emergency circumstances warrant. Ten known upset cases wherein the aircraft exceeded ultimate load during recovery and landed safely emphasize the importance of this versatility. Artificial feel forces have a long history of successful application for aircraft with fully powered controls and for aircraft operating through the transonic regime.

Other forms of envelope limiting are also useful. The DC-8, 747, and possibly other modern transports have automatic flap retraction with increasing airspeed. The 747 and DC-9 have rudder surface stops which are programmed with airspeed and flap setting. The L-1011 has a programmed variation with airspeed in the number of rudder segments which are used for control. Envelope limiting is also an inherent part of any power-actuation system, primarily because of authority limits in the low-frequency regime and because of rate limiting in the high-frequency regime.

It is important to note, however, that the nature of envelope limiting is to provide a means for complying with requirements such as structural criteria. Envelope limiting does not result in any new structural criteria because its function is to artificially reduce the excessive capabilities of the aircraft to a level commensurate with the least capability of the aircraft at a given operating point.

---

\* For example, this phenomenon occurs in connection with the F-104 g-limiting system.

\*\* This envelope limiting in approach couplers satisfies pilot acceptance limitations rather than aerodynamic or load limitations.

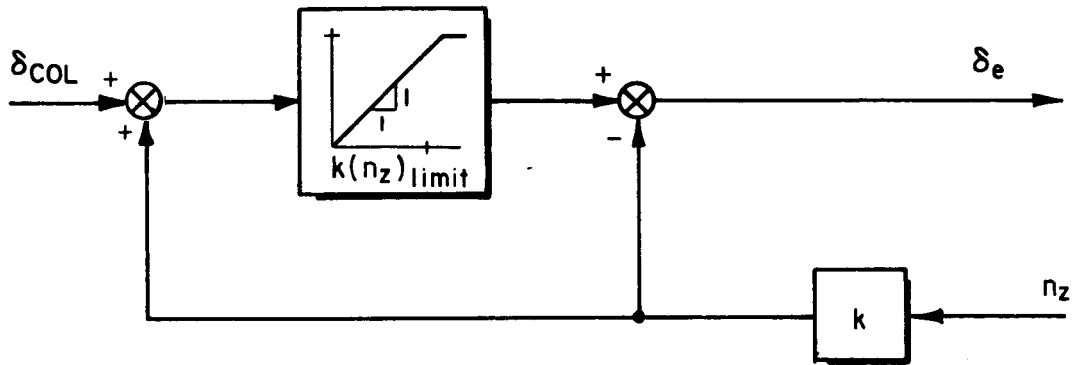


Figure 4. — A Form of Positive Automatic Load Factor Limiting

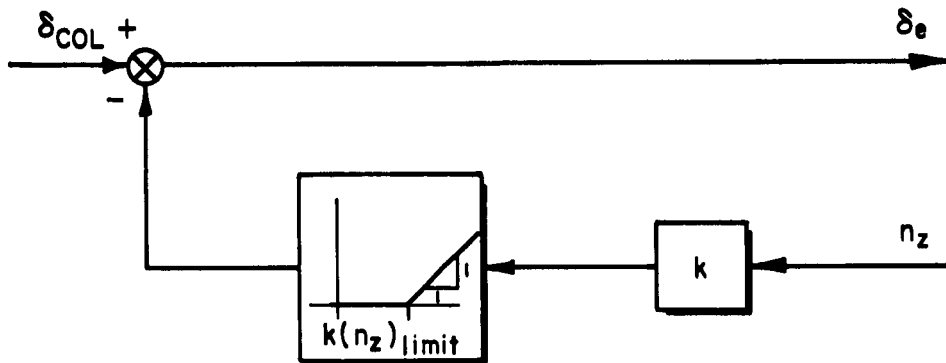


Figure 5. — An Alternate Form of Positive Automatic Load Factor Limiting

The general principles involved in envelope limiting by either pilot strength limitations or by positive automatic means are presently well understood. For use in active control technology systems, these general principles can be applied in more sophisticated ways. That is, force levels in artificial feel system can be more complex functions of variables which are more closely indicative of critical load factor effects (e.g., wing root bending moment) rather than of load factor alone. Similarly, in the case of positive automatic limiting, the limit levels can be functions of variables which more closely define the critical loadings. Future research on envelope limiting should address the effective use of computed air data and the flexibility of airborne digital computation to produce more finely tailored limiting functions and to implement more sophisticated limiting functions. The need for these will arise in connection with the possible unique aerodynamics, structural load, safety or pilot acceptance limitations of advanced aircraft.

## 2.7 PILOT INTERFACE WITH ACT SYSTEMS

The pilot interface with ACT systems involves two major areas: pilot acceptance of and operation of ACT systems, and loading conditions which may be pilot induced because of novel ACT system features. The pilot interface is a configuration design consideration and not a function of the ACT system. It provides the means for managing ACT system operation and the means for direct manual control of the aircraft.

ACT system acceptance requires provision of satisfactory handling qualities, workload levels, confidence and manageability. Handling qualities requirements, in the traditional sense (e.g., short-period damping and frequency requirements) may be inappropriate for application to ACT systems as has been stated previously. This is because ACT systems may introduce additional modes in which there is significant response. When this is the case, it will be necessary to appeal to more fundamental requirements such as the crossover model concept (ref. 33) or an equivalent embodiment of that concept such as is given in references 34 to 36, for example. Appropriate artificial feel forces are an important aspect of aircraft handling qualities. Greater computation capability available with ACT systems will make more finely tailored feel force functions possible, as mentioned in the previous subsection. Feel forces should also be tailored to discourage operation of the aircraft outside its design envelope. Automatic envelope limiting used for this purpose must be designed to operate in a way which makes the artificially imposed limits appear as inherent aircraft limits to the pilot.

Pilot confidence in status must be retained at least at current levels. This means that unusually rapid or large changes in linear and angular accelerations must be avoided in ACT systems as they are in current automatic systems. Furthermore, ACT system inputs to the controls must be made by means of a series of servo configuration so the pilot is not so keenly aware of their presence by virtue of motion of his cockpit controls. The need for this in connection with load distribution control and flutter control is self-evident. With relaxed inherent stability, the pitching-moment control-surface deflection required at low frequencies is reversed with respect to normal control-surface deflection if the unaugmented maneuver margin is negative. It is undesirable to reflect this reversed control-surface deflection in the cockpit controls. Even when

the unaugmented maneuver margin is positive, nearly zero, the situation tends to be undesirable because the low-frequency control column displacements from trim are greatly attenuated. This degrades the pilot's sense of pitch-attitude confirmation via control-column displacement. Static control-column forces must result in a stable force-per-knot gradient regardless of maneuver margin. This is presently required by 25.173 and 25.175 of reference 2.

Other aspects of pilot confidence arise in connection with control system reliability. The matter is not so much the ACT system reliability itself, which must be assumed to be at a level appropriate to the criticality for safety of its various functions, but rather it is the aspect of ACT system management in the face of a failure which degrades performance or capability. Appropriate failure mode annunciation and non-flight critical disconnect features are essential. Even with sophisticated redundancy, there is a level of failure degradation which requires the crew to make decisions concerning appropriate action, e.g., retreat to a more restricted flight envelope, reconfigure aircraft, and so on. These management tasks can cause considerable increase in cockpit workload peaks.

The consequences of increased workload peaks can be increased levels of pilot-induced loads through greater intermittancy in attention to the primary control task, and decreases in aircrew reliability, which can result in improper procedure or operation.

This situation can be further aggravated by the fact that the really crucial emergency situations wherein pilot take-over can have potentially good effect, will perhaps tend to occur less frequently, but the degradations in handling qualities will perhaps also be more severe. These factors both tend to make the transition from normal to degraded operation more difficult. It has been suggested in the "graceful degradation hypothesis" (ref. 37) that the augmentation used in the normal mode be such that the difference in handling qualities with respect to the degraded mode is the minimum which results in acceptable normal operation. This is hypothesized to render the transitions less demanding. The loads, one suspects, would tend to be greater for normal operation, but less in the course of transition to degraded operation.

Loading conditions which may be pilot induced may be more numerous and varied than in current transport aircraft. However, much more can be done within the ACT framework toward achieving a closer match between the pilot's capability to induce loads and the airframe's ability to withstand loads than is done in current practice. This is possible mainly through the increased level of automatic system complexity which will be acceptable for ACT applications. This increased complexity may be used to implement more sophisticated automatic limiting systems and more sophisticated artificial feel systems.

Automatic limiting systems can be used in effect to preserve control authority for the innermost control loops. These loops are the most crucial for providing the augmentation required in the presence of relaxed inherent stability. At the same time, automatic limiting systems can control the variables of the outer loops to safe and adequate values. In turn, the loads applied to the airframe will also be controlled. The particular details and considerations for this have been discussed previously in connection with envelope limiting.

Under certain emergency circumstances it is essential that the pilot be able to exert virutally full control authority. However, it must be extremely unlikely that this authority would be exercised inadvertently. Therefore, the artificial feel forces should be tailored in ways consistent with pilot strength limitations and the ultimate loads which the airframe can withstand. Again, the particular details and considerations for this have been discussed previously in connection with envelope limiting.

The principles which must be observed when developing the pilot's interface with the ACT system are the same as those which must be observed when conventional flight control systems are involved. These are outlined in Appendix D of reference 2 and in reference 38, for example. The relatively few quantitative techniques available such as are used for handling qualities analysis and work-load analysis are rather fully developed. The process of developing the pilot's interface with any automatic system is traditionally evolved through mockups and simulated operation. Pilot comments and engineering judgments provide the basis for optimizing the intérface. This procedure will continue to be used for ACT systems.

Section 3  
DESIGN CONSIDERATIONS IN APPLYING ACT TO  
SUBSONIC CTOL TRANSPORT AIRCRAFT

There are four key elements in bringing ACT to the point of commercial application in the 1980's:

- Projected risk in applying ACT functions
- Limitations upon ACT applications that may be imposed by regulations
- Availability of proven design criteria
- Availability of proven design practices to guide the combined application of ACT functions

These four elements are considered in turn in the following subsections.

### 3.1 PROJECTED RISK IN APPLYING ACT FUNCTIONS

Risk itself must be examined from three viewpoints for each ACT function:

- Basic dependence of safety upon the ACT function
- Means available for modifying risks presented by failures in the ACT function implementation
- Economic risk to manufacturer presented by dependency upon the ACT function

The rapidity with which system life or safety degrades following the loss of each ACT function is used to assess the basic dependency upon that ACT function (table 1). The horizontal bars in this table span the extremes which may be expected in the rapidity with which system life or safety degrades following loss of each ACT function. Points characterizing particular applications will lie between the extremes according to the degree of conservatism in the application. (The more conservative applications tend toward the right hand ends of the bars.) The dashed vertical line indicates the current state of the art. As the art advances this line will move toward the left. Interestingly enough, the state of the art seems to progress evenly for each ACT function according to the rapidity of degradation measure. This trend suggests an appropriate emphasis for applying each ACT function. Specifically, relaxed inherent stability, maneuver and gust load control, ride quality control, envelope limiting, c.g. control, and fatigue damage control are ready for application if needed. Flutter control is not ready.

In table 1, those horizontal bars which have segments in the same vertical columns also happen to indicate those ACT functions which when used in combination tend to produce synergistically favorable results. The appropriate degree of conservatism which should characterize the application of each function might also be inferred as explained previously.

TABLE 1. - RAPIDITY WITH WHICH SYSTEM IS COMPROMISED AFTER LOSS OF AN ACT FUNCTION

FUNCTION	RAPIDITY OF COMPROMISE RESULTING FROM LOSS OF ACT FUNCTION Safety of Moment    Safety of Flight    Life of Aircraft    Life of Fleet	COMMENTS
Relaxed Inherent Stability Augmentation		Pilot takeover if failure occurs at altitude; c.g. man-agement may assist in unaug-mented landing
Maneuver		Safety or economic aspects are critical according to degree of reliance upon ACT function
Load Control		
Flutter Control		Economic aspect is critical
Ride Quality Control		Whether or not aircraft loss occurs depends upon aircraft flight condition when failure occurs
Envelope Limiting		Critical only if ride degrada-tion interferes with crew per-formance
C.G. Control		

CURRENT STATE-OF-THE-ART

DECREASING SAFETY CRITICALITY

The criticality of safety considerations tends to be paramount at the left side of table 1 and diminished at the right side, where economic considerations tend to predominate.

An assessment of situation severity and a list of means available for modifying risks presented by failures in ACT functions is given in table 2. There are three principal means for modifying the risk:

- Control system redundancy
- Actuation and/or surface authority distributions
- Reduced operating envelope

Provision of a gracefully degrading system and use of c.g. management apply only for relatively conservative applications of the relaxed inherent stability augmentation function. None of these means for modifying the failure risk are new in commercial air transport operation. What will be unprecedented, however, is the degree of automation employed in failure detection, analysis, and reduced operating capability assessment.

TABLE 2. - DEGRADED SITUATION SEVERITY AND MEANS AVAILABLE FOR MODIFYING RISKS PRESENTED BY FAILURES

FUNCTION	SEVERITY OF SITUATION WITH FUNCTION DEGRADATION	MEANS AVAILABLE FOR MODIFYING RISKS PRESENTED BY FAILURES
Relaxed Inherent Stability Augmentation	Moderate-Very	Redundancy + Authority distribution Reduced operating envelope Gracefully degrading system CG management
Maneuver	Negligible-Moderate	Redundancy + Authority distribution Reduced operating envelope
Load Control Gust	Negligible-Moderate*	Redundancy + Authority distribution Reduced operating envelope
Fatigue Damage	Negligible	Reduced operating envelope
Flutter Control	Very-Extreme	Redundancy + Authority distribution Reduced operating envelope
Ride Quality Control	Negligible-Very	Redundancy + Authority distribution Reduced operating envelope
Envelope Limiting	Negligible-Moderate	Redundancy Reduced operating envelope
CG Control	Negligible	Reduced operating envelope

\*When damping of structural modes is involved, the risk of failure of malfunction would be moderate-very.

Control authority will tend to be distributed to a much greater extent. If first and second failures (assuming dissimilar failures) are to result in fair operational status, then at least three-channel redundancy through the point of actuation is required. For ACT functions such as maneuver and gust load control, which require distributed control forces over the airframe, the control surfaces must be split so that jamming of one surface, for example, will not require disabling of the control functions for which distributed control forces are essential.

Reduced operating envelopes may be varied according to which specific components have failed; and once selected, the reduced envelope may be automatically enforced by the envelope-limiting ACT function itself. For example, failures which affect the available hinge moment, the available stroke, or merely the number of channels remaining, all imply potentially different reduced operating envelopes.

The third area of criticality, economic risk to the manufacturer presented by dependency upon an ACT function, must be balanced against the risk of being less competitive in the marketplace because of its omission. Decisions involving this area of criticality tend to be made at a time when little if any actual performance data and little knowledge of the ultimate competitive position are in hand. For this reason, new designs tend to evolve as modest extrapolations of the previous successful design. This practice tends to minimize dependence upon paper estimates of performance while allowing a small amount of innovation. The following points represent the interpretation of this conventional wisdom in the context of guidelines for commercial ACT application.

- A potential aircraft configuration should be examined to identify critical areas which might benefit from ACT application
- Payoff from ACT application must be evaluated carefully to determine that it is clearly significant. "Carefully" virtually excludes concepts that are not completely developed which might incur large costs in design and verification
- The ACT application must be cost effective. The payoff, in quantitative terms, must dominate the quantitative estimates of risks in the areas of safety, reliability, maintainability, and inadequate performance presented by the application

In light of the above guidelines, recent past flight research experience and recent applications for military aircraft are good indicators of those new technology areas which are ready to be considered for commercial application. The state of research in other, more novel, technology areas can, by similar reasoning, be the basis for estimating when these technology areas may be ready for consideration in commercial applications. Table 3 gives a partial list of ACT function applications in research or research and development programs involving specific aircraft. Generally, higher states of readiness for the various ACT functions are indicated by the length of the horizontal bars and the number of different aircraft receiving application.



### 3.2 POTENTIAL REGULATORY LIMITATIONS UPON ACT APPLICATIONS

Existing Federal Airworthiness Regulations (FARs) in Part 25 (ref. 2) do not place many significant constraints on the application of ACT. Those constraints which are imposed tend to be of the following kinds, as will be appreciated from the detailed review which follows.

- Interpretations of the fundamental regulation intent were not made in a context which included ACT
- Practical considerations for demonstrating compliance sometimes require arbitrary maneuvers, tests, or environments which have no counterparts in normal or degraded modes of operation
- The view of acceptable safe practice tends to be consistent with the current or recent past state of the art but not to the projected state of the art

Detailed examination of FAR 25 reveals many areas wherein ACT considerations can be involved and the existing regulation is adequate even in this broader context. These areas are not reported here. The following paragraphs list specific regulations by number and title and suggest reasons that additions or changes should be considered.

Existing regulations already recognize that acceptable flight characteristics for some aircraft may depend upon a stability augmentation system or upon any other automatic or power-operated system in subparagraph 25.21(e). This clearly admits ACT systems as well.

#### 3.2.1 Flight, Performance: Turbine Engine Powered Airplanes

Regulation. 25.103 Stalling Speed.

Aircraft with negative maneuver margins cannot be allowed to stall because of elevator or stabilator saturation. Requirements that are referenced to the stalling speed are then inappropriate, as pointed out in reference 3.

#### 3.2.2 Flight, Controllability and Maneuverability Regulation

Regulation. 25.143 General.

The requirements "the airplane must be safely controllable and maneuverable: [subparagraph 25.143(a)] and "it must be possible to make a smooth transition from one flight condition to any other without exceptional pilot skill, alertness" [subparagraph 25.143(b)] are pertinent to the average gradient for the stick force per knot requirement of subparagraph 25.173(c). A stable gradient of the stick force per knot curve is required only if it is possible to drive the elevator (or stabilator) to the control surface stops with a steady force or displacement of the elevator (or stabilator) cockpit control. The stable gradient, in that case, is necessary to serve as an indicator of the amount of elevator (or stabilator) control surface throw available for regulation of pitch attitude in the short-period frequency range. Inasmuch as flight-path angle is controlled via pitch attitude in this frequency range, the stable gradient is essential to safe operation in that case. If a portion of the total elevator (or stabilator) control surface throw is reserved for pitch attitude regulation in the short-period frequency range and is operated by means of pitch-command augmentation, then the stable gradient is not essential to safe operation.

For conventional aircraft having a substantial positive inherent maneuver margin (and therefore downward tail trim load), the result of inadequate stable values of stick force per knot can be a tendency for the pilot to neglect the task of close continuous control of airspeed with elevator when pitch attitude is being controlled with elevator. This is a particularly crucial combination of conditions. It is crucial because changes in airspeed with respect to trim are no longer statically related to changes in pitch attitude. Changes in airspeed,  $u$ , are usually related to changes in pitch attitude,  $\theta$ , by the transfer function

$$\frac{u}{\theta} = \frac{g}{s + 1/T_{\theta_1}}$$

$$1/T_{\theta_1} = X_u + X_w (M_{\delta_e} Z_u - Z_{\delta_e} M_u) / (M_{\delta_e} Z_w - Z_{\delta_e} M_w)$$

when pitch attitude is closely controlled with the elevator. As  $1/T_{\theta_1}$  tends to zero, the stick-force-per-knot gradient tends to zero. If the stick-force-per-knot gradient is zero, the change in airspeed is proportional to the integral of the change in pitch attitude and not merely proportional to the change in pitch attitude. This situation demands that airspeed be continuously controlled with the elevator. This is an unusual piloting technique which is somewhat undesirable because of the increased attention it requires, but it is a practical and feasible technique nevertheless. Changes in pitch attitude (e.g., changes in power setting) require greater piloting skill in this special case than in the ordinary case.

An additional consideration in ACT applications, where relaxed inherent stability may entail operation of aircraft with negative inherent maneuver margin (and therefore an upward tail trim load), is that the result of reaching the elevator (or stabilator) trailing-edge-down stop can be an uncontrollable pitch-up maneuver which has very dangerous stall implications. A stable stick-force-per-knot gradient provides an indication that the elevator (or stabilator) is approaching the trailing-edge-down stop, and in so doing warns the pilot that pitch-up may be imminent.

The existing specification of a minimum average gradient of the stable stick-force-per-knot curve even when essential to safe operation is inappropriate. The existing average gradient specification of a minimum of 4.448 newtons (1 pound) for each 6 knots is so small as to be appropriate only for high-speed, high-altitude flight conditions. Larger minimum values are appropriate to low-speed, low-altitude flight conditions since the classical stick-force-per-knot gradient varies inversely as the trim airspeed.

Changes to the wording of subparagraphs 25.143(a) and (b) seem unnecessary. However, those paragraphs occasionally imply requirements more stringent than already exist in subparagraphs 25.173(b) through (d).

#### Regulation. 25.145 Longitudinal control

Aircraft with negative maneuver margins cannot be allowed to stall because of elevator or stabilator control saturation. Requirements referenced to stall speed are then inappropriate, as pointed out in reference 3. In addition, paragraph 25.145 may not provide for sufficient maneuvering capability.

### 3.2.3 Flight, Trim

#### Regulation. 25.161 Trim.

The interpretation of trim which is appropriate here is that a given combination of power setting and elevator, stabilizer, or stabilator trim setting should produce unique and stable trimmed values of pitch attitude and airspeed. If the stick-force-per-knot gradient is zero (or very small), airspeed requires continuous control if pitch attitude is being controlled. This situation is inimical to safe operation only if uncontrollable pitch-up maneuvers can occur. Such maneuvers can occur, for example, when the inherent maneuver margin of the airplane is negative and the elevator can reach its trailing-edge-down stop. The reasons for this are discussed in depth in connection with subparagraph 25.143.

### 3.2.4 Flight, Stability

#### Regulation. 25.171 General.

The sentence, "In addition, suitable stability and control feel (static stability) is required in any condition normally encountered in service, if flight tests show it is necessary for safe operation," must be interpreted in the light of the discussion accompanying subparagraph 25.143.

Changes in the wording of this regulation seem unnecessary, but broader interpretation may be required.

#### Regulation. 25.173 Static longitudinal stability.

Paragraphs 25.173(b) through (d) dictate design and should be reconsidered. Paragraph 25.171 and subparagraph 25.173(a) already make adequate provision for a stable static longitudinal force-feel gradient when this is essential to safety.

#### Regulation. 25.175 Demonstration of static longitudinal stability.

Static longitudinal stability demonstrations should be contingent upon the requirement for static longitudinal stability as discussed in connection with paragraphs 25.171 and 25.173. Minimum demonstrated speed should be an allowable alternative to  $V_{s1}$ .

#### Regulation. 25.177 Static directional and lateral stability.

The requirement of 25.177 for "the rudder free" dictates design and should be reconsidered in terms of "rudder control free."

#### Regulation. 25.181 Dynamic longitudinal, directional, and lateral stability.

Additional requirements upon the stability of modes of motion at higher and lower frequencies than the short-period attitude mode frequencies should be stated. The special conditions of reference 4 may be appropriate.

### 3.2.5 Flight, Stalls

#### Regulation. 25.201 Stall demonstration.

Demonstration of stall is not appropriate for aircraft which will not normally be operated near stalling speed. An alternative requirement has been proposed for these cases in reference 3. It requires a demonstration of the minimum flight speed or the maximum angle of attack.

Regulation. 25.203 Stall characteristics.

Refer to discussion for 25.201.

Regulation. 25.205 Stalls: Critical engine inoperative.

Refer to discussion for 25.201.

### 3.2.6 Structure, General

Regulation. 25.301 Loads.

Present regulations do not specifically require consideration of dynamic control loads appropriate to the stability of the airplane. These loadings must be provided for especially when the airplane is inherently unstable as may be the case when ACT is applied. Furthermore, loads resulting from stability augmentation system and automatic flight control system failures require consideration.

### 3.2.7 Structure, Flight Maneuver and Gust Conditions

Regulation. 25.351 General.

The maneuver described in 25.331(c)(1) has no counterpart in normal or emergency aircraft operation. It therefore dictates design and should be reconsidered. The benefits to be derived from ACT may be compromised by this requirement.

Regulation. 25.337 Limit maneuvering load factors.

Use of word "impossible" in 25.337(d) is inappropriate. Furthermore, it tends to unnecessarily restrict application of envelope limiting.

Regulation. 25.341 Gust loads.

Paragraph 25.341 may penalize ACT designs. It should also permit use of probabilistic design techniques such as a mission analysis or design envelope analysis of combined longitudinal maneuver, control, and gust-induced loading (refer to pp. 47-50 of reference 3). Requirements in the form of the maximum expected number of exceedences per hour of the limit load and ultimate load levels which are permissible should be stated. Values on the order of  $2 \times 10^{-5}$  exceedences of the limit load level per hour and  $10^{-7}$  exceedences of the ultimate load level per hour are suggested.

Regulation. 25.349 Rolling conditions.

Aileron deflections rather than aileron control deflections are specified. This regulation therefore dictates design and should be reconsidered.

The effects of unsymmetrical gusts should be determined in connection with the revision suggested for 25.351(b).

Regulation. 25.351 Yawing conditions.

In subparagraph 25.351(a), rudder deflection may be limited by means other than the control-surface stops or a 300-pound rudder pedal force. This regulation therefore may limit ACT design unnecessarily and should be reconsidered.

Paragraph 25.351(b) may restrict ACT designs unnecessarily. Requirements should be based only on probabilistic design techniques such as a mission analysis or design envelope analysis of combined lateral-directional maneuvers, and control- and gust-induced loading (refer to pp. 47-50 of reference 3). Requirements in the form of the maximum expected number of exceedences per

hour of the limit load and ultimate load levels which are permissible should be stated. Values on the order of  $2 \times 10^{-5}$  exceedences of the limit load level per hour and  $10^{-7}$  exceedences of the ultimate load level are suggested.

### 3.2.8 Structure, Control Surface and System Loads

Regulations. 25.397 Control system loads.

The existing regulation does not seem to cover all possible sources of control system loading in the context of artificial feel and power-boosted or fully powered control and control-surface actuation systems. However, provision for these systems seems implicit in the last sentence of paragraph 25.397(b).

### 3.2.9 Structure, Ground Loads

Regulation. 25.473 Ground load conditions and assumptions.

Subparagraph 25.473(b) potentially permits reduction in design limit descent velocity such as might be obtained with a highly reliable (ground-based and airborne) automatic landing system.

### 3.2.10 Structure, Fatigue Evaluation

Regulation. 25.571 Fatigue evaluation of flight structure.

Subparagraph 25.571(b)(1)(i) should specifically state that the typical loading spectrum expected in service includes loadings imposed by the control system and loadings encountered during periods when the control system is inoperative unless such periods are extremely improbable.

Subparagraph 25.571(c)(2) should be replaced by a requirement for probabilistic design techniques similar to those recommended in connection with paragraphs 25.341 and 25.351(b). The maximum expected number of exceedences per hour of the ultimate load level resulting after fatigue failure or obvious partial failure of a single principal structural element should be less than a frequency on the order of  $2 \times 10^{-5}$  per hour.

### 3.2.11 Design and Construction, General

Regulation. 25.629 Flutter, deformation, and fail-safe criteria.

Paragraph 25.629(d) does not in any way inhibit application of flutter control systems. However, it is not clear that the prospect of flutter control was considered. The provision in subparagraph 25.629(d)(4)(vi) governing the consequences of control-system failure should be revised so that it is appropriate for control systems having high redundancy. It will then be appropriate for systems incorporating flutter control systems as well.

### 3.2.12 Design and Construction, Control Systems

Regulation. 25.671 General.

Satisfaction of the paragraph 25.671(d) requirement would seem to require considerable ingenuity of ACT system designers when those systems are flight-critical. However, the requirement nevertheless seems to serve safety in a significant way. It therefore should apply to ACT systems even though substantial design limitations are implied.

Changes in the wording of this regulation seem unnecessary, but broader interpretation may be required.

Regulation. 25.672 Stability augmentation and automatic power-operated systems.

In subparagraph 25.672(b), the capability to initially counteract failures is necessary only when those failures are not extremely improbable. Consequently this subparagraph contains requirements inappropriate for highly redundant systems.

The reference to "any single failure" in subparagraph 25.672(c) is inappropriate in the context of systems having high redundancy. For such systems, critical situations should include any single failure or combination of failures which is not extremely improbable and which results in degraded controllability or maneuverability.

### 3.2.13 Equipment, General

Regulation. 25.1309 Equipment systems and installations.

Combinations of failures which are not extremely improbable, and which are not readily counteracted by the crew, are not specifically mentioned in subparagraph 25.1309(b)(1). Such a requirement is conceivably implied, however. Possible presence of flight-critical SAS functions in ACT applications makes consideration of the addition proposed in reference 3 essential.

Subparagraph 25.1309(d)(4) does not specifically require verification that crew workload remains within an acceptable level with the addition of the fault-detection and failure-management workload increment. Reference 3 suggests rewording.

In ACT aircraft, the requirements of subparagraph 25.1309(e) seem incomplete in light of the requirements for landing with all engines inoperative [25.671(d) of reference 2]. Requirements for 5 minutes of operation VFR with normal electrical power system inoperative are difficult to fulfill for flight-critical ACT applications. It is suggested that these requirements be reconsidered.

## 3.3 DESIGN CRITERIA

This subsection summarizes the basic design criteria for structural and structural-control systems which have been identified from review of the state of the art and of the existing regulatory documents and from the assessment of criticality of ACT functions.

This subsection is organized into six topical areas:

- Loading and strength in the context of the combined structure-control system
- Flight control system characteristics
- Automatic center-of-gravity control system characteristics
- Ride quality
- Automatic envelope limiting functions
- Flutter characteristics

In the paragraphs which follow, the words "improbable" and "extremely improbable" are frequently used to indicate the expected frequency of occurrence of certain events in qualitative terms. These qualitative terms are often given specific numerical valuations for the purpose of a priori analysis. For example, an "improbable" event might be interpreted quantitatively as an event occurring

with an expected frequency of  $2 \times 10^{-5}$  per hour or less. An "extremely improbable" event might be interpreted as an event occurring with an expected frequency of  $10^{-7}$  per hour or less. "Probable" events, which receive frequent mention in reference 2, are events which are not "improbable" or "extremely improbable."

### 3.3.1 Structure Plus Control System

- A. The limit strength requirements must be met at each combination of airspeed and load factor on and within the boundaries of the representative maneuvering envelope (V-n diagram) of figure 6. This envelope must be used in determining the airplane structural operating limitations.

The selected design airspeeds are equivalent airspeeds (EAS).

Design cruising speed,  $V_C$

Design dive speed,  $V_D$

Design maneuvering speed,  $V_A$

Design flap speed,  $V_F$

Demonstrated stall speed,  $V_{S1}$  (the minimum demonstrated speed,  $V_{MIN}$ , may be used in lieu of  $V_{S1}$ )

Except where limited by maximum (static) lift coefficients, the airplane is assumed to be subjected to symmetrical maneuvers resulting in the limit maneuvering load factors prescribed in this section.

Pitching velocities appropriate to the corresponding pull-up and steady-turn maneuvers must be taken into account.

The positive limit maneuvering load factor "n" for any speed up to  $V_D$  may not be less than:

$$2.1 + \left( \frac{24\ 000}{W + 10\ 000} \right)$$

except that "n" may not be less than 2.5 and need not be greater than 3.8 — where "W" is the design maximum takeoff weight.

The negative limit maneuvering load factor —

May not be less than -1.0 at speeds up to  $V_C$ ; and

Must vary linearly with speed from the value at  $V_C$  to zero at  $V_D$ .

Maneuvering load factors lower than those specified above may be used if the airplane has design features that make exceeding these values in flight extremely improbable.

If flight-critical automatic control systems are a design feature of the airplane, they are to be assumed to be operating normally.

- B. A mission analysis or design envelope analysis of combined longitudinal maneuver, control, and gust-induced loading, and of combined lateral-directional maneuver, control, and gust-induced loading must be conducted. The maximum expected number of exceedences per hour of the limit load and ultimate load levels shall be less than  $2 \times 10^{-5}$  and  $10^{-7}$ , respectively. This analysis must be accomplished

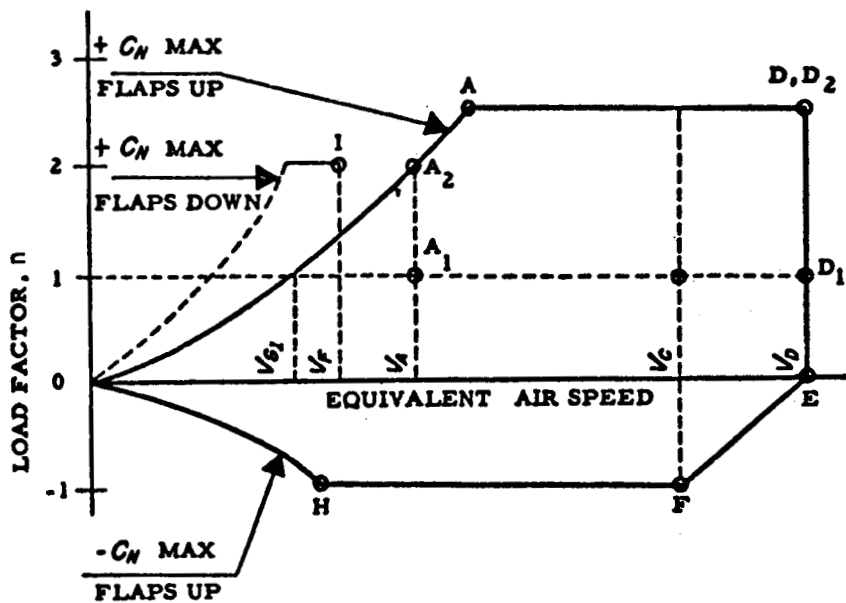


Figure 6. — Maneuvering Envelope

by application of rational probability concepts wherein the joint probability of occurrence of system failures and malfunctions and independent loading events is the basis for evaluation. This approach is necessary in order to develop a comprehensive appreciation for the total impact of control (including its failure modes) upon all facets of loading (maneuver, gust, and fatigue damage) in the context of actual system operation.

- C. If a control system operates in a substantially nonlinear way, the effects of nonlinearity must be represented in a conservative way with respect to the impact upon loads.
- D. Structural strength requirements must be insensitive to the detail features of control laws.
- E. Commitment to a specific degree of distribution of control authority and to a specific actuation bandwidth must be made at the outset for each airplane configuration in order that structural strength requirements be consistent with control capability.

### 3.3.2 Flight Control System

- A. Current technology limits the frequency range of transport aircraft motions that can be actively controlled
  - Motions at frequencies up to 3 Hz can be controlled
  - Motions at frequencies between 3 and 10 Hz will be difficult to control

- Motions at frequencies greater than 10 Hz probably cannot be controlled
- B. Dispatch reliability goals of 99% on-time within 2 years after new airplane introduction must be balanced against the number of systems required for dispatch.
- C. Provision for check-out of safety-related systems prior to flight is essential.
- D. Distribution of control force and moment generating capability over the airplane must be consistent with requirements for reliability.
- E. Distribution of control force and moment generating capability over the airplane must be consistent with controllability requirements for the modes of motion to be controlled.
- F. Augmentation systems for relaxed inherent stability must be fail-operational for all failure modes which are not extremely improbable or which cannot be readily counteracted by the pilot at every point in the normal flight envelope.
- G. Airplanes which operate at zero or negative inherent maneuver margin at any point in the normal flight envelope must have positive automatic protection against pitch-up.
- H. If a functioning control system is critical for safe flight because of the artificial stability or load protection or both which it provides, the control authority required to provide artificial stabilization and load protection must itself be protected from the authority demands for all non-flight-critical control purposes.
- I. If a functioning control system is critical for safe flight because of the artificial stability which it provides, the control authority required to provide artificial stabilization must be protected from the authority demands for all other systems and the pilot.

### 3.3.3 Automatic Center-of-Gravity Control System

- A. Automatic fuel transfer system must incorporate a positive means of disengagement.
- B. Disengagement must be such that isolation between fuel tanks is achieved in the absence of manually controlled fuel transfer.
- C. Manual control of fuel transfer must be possible after failure of the automatic transfer system.
- D. Maximum rate of fuel transfer possible under manual control must equal or exceed the maximum rate possible under automatic control.
- E. Provision must be made for manually controlled fuel jettisoning.

### 3.3.4 Ride Quality

- A. Ride quality, if not so poor as to result in infliction of injury, is a subordinate consideration with respect to those affecting flight safety.

- B. Ride quality must be sufficient to:
- Be acceptable to passengers
  - Not inhibit crew performance (refs. 39 and 40)
  - Be comparable to that for other commercial aircraft
- C. Ride quality limits for maximum acceptable rms g vibration exposure which have been applied in the aircraft industry are:
- 0.11 g for normal acceleration at any point in the passenger cabin and flight deck
  - 0.055 g for lateral acceleration at any point in the passenger cabin and flight deck

where the probability of exceeding these limits is less than or equal to  $10^{-3}$  per hour. Further guidance on the limits for maximum acceptable rms g vibration exposure in a commercial transport-like environment is provided by tables 1 and 2 of reference 41. Table 4 gives objectionable rms g levels for vertical vibration with varying spectral content. Table 2 gives similar results for lateral vibration. Figure 11 in reference 41 relates the rms vibration levels present in both vertical and lateral axes to a passenger ride acceptance criterion. The proposed International Standards Organization limits (the "Reduced Comfort Boundary" is appropriate for defining acceptable ride quality) are given in figures 6A and 6B of reference 42 for vertical and lateral (or longitudinal) vibration, respectively. These limits are given as function of exposure durations ranging from 1 minute to 8 hours. The vibration input power spectrum is that for a narrow band (1/3 of an octave) random process with center frequency as indicated on the abscissa.

- D. Ride quality limits which apply for avoidance of motion sickness are not well established. The susceptibility of motion sickness from vertical, low-frequency vibration (in the absence of other factors) is indicated in figure 1 of reference 43. Other mechanisms underlying motion sickness are discussed by Graybiel in reference 44.

### 3.3.5 Envelope Limiting

- A. If automatic envelope limiting is used to protect the airplane from loads exceeding design values, adequate provision must be made to arrest the rate at which the design envelope limits are approached so that overshoots are either eliminated or do not result in overloads.
- B. Failures of automatic envelope limiting systems must be annunciated visually and aurally in the cockpit if those systems protect the airplane from overload or instability.
- C. It is desirable that the limits of automatic envelope limiting systems be adjusted automatically in a manner consistent with identified airplane failure modes.

- D. If a hierarchy of automatic envelope limiting functions exists with respect to criticality for safe flight, then the satisfaction of the less critical automatic envelope limiting functions must be subordinated with respect to the more critical functions.

### 3.3.6 Flutter (ref. 45)

- A. The airplane must be designed to be free from flutter and divergence for all combinations of altitude and speed encompassed by  $V_D$  (or  $M_D$ ) versus altitude envelope enlarged at all points by an increase of 20 percent in equivalent airspeed at both constant Mach number and constant altitude except that Mach numbers greater than 1.0 need not be included when  $M_D$  is less than 1.0 at all design altitudes and when the following is established:
- A proper margin of damping exists at all speeds up to  $M_D$ , and
  - There is no large and rapid reduction in damping as  $M_D$  is approached
- B. The airplane must be free from flutter and divergence over its current operating envelope after any failure or malfunction of the structure or flight control system (including automatic flight control systems) which affects stability or strength and which is not extremely improbable.
- C. If the airplane depends upon a flutter control system for satisfying either of the requirements in paragraphs A and B, then a reduced operating envelope must be observed following any failure or malfunction which affects stability or strength. The reduced envelope for the failed or malfunctioning system must meet the two previous requirements.
- D. If the airplane depends upon a flutter control system for satisfying any of the requirements in paragraphs A, B, and C, the control authority required for flutter control must be protected from the authority demands for all other control purposes.

## Section 4

### RECOMMENDED DESIGN PRACTICES

Recommendations for design practice in areas involving ACT can only be tentative at most given the limited amount of design experience. Many details of ACT system design are either well understood or will come to that state in the near future as the result of ongoing research. However, the total impact that incorporation of ACT functions may have upon an aircraft configuration is currently not well understood. NASA-sponsored studies performed by major airframe companies in connection with Advanced Transport Technology have advanced the art of incorporating ACT into the aircraft configuration cycle, but only modestly. The material which follows outlines current understanding of the impact of ACT upon the aircraft configuration cycle. This is followed in turn by a more detailed discussion of the technical aspects.

#### 4.1 ACT IMPACT UPON THE CONFIGURATION CYCLE

An aircraft configuration cycle begins with a preliminary definition of basic airplane requirements which derive from its intended "mission." These requirements typically specify number of passengers (or payload weight or volume), range, speed, and definitions of the levels of technology to be employed with respect to aerodynamics, structures, and propulsion. Typically the latter three areas--aerodynamics, structures, and propulsion--include a vast number of subsidiary considerations which are only given very broad-brush treatment in the preliminary definition. One such subsidiary area is aircraft handling qualities, which in preliminary definition is considered in connection with "aerodynamics."

A specific commitment to a given level of capability in active control is required for preliminary definition. This commitment is required because lower bounds upon drag and structural stiffness and weight may be affected in a sensitive way by the potential capability available through active control. However, the details of ACT control laws and their implementation tend to have a subsidiary role with respect to both aerodynamics and structures because the aircraft configuration is much less sensitive to these details than it is to weight and specific fuel consumption.

The particular way in which provision of active control capability interacts with drag, structural stiffness, and weight must be established in quantitative terms. The interaction of active control capability with drag is quantitatively established as will be shown below. However, the interaction of active control capability with structural stiffness and weight and, indeed, the weight increments associated with the distributed control surfaces and power actuation required for structural control are not, or at least not as well, quantitatively established. These quantitative relationships must be established through research and development.

Once the preliminary definition for the aircraft configuration is established, it is turned into a preliminary configuration design for a full-scale

aircraft. The preliminary configuration design is analyzed to determine its performance parameters with respect to the defined performance parameter goals, and the sensitivity of its performance parameters with respect to the design degrees of freedom (e.g., aircraft size).

On the basis of the performance parameters, the performance parameter goals and the performance parameter sensitivities and changes required in the definition for the aircraft configuration are estimated which will bring the performance parameters toward the performance parameter goals. From this point, the "design cycle" is repeated until the performance goals are achieved.

When the performance goals are achieved, the level of detail in analysis of the full-scale aircraft design is gradually increased to verify satisfaction of the performance goals with increasing confidence.\* It is only at this point that the specific control law details for ACT functions begin to receive attention.

#### 4.2 POSSIBLE WEIGHT AND DRAG REDUCTION WITH RELAXED INHERENT STABILITY (refs. 45 to 50)

Experience indicates that the largest and most attractive economic payoff results from reducing the inherent stability requirements and incorporating a stability augmentation system of commensurate reliability.

Relaxing the inherent stability offers potential net economic performance-and-payload benefits by reducing the trim drag and reducing the weight in empennage, trim control surfaces, wing, and fuselage at the cost of relatively smaller increases in the weight of equally reliable feedback stabilization, i.e., power sources, sensors, computers, actuators, and control surfaces, including the equipment-to-gross-weight multiplication factor, which is typically greater than the structural-to-gross-weight multiplication factor of three (ref. 51). Performance improvements can be measured in terms of reduced gross weight, increased range, increased payload, higher maximum speed, and increased maneuverability, for example. Most contemporary design studies (refs. 51 and 52) have adopted the reduction in aircraft gross weight at constant payload as the primary measure of economic performance improvement rather than the increased range at constant gross weight.

The benefits of relaxed inherent stability are so important that they should be evaluated at the start of any preliminary design activity. Design studies based on an existing configuration may show only slight benefit, because the design features that affect weight and drag significantly cannot be changed easily. Takeoff gross weight reductions of at least 3 or 4 percent are possible under these circumstances. However, reduction takeoff gross weight on the order of 15 percent and drag reduction on the order of 2 or 3 percent are possible if the tail sizes can be reduced. This, in turn, may offer unit cost reductions on the order of 20 percent on a run of as few as 100 aircraft.

#### 4.3 HORIZONTAL TAIL SIZING CRITERIA

Inherent longitudinal stability may be relaxed by reducing the horizontal tail "volume," that is, the product of horizontal tail area and its moment arm

---

\*At some point in this process, it often happens that more detailed analyses fail to verify satisfaction of the performance goals. In this case, the basic aircraft configuration design must be recycled with the newly discovered performance restriction taken into account.

about the aircraft center of gravity. In the limiting case, the horizontal tail may be completely eliminated and longitudinal control then accomplished by means of elevons. There are powerful incentives both for designs with reduced horizontal tail volumes and for designs with no horizontal tail whatsoever. These incentives will be examined in this subsection along with the attendant disadvantages. This examination covers the trim drag characteristics, the short-period requirements, and the control rate and authority requirements involved. Together, these three considerations provide the basis for sizing the horizontal tail.

Appendixes A, B, and C have been provided to summarize the relevant technical details in a compact treatment not available elsewhere. Appendixes A, B, and C cover horizontal tail sizing criteria and practices with angle-of-attack stability augmentation via active control; horizontal tail sizing criteria and practices with pitch-attitude stability augmentation via active control; and trim drag, respectively.

#### 4.3.1 Trim Drag for Horizontal Tailless Designs

Under certain operating conditions, the static margin for the wing-fuselage combination can be positive. This tends to produce the most unfavorable trim drag condition. When the inherent static margin of the wing-fuselage combination is positive, the horizontal tail must provide a downward (negative lift) force to maintain balance (See Appendix C). Wing lift must be increased to make up for this negative tail lift. The resulting increase in wing drag, combined with the tail-plane drag, is the trim drag. By relaxing (i.e., reducing) the inherent static margin, the size of the tail plane and/or the length of the tail moment arm can be reduced, and in the limiting case the horizontal tail may even be eliminated, as in figure 2, provided adequate trim, stabilization, and maneuvering control authority is made available on the wing to compensate for the inevitable center of gravity shifting caused by consumables, crew, and passengers, and the inevitable neutral point shifting caused by compressibility and aeroelastic effects. Thus the parasite and induced trim drag caused by the horizontal tail can be traded for the parasite trim drag of elevons. However, the parasite trim drag of elevons is about twenty times more sensitive to the inherent static margin of the wing-fuselage combination than the induced trim drag of a horizontal tail (Appendix C). Therefore, if the greatest possible reduction in total drag is to result by eliminating the horizontal tail, more precise or perhaps automatic c.g. control as well as feedback stabilization will be necessary.

Three of the disadvantages of the horizontal tailless aircraft are:

- Difficulty in trimming pitching moments created by high-lift flaps
- The almost complete loss of inherent rotational damping in pitch
- The complete loss of the inherent rotational damping in angle attack provided by the lag in the action of the wing downwash on the horizontal tail

Approximately half of the short-period damping coefficient is lost as a result of the latter two disadvantages. Obviously, such significant loss must be recovered through feedback stabilization, utilizing automatically actuated elevons on the wing. Increased control power and authority are therefore required for the elevons.

Notwithstanding these disadvantages, the aircraft without a horizontal tail appears attractive even with a slightly negative inherent static margin, because of the following beneficial effects:

- Down (rather than up) elevon is required to trim with increasing lift coefficient,  $C_L$ ; therefore, both  $C_{L_{max}}$  and  $C_{L_{\alpha_{trim}}}$  will be larger and camber will be positive
- Increased  $C_{L_{max}}$  can be used to reduce landing speed or to reduce wing area and thereby to exchange wing weight for payload
- Increased  $C_{L_{\alpha_{trim}}}$  decreases the flight-path time constant, thereby affording some improvement in flight path control and some reduction in  $\alpha_{trim}$  for improved visibility over the nose, but probably resulting in less favorable  $I_{xz}$ -product of inertia effects on lateral stability, unless a reduction in vertical tail area also reduces  $I_{xz}$  and hence reduces the inclination between the fuselage reference line and the longitudinal principal axis commensurately
- Positive camber can increase lift-to-drag ratio and improve range.
- The supercritical airfoil is compatible with all of the foregoing beneficial effects and can provide either a higher cruise Mach number with comparable wing thickness or increased structural efficiency by increasing wing thickness with comparable cruise Mach number
- Since down elevon is required to trim, proper spanwise placement of elevons can also reduce average wing root bending moments, e.g., inboard elevons should be deflected down to shift more of the spanwise lift distribution inboard at the price of a small increase in profile drag. Reference 53 offers a method for optimizing a linear combination of drag and wing root bending moment in trimmed flight for aircraft with or without a tail plane
- For the horizontal tailless configuration, reducing wing root bending moments need not affect the magnitude of wing torsional moments, because up elevon is traded for down elevon to trim, whereas a configuration which uses the tail plane to trim must employ wing flaps to reduce root bending moment at the expense of increased torsional moments
- If the inboard elevons are deflected downward to trim and outboard elevons are deflected differentially as ailerons, there will not be as much increase in adverse aileron yaw as there would be if outboard elevons were deflected downward to trim, because the outboard section-lift coefficient and induced drag are less than otherwise
- Since down elevon is required to trim, wing contributions to dihedral effect and weather cock effect will be greater than otherwise, because both are increased by positive camber

#### 4.3.2 Trim Drag for Designs Having a Horizontal Tail

The low sensitivity of trim drag to the inherent static margin and the considerable inherent short-period damping provided by the horizontal tail offer incentives to retain the horizontal tail plane, albeit reduced in volume in accord with a set of rational criteria which are summarized in this topic. The first of these criteria is minimization of total drag in trimmed flight.

The analysis in Appendix C shows why reducing the inherent static margin can reduce the total drag in trimmed flight with a tail plane, and why there is an optimum horizontal tail volume which minimizes total drag in trimmed flight. Not included in the analysis in Appendix C is the root-mean-square (rms) drag deviation caused by variability in angle of attack and control surface displacement. The rms drag is a very real and important operational fact which does not appear to receive attention in preliminary design by current practice. The rms drag is affected not only by the partition between inherent and feedback stabilization, but also by the nonlinear variation of the pitching moment coefficient ( $C_m$ ) with lift coefficient ( $C_L$ ).

Unnecessarily large rms control authority required by reduced tail volume also results in increased gross weight and drag. The rms control authority required can be reduced by proper shaping of the  $C_m$ - $C_L$  characteristic. For inherently statically unstable  $C_m$ - $C_L$  characteristics, it is desirable that a stable break occur above the normal trim  $C_L$  range (ref. 54). This will not only inhibit catastrophic upset in case of an extremely large transient gust velocity, but also reduce rms control authority requirements and rms trim drag.

Lift coefficient alone does not uniquely determine the drag coefficient, because the drag coefficient will depend on the relative proportions of the lift coefficient contributed by the horizontal tail incidence and/or elevator angle and by the wing angle of attack. In turn, these relative proportions of lift coefficient are governed by the inherent static margin of the wing-fuselage combination and the horizontal tail volume. Reducing the inherent static margin will reduce the optimum horizontal tail volume for minimizing trim drag and so lead to correspondingly reduced drag and gross weight for constant payload. Following the conventional practice of maintaining ample inherent static margin for unaugmented manual control, a designer could also minimize overall drag. However, he would have to trade increased tail volume (and weight) for reduced incidence and/or elevator angle, so that the increased tail friction drag would tend to offset any reduction in pressure and induced tail drag thus keeping total tail drag essentially constant. The result would be a larger minimum total drag than for a relaxed inherent stability design, because the larger induced wing drag caused by the positive inherent static margin of the wing-fuselage combination is not changed.\*

Minimization of total drag in trimmed flight is a criterion for sizing the tail plane which is applicable throughout the flight profile at the relatively lower lift coefficients typical of climb and cruise. The next criterion for sizing the tail plane is the ability to trim (i.e., balance) at the high lift coefficients necessary for low-speed flight.

#### 4.3.3 Trim at High Lift Coefficients

Figure 7 illustrates typical horizontal tail sizing criteria for configurations with a tail plane as a function of the fore/aft wing location on the fuselage (or the aft/forward center-of-gravity location on the projected mean aerodynamic chord). There is an aft bound on the wing location at which a given size, moment arm, and control authority of the tail plane can trim or balance

---

\*Recall that when the inherent static margin of the wing-fuselage combination is positive, the horizontal tail must provide a downward (negative lift) force to maintain balance. Wing lift must be increased to make up for the negative tail lift which is necessary for trim.

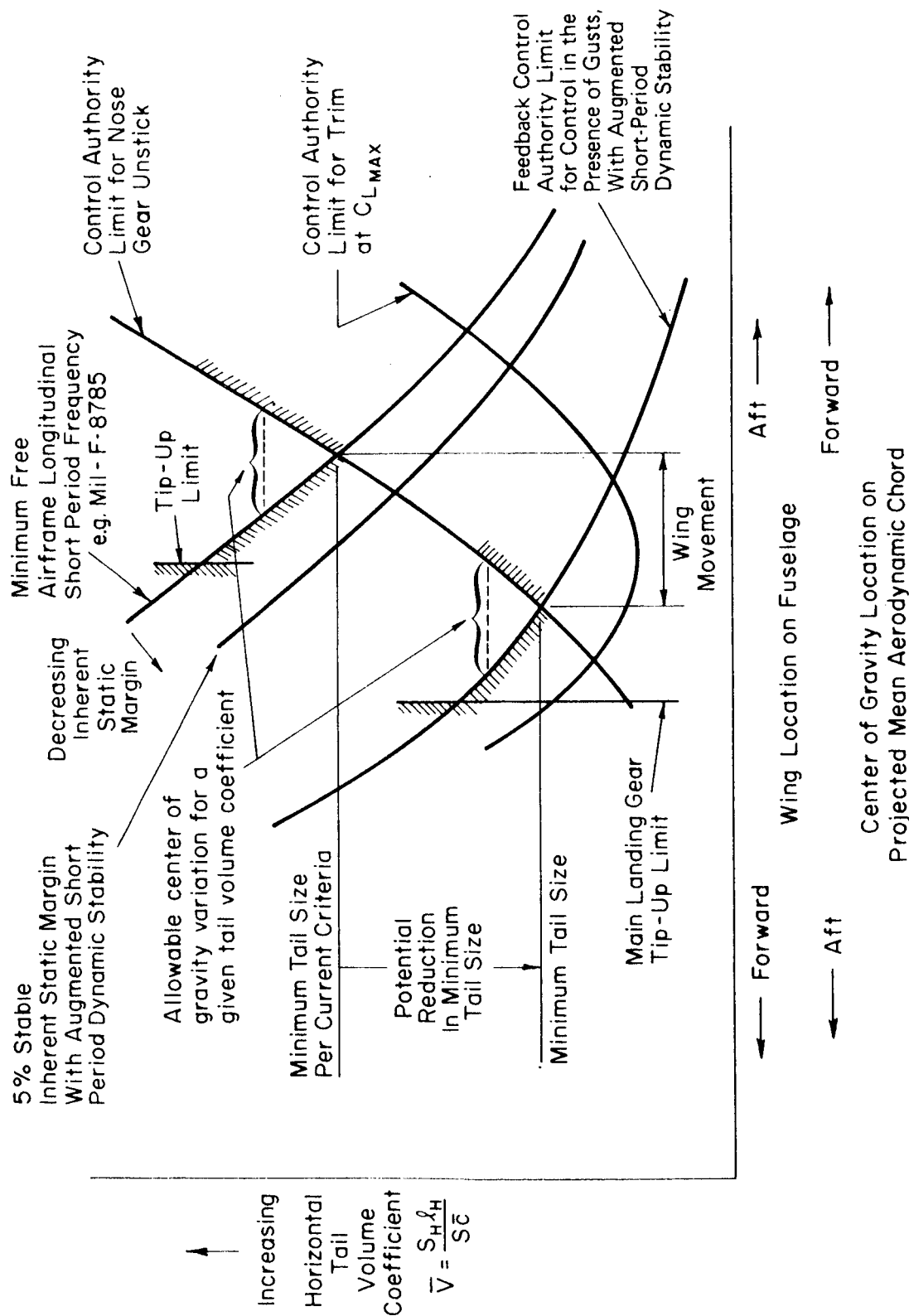


Figure 7. — Horizontal Tail Sizing Criteria

the moment from a static margin at maximum lift coefficient,  $C_{L_{max}}$ . That this is so can be shown by laying figure 8 over figure 9. Figure 8 illustrates how the wing location and horizontal tail volume coefficient,  $\bar{V}$ ,\* affect the static margin. Figure 9 illustrates the relative control authority of the tail plane which is required to trim at a given lift coefficient,  $C_L$ . The overlay of figure 8 on figure 9 shows that if the wing-body aerodynamic center\*\* is aft of the center of gravity, a constant upper bound on control authority to trim at  $C_{L_{max}}$  will force the wing location forward as  $\bar{V}$  is decreased, because the slope of the static margin with  $\bar{V}$  at constant trim authority is greater than the slope of the static margin with  $\bar{V}$  at constant wing location. Conversely, if the wing-body aerodynamic center is forward of the center of gravity, a smaller constant upper bound on control authority to trim at  $C_{L_{max}}$  will permit the wing location to retreat aft as  $\bar{V}$  is decreased, because the slope of the static margin with  $\bar{V}$  at constant trim authority is less than the slope of the static margin with  $\bar{V}$  at constant wing location. Clearly the smallest  $\bar{V}$  can be realized with the least trim authority, if the wing-body aerodynamic center is at or forward of the center of gravity.

However, there is a practical limit to the reduction in  $\bar{V}$  from a different lower bound: that on the maneuver margin. The ordinate in either figure 8 or 9 shows that the square of the short-period undamped natural frequency,  $\omega_{sp}^2$ , is approximately proportional to the static margin, if  $-C_{m_{C_L}} - C_{m_q} / 4\mu_c$ , where  $-C_{m_{C_L}}$  is the static margin,  $C_{m_q}$  is the damping-in-pitch stability derivative, and  $\mu_c = m/\rho S\bar{c}$  is the relative airplane density based on the mean aerodynamic chord,  $\bar{c}$ . (More correctly,  $\omega_{sp}^2$  is proportional to the maneuver margin as discussed in Appendix A.) As  $\bar{V}$  decreases,  $\omega_{sp}$  decreases, unless control

---

\* The product of the size and moment arm of the tail plane is customarily expressed in terms of the nondimensional horizontal tail volume coefficient,  $\bar{V} = S_H l_H / S\bar{c}$ , where  $S_H$  is the horizontal tail area,  $S$  is the wing reference area,  $l_H$  is the effective moment arm of the center of the lift of the horizontal tail with respect to the center of gravity, and  $\bar{c}$  is the mean aerodynamic chord of the wing.

\*\*The aerodynamic center is a point referred to the mean aerodynamic chord about which the pitching moment coefficient is invariant with lift coefficient.

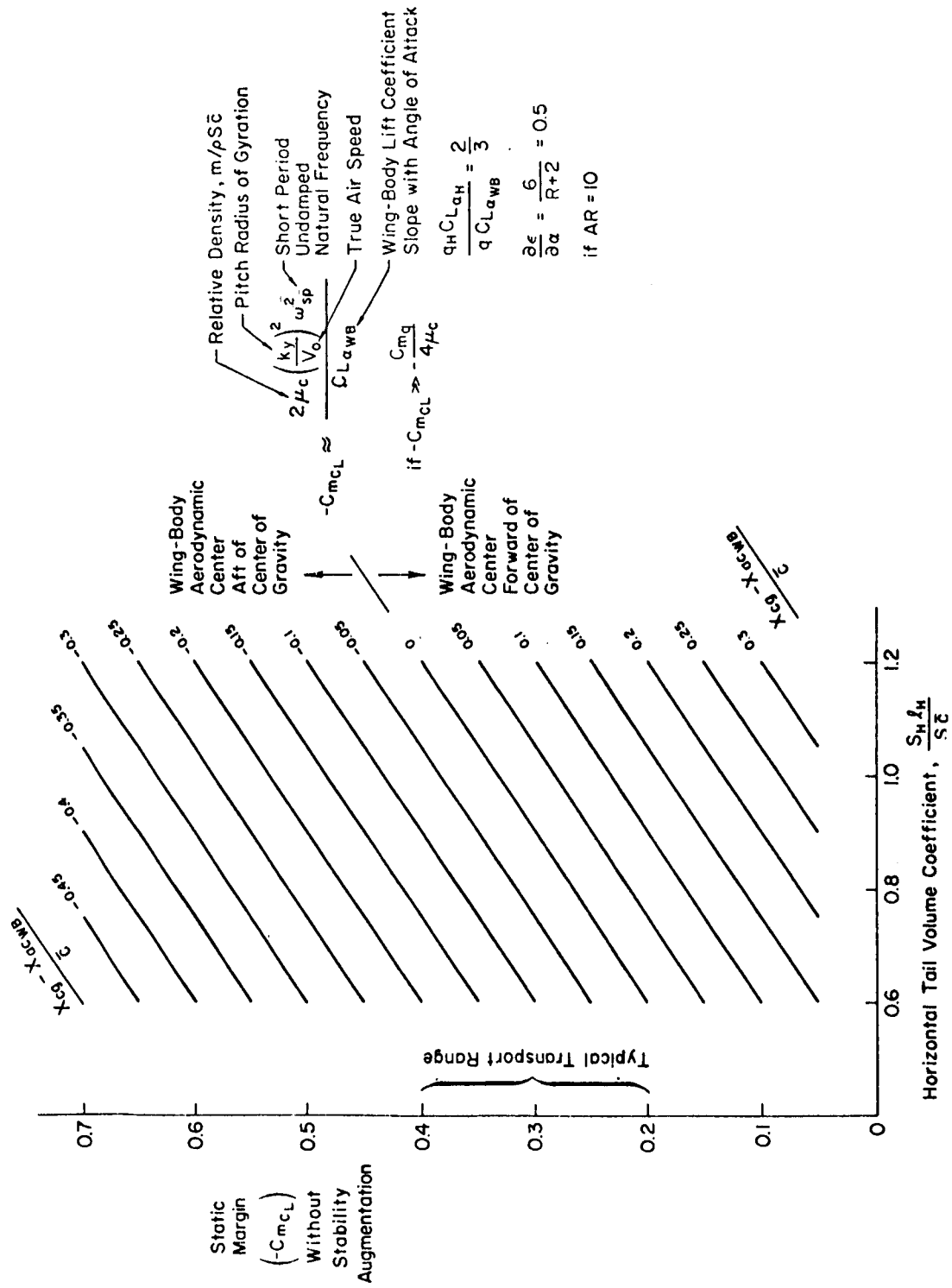


Figure 8. — Unaugmented Static Margin Versus Horizontal Tail Volume Coefficient as a Function of Location

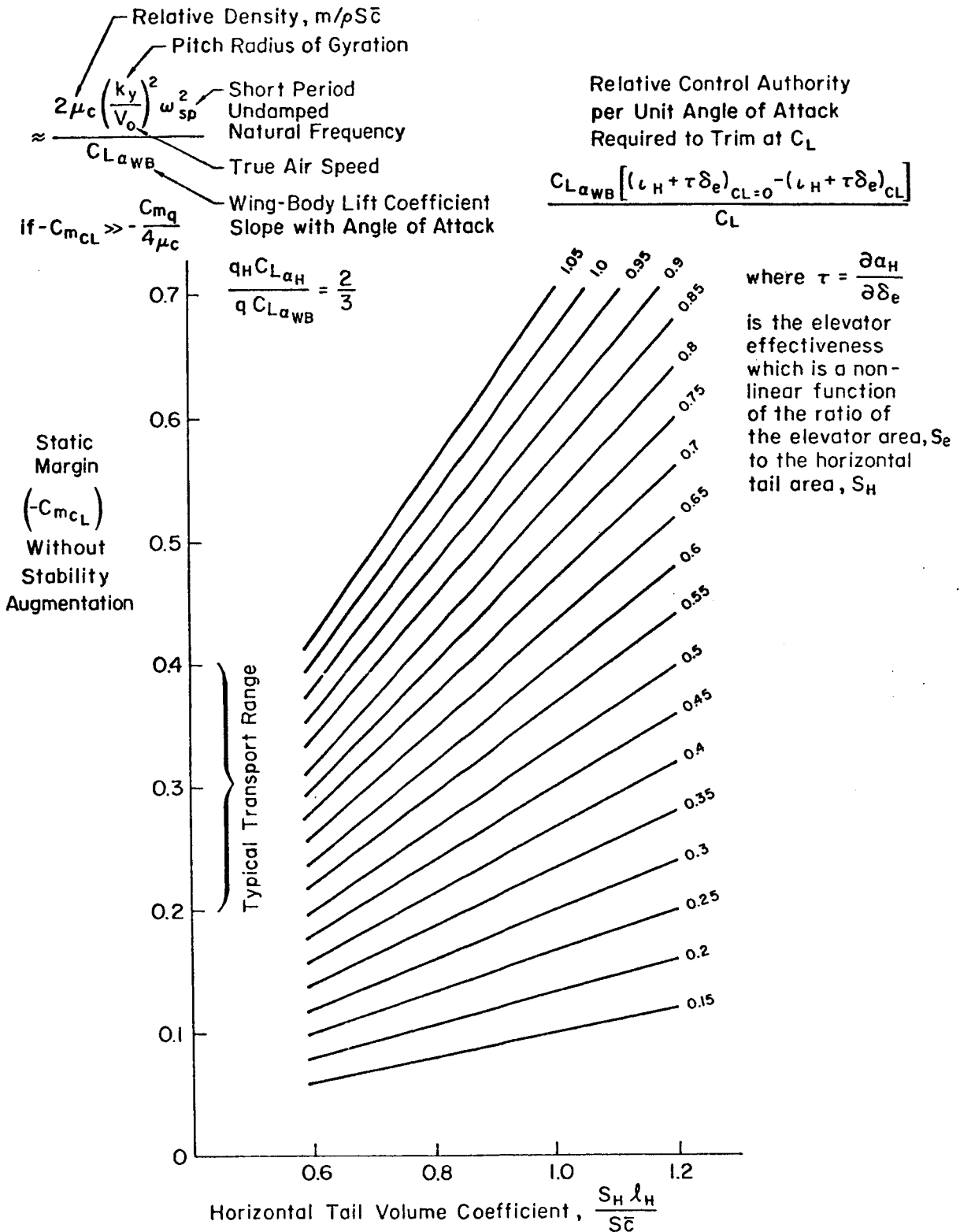


Figure 9. — Unaugmented Static Margin Versus Horizontal Tail Volume Coefficient as a Function of Relative Control Authority Required to Trim

effectiveness\* and authority are provided for augmentation of feedback stability, a subject which will be discussed in more detail subsequently. Flying- or handling-quality requirements place lower bounds on  $\omega_{sp}$  in various flight phases (e.g., ref. 38). Therefore, control effectiveness and control authority available for feedback stability augmentation ultimately determine the minimum practical  $\bar{V}$  -- usually in the power approach flight condition. Figure 7 illustrates the minimum in horizontal tail volume coefficient as a function of wing location on the fuselage for trim at  $C_{L_{max}}$  with constant control authority.

In practice, the horizontal tail volume coefficient,  $\bar{V}$ , can seldom, if ever, approach its minimum value for trim at  $C_{L_{max}}$ , because other sizing criteria intervene to constrain  $\bar{V}$ . For example, it must be possible to unstick the nose gear at rotation speed in the takeoff roll, and it must be possible to rotate nose-up in ground effect to flare and to maintain the touchdown attitude prior to landing, yet the center of gravity cannot transgress the aft tip-up limit imposed by the location of the main landing gear.

Figure 7 illustrates the nose gear unstick constraint with constant control authority and the tip-up limit. However, these are not the only constraints on sizing criteria, because, as noted above, a reduction in horizontal tail volume coefficient will cause a reduction in longitudinal stability and a deterioration in longitudinal maneuvering characteristics, if both stability and control are not otherwise augmented by feedback control having sufficient actuation power and authority.

#### 4.3.4 Short-Period Stability

Constraints on longitudinal stability and control can be characterized in terms of longitudinal short-period dynamic properties, such as undamped natural frequency,  $\omega_{sp}$ , damping ratio,  $\zeta_{sp}$ , and the larger inverse time constant,  $1/T_{\theta 2} \doteq \rho S U_0 C_{L\alpha} / 2m$ , in the numerator of the pitching response to pitching control displacement. ( $T_{\theta 2}$  is also called the "flight path time constant" in response to a change in trimmed pitch attitude, and  $1/T_{\theta 2}$  closely approximates the short-period response ratio of the time rate of change of flight path angle to a change in angle of attack from its trimmed value; the flight-path-angle deviation resulting from a gust-induced angle of attack is also proportional to  $1/T_{\theta 2}$ .) Obviously the inverse time constant,  $1/T_{\theta 2}$ , is composed of factors determined largely, if not entirely, by airplane

---

\*Control effectiveness here means precisely the dimensional partial derivative  $M_\delta = (1/I_y) (\partial M / \partial \delta)$  in units of rotational acceleration/angle, e.g.,  $1/\text{sec}^2\text{-rad}$ , where  $M$  is the pitching moment,  $I_y$  is the pitching moment of inertia and  $\delta = \alpha_H + \tau \delta_e$ .  $\alpha_H$  is the incidence of the horizontal tail,  $\delta_e$  is the elevator displacement, and  $\tau = \partial \alpha_H / \partial \delta_e$  is (unfortunately) also called the elevator effectiveness parameter (in rotating the zero lift axis of the horizontal tail), (ref. 55). By control displacement authority here we mean precisely the maximum allowable limits on  $\delta$  and by control rate authority, the maximum value of the absolute time derivative  $|\dot{\delta}| = |d\delta/dt|$ . Unfortunately, the nondimensional partial derivative  $C_{m\delta} = 2I_y M_\delta / \rho S U_0^2 \bar{c}$  is called a measure of control power (ref. 55) and also control effectiveness (ref. 56). To confuse the terminology further, reference 54 has also called the (negative) product,  $-C_{m\delta} \delta$ , control power by virtue of an unconventional definition for positive  $\delta$ .

performance requirements and is therefore not usually subject to change for stability and control purposes, except by direct wing lift control for load alleviation, ride quality modification, or precise vertical path regulation.

However, there are three feedback variables for augmenting both  $\omega_{sp}$  and  $\zeta_{sp}$  by means of controlling the incidence of the horizontal tail plane and/or the elevator displacement. These three variables (and what they augment, listed in order of decreasing practicality and reliability, are: (1) pitch attitude ( $\omega_{sp}$ ) and its time rate of change ( $\zeta_{sp}$ ); (2) normal acceleration ( $\omega_{sp}$ ) and its time rate of change ( $\zeta_{sp}$ ) measured near the center of percussion; and (3) angle of attack ( $\omega_{sp}$ ) and its time rate of change ( $\zeta_{sp}$ ). All of these feedback techniques are described in reference 56. The short-period approximations for the pitch rate and attitude feedback technique are derived in Appendix B for airplanes with negligible inherent static margin and negligible downwash lag effect on the tail plane. The following discussion will concentrate on the pitch rate and attitude feedback technique because it is the most common technique used in commercial transport aircraft.

The short-period approximations for the angle of attack and rate feedback ( $\alpha, \dot{\alpha} \rightarrow \iota_H + \tau\delta_e$ ) technique are discussed in Appendix A. The favorable effects of  $\alpha, \dot{\alpha} \rightarrow \iota_H + \tau\delta_e$  on the short-period dynamic stability are often difficult to achieve with practical control, because of angle-of-attack sensor problems. However, the alternative feedback technique using normal acceleration and rate feedback ( $a_z', \dot{a}_z' \rightarrow \iota_H + \tau\delta_e$ ) when measured at the center of percussion has features similar to  $\alpha, \dot{\alpha} \rightarrow \iota_H + \tau\delta_e$ , because  $\alpha$  is a major component in the  $a_z'$  signal (ref. 56).

#### 4.3.5 Short-Period Frequency

The square of the longitudinal short-period undamped natural frequency with pitch attitude feedback to the tail-plane control can be expressed with good approximation from Appendix B as:

$$\omega_{sp}^2 = \frac{\bar{V}\eta_H C_{L\alpha_H}}{2\mu_c \left(\frac{k_y}{U_0}\right)^2} \frac{\partial(\iota_H + \tau\delta_e)}{\partial\theta} \quad (1)$$

by virtue of the assumptions that the inherent static margin and downwash lag effect are negligible, and where:

$\mu_c = m/\rho S\bar{c}$  is the longitudinal relative density

$k_y$  is the pitching radius of gyration

$U_0$  is the trimmed true airspeed

$\bar{V} = S_H \ell_H / S\bar{c}$  is the horizontal tail volume coefficient

$\eta_H = q_H/q$  is the dynamic pressure ratio at the horizontal tail plane

- $C_{L\alpha_H}$  is the partial derivative of the horizontal tail lift coefficient with angle of attack,  $\alpha$
- $[\partial(\iota_H + \tau\delta_e)/\partial\theta]$  is the pitch attitude feedback gain to the tail plane controls  $\iota_H$ ,  $\delta_e$
- $\iota_H$  is the incidence of the tail plane
- $\delta_e$  is the elevator displacement
- $\tau = \partial\alpha_H/\partial\delta_e$  is the elevator effectiveness, a nonlinear function of  $S_e/S_H$ , the ratio of the elevator area to the horizontal tail area

Equation (1) connects  $\omega_{sp}$  with design parameters such as tail length, tail plane size, elevator area, and pitch attitude feedback gain in a form suitable for preliminary design calculations. A graph of a rearrangement of equation (1) is shown in figure 10, after dividing equation (1) by the wing-body lift coefficient derivative with respect to angle of attack,  $C_{L\alpha_{WB}}$ , to express the effective maneuver margin. (Figure 10 is identical to Figure 9, except for the difference in interpretation of control gain and the proper identification of the ordinate as the effective maneuver margin.)\* Increasing the nondimensional feedback control gain,  $\partial(\iota_H + \tau\delta_e)/\partial\theta$ , in figure 10 as  $\bar{V}$  is reduced makes it possible to maintain the effective static margin (or short-period frequency) required by flying qualities criteria in each flight phase at the expense of control actuation power and authority.

The feedback control gain,  $\partial(\iota_H + \tau\delta_e)/\partial\theta$ , provides the preliminary designer with one connection between control surface authority required for gust regulation and the (closed-loop) variability in pitch attitude (about its trimmed value) induced by a given level of variability in gust velocity with stability augmentation. Obviously there is a limit to the control authority available for gust regulation. This control authority limit restricts the allowable covariation between  $\bar{V}$  and wing location to that depicted in figure 7. The intersection of the control authority limit for gust regulation with the nose gear unstick limit in figure 7 determines the potential reduction in the horizontal tail volume coefficient which represents the potential reduction in weight.

#### 4.3.6 Short-Period Damping

Before discussing the application of control authority criteria, however, it is necessary to introduce the relationship, derived in Appendix B, between the short-period damping coefficient,  $2\zeta_{sp}\omega_{sp}$ , and the dimensionless pitch rate feedback gain,  $[\partial(\iota_H + \tau\delta_e)/\partial(\dot{\theta}\iota_H/2U_0)]$ , to the tail plane controls. The

---

\*Figure 10 presumes that the wing location on the fuselage covaries with  $\bar{V}$  sufficiently forward of the center of gravity so as to render the inherent static margin negligible (Appendix A).

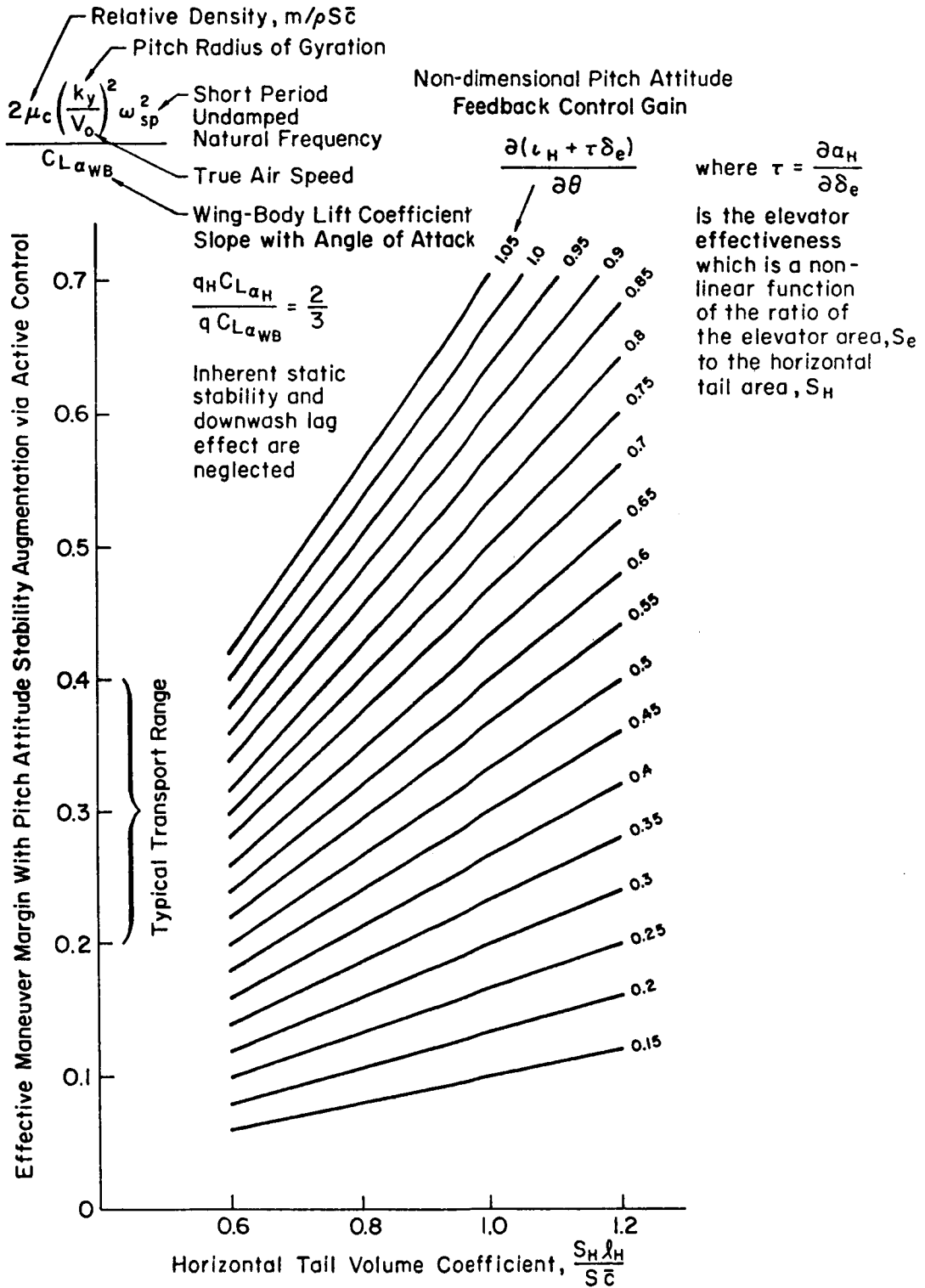


Figure 10. – Effective Maneuver Margin With Pitch Attitude Stability Augmentation Versus Horizontal Tail Volume Coefficient as a Function of Pitch Attitude Feedback Control Gain

short-period damping coefficient can be expressed with good approximation from Appendix B as:

$$2\zeta_{sp}^{\omega_{sp}} = \frac{\bar{c}}{2U_0} \left\{ -C_{mq_{WB}} + \frac{l_H}{\bar{c}} \bar{V}_{\eta_H} C_{L\alpha_H} \left[ 2 + \frac{\partial(\iota_H + \tau\delta_e)}{\partial(\dot{\theta}l_H/2U_0)} \right] \right\} \quad (2)$$

where  $C_{mq_{WB}}$  is the nondimensional wing-body damping-in-pitch derivative,  $\partial C_{mq_{WB}}/\partial(\dot{\theta}\bar{c}/2U_0)$ ;  $[\partial(\iota_H + \tau\delta_e)/\partial(\dot{\theta}l_H/2U_0)]$  is the nondimensional pitch rate feedback gain to the tail plane controls;  $\iota_H$ ,  $\delta_e$ , and all other symbols are the same as defined for equation (1). Equation (2) connects  $2\zeta_{sp}^{\omega_{sp}}$  with design parameters such as tail length, tail plane size, elevator area, and pitch rate feedback gain in a form suitable for preliminary design calculations. A graph of a rearrangement of Equation (2) is shown in figure 11, after dividing Equation (2) by the horizontal tail lift coefficient derivative with respect to tail angle of attack,  $C_{L\alpha_H}$ , to express the augmented short-period damping coefficient under the assumption that the inherent downwash lag effect is negligible. Increasing the nondimensional feedback control gain,  $[\partial(\iota_H + \tau\delta_e)/\partial(\dot{\theta}l_H/2U_0)]$  in figure 11 as  $\bar{V}_{\eta_H}/\bar{c}$  is reduced makes it possible to maintain the effective short-period damping coefficient (i.e.,  $2\zeta_{sp}^{\omega_{sp}} > \rho S U_0 C_{L\alpha} / 2m$ ) required by flying qualities criteria in each flight phase at the expense of control actuation power and authority.

The feedback control gain  $[\partial(\iota_H + \tau\delta_e)/\partial(\dot{\theta}l_H/2U_0)]$  provides the preliminary designer with another connection between control surface authority required for gust regulation and the (closed-loop) variability in pitch rate induced by a given level of variability in gust velocity with stability augmentation. Having established both connections between augmented short period dynamic stability and control displacement variability about the trimmed condition, it is next appropriate to discuss the application of control authority criteria with the help of Appendix B.

#### 4.3.7 Control Authority Limitations

The relationships between the variances in control displacement,  $\sigma^2(\iota_H + \tau\delta_e)$ , and control rate,  $\sigma^2(\dot{\iota}_H + \tau\dot{\delta}_e)$ , and the variance in normal gust velocity,  $\sigma_{w_g}^2$ , are derived in Appendix B. These variance relationships are called variance ratios and are predicated on the linear stationary properties of the short-period model of the airframe as well as the Gaussian (amplitude) distribution of normal gust velocity. When a time-invariant linear system, such as the short period perturbed model of the rigid airframe with pitch attitude and rate stability augmentation is subjected to a Gaussian random disturbance in normal gust velocity, the distributions of control displacement and rate will also be Gaussian. Therefore, complete information about the (first) probability distributions of control displacement and rate can be obtained from their variances.

For commercial transport aircraft, the control (displacement and rate) variances (about the mean trimmed control displacement) induced by stochastic gust disturbances are more crucial from the standpoint of authority limits than the variances contributed by guidance and maneuvering commands which primarily determine the trim control displacement and rate. Since the



application of control authority limits is best served by probabilistic criteria, the use of a versine gust velocity model at a single wavelength is inappropriate for this purpose.

Instead, relationships are presented in Appendix B by which the preliminary designer may adjust proposed values for upper and lower bounds on control displacement and rate authority to establish an acceptably low value of the overall probability of exceeding the limits as the trim control displacement varies over the operating profile. The limits and the probability of exceedence thereof depend on both feedback control gains to the horizontal tail plane discussed previously, the geometry of the horizontal tail, and the elevator effectiveness.

The designer's problem is to find an equitable compromise among all of the variables open to choice so that the control authority (and rate) limits, while not unduly restrictive from the probabilistic viewpoint, are sufficiently generous to allow a worthwhile net reduction in weight to accompany the reduction in  $V$ .

Simplified design practices are offered in Appendix B, if the desired probabilities of exceedence of control displacement (and rate) authority limits are very low. If, however, the designer must cope with unduly restrictive authority (and/or rate) limits, the design practices become even more interactive, because the feedback gains are no longer relatively independent of control displacement (and/or rate). In such a case where control authority must be unduly limited, describing functions may be used to estimate the average feedback control gains. Design practices, criteria, and examples are presented in reference 57.

This concludes the discussion of horizontal tail sizing criteria from the probabilistic viewpoint of providing satisfactory dynamic stability through active control.

#### 4.4 VERTICAL TAIL SIZING CRITERIA

Figure 12 illustrates typical area sizing criteria for the vertical tail as a function of the same abscissae as in figure 7 for the horizontal tail. The use of area ratio (rather than a volume coefficient) as the ordinate and the use of common abscissae are intended to emphasize that design decisions regarding horizontal tail length (with respect to the center of gravity) may impose a constraint on vertical tail length. Thus, vertical tail length is no longer an independent variable. Fore/aft wing location on the fuselage, per se, has not the aerodynamic influence on vertical tail sizing that it did on horizontal tail sizing, because even swept wings generate little asymmetric side force and yawing moment in a steady sideslip when compared with the vertical tail. The center-of-gravity location does, however, affect the vertical tail length (by definition) and the yawing radius of gyration. Consequently, the vertical tail area ratio required to satisfy the constant dutch roll frequency criterion in figure 12 decreases as the vertical tail moment arm with respect to the center of gravity increases.

There is a lower bound on the vertical tail area ratio at which the control authority of the vertical tail-and-rudder can trim (or balance) the largest asymmetric thrust moment at the (lowest) critical speed or remove the greatest crab angle in a crosswind approach. This area ratio limit also decreases as the tail moment arm increases.

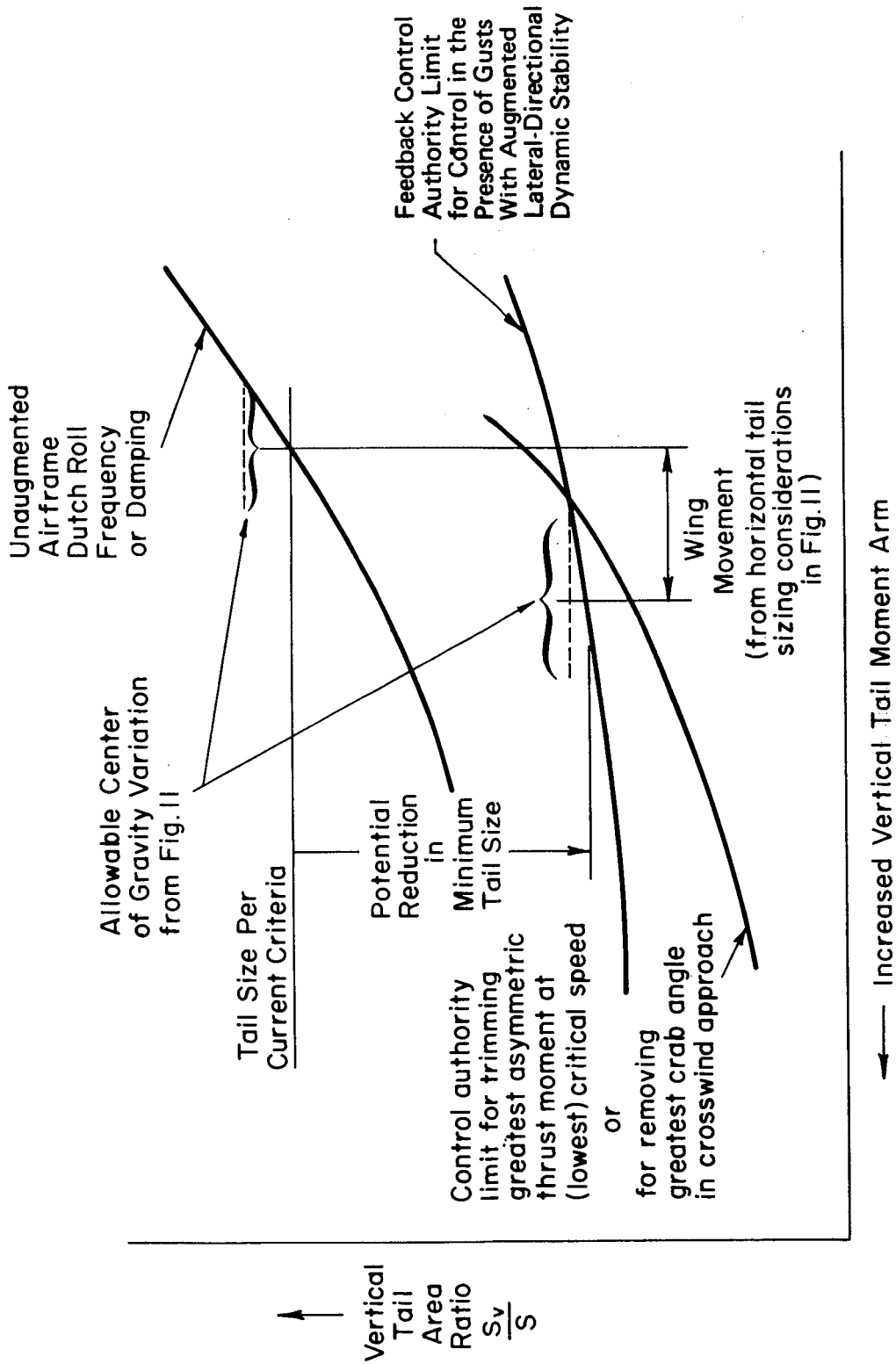


Figure 12. — Vertical Tail Sizing Criteria

In the absence of a yaw damper, the vertical tail area ratio can seldom, if ever, approach its minimum value for trimming asymmetric thrust or removing crosswind crab angle because handling qualities criteria intervene. Without feedback stability augmentation, a reduction in vertical tail area will degrade directional stability and control with the rudder, especially at the high angles of attack characteristic of the power-approach flight condition. However, if the vertical tail area reduction is accompanied by augmented dynamic directional stability having feedback control surface effectiveness and actuation power and authority, the vertical tail area ratio usually will be constrained by the control authority limit for trimming asymmetric thrust or decrabbing, as shown in figure 12.

#### 4.4.1 Directional Dynamic Stability

Directional dynamic stability is characterized by the coupled yawing-rolling oscillation which is termed the "dutch roll." Constraints on directional stability can, in turn, be characterized in terms of the undamped natural frequency,  $\omega_d$ , and the damping ratio,  $\zeta_d$ , of the dutch roll. Additional constraints on directional control power can be characterized in terms of the undamped natural frequency,  $\omega_r$ , and damping ratio,  $\zeta_r$ , in the numerator of the yawing velocity response to yawing control displacement.

Washed-out yawing velocity is a common feedback variable for augmenting the customarily deficient  $\zeta_d$  by controlling the rudder (or even the incidence of the vertical tail, if the tail area is reduced). For straight-wing aircraft of high aspect ratio in cruising flight, yawing velocity feedback to the directional control surface can provide an augmented  $\zeta_d$  on the order of 0.7 or more because  $\omega_r \ll \omega_d$  even though both  $\zeta_d$  and  $\zeta_r$  may be inherently very small and even slightly negative.

A less favorable configuration of  $\omega_r$  is easily possible for swept-wing aircraft of low-to-medium aspect ratio operating at high lift coefficient, so that either dihedral effect (lateral static stability) or roll damping predominate over directional static stability and damping. In either unfavorable case,  $\omega_r$  will be only slightly smaller than  $\omega_d$ , both  $\zeta_d$  and  $\zeta_r$  will be inherently very small, and  $\zeta_r$  may even become negative. Consequently, the yawing velocity feedback to the directional control surface will increase dutch roll damping little, if at all.

The difficulties in improving dutch roll damping occasioned by  $\omega_r$  approaching  $\omega_d$  can be overcome by feeding rolling velocity to the ailerons to augment the roll damping. This has the beneficial effect of reducing  $\omega_r$  so that  $\omega_r \ll \omega_d$  as in the former favorable case.

If augmented damping ratio,  $\zeta_d'$ , is to remain substantially invariant with flight condition, the yawing velocity feedback gain to the directional control surface must vary inversely with the square root of dynamic pressure. On the other hand, if the augmented damping coefficient,  $2\zeta_d'\omega_d'$ , is to be invariant, the same feedback gain must vary inversely with the dynamic pressure itself.

The feedback of heading angle to the directional control surface offers the most practical means of increasing or maintaining  $\omega_d$  sufficiently large by augmenting static directional stability in spite of reduced vertical tail area ratio. The feedback of sideslip angle or sideslipping velocity to the directional control surface directly augments the static directional (weathercock) stability derivative  $N_\beta$  (or  $N_v$ ) and increases  $\omega_d$ . To improve the dutch roll damping a rate-of-change of sideslip angle or sideslipping

acceleration component of limited bandwidth can be introduced. The primary deficiency in using sideslip feedback is a practical one in instrumenting an adequate sensor. This can be, to some extent, alleviated by substituting a properly located lateral accelerometer for the sideslip sensor. As in the analogous longitudinal case, the proper location is near the center of percussion for the directional control. All of the feedback techniques mentioned are described in reference 56 along with suitable approximations for  $\zeta_d$ ,  $\omega_d$ ,  $\zeta_r$ , and  $\omega_r$  in terms of the aerodynamic, geometric, and inertial properties required for preliminary design.

#### 4.4.2 Control Authority Limitations

The feedback control gains to the directional control surface provide the designer with the connections between control surface rate and displacement authority required for gust regulation and the (closed-loop) variability in each measured feedback variable (e.g., yaw rate and heading) with respect to the trimmed flight condition. After establishing these connections in terms of variance ratios, the designer may proceed in a manner analogous to that described previously for augmenting longitudinal short-period dynamic stability in order to apply the control authority limits for gust regulation to the allowable reduction in vertical tail area in figure 12 while maintaining  $\zeta_d$  and  $\omega_d$  at levels which are satisfactory for handling qualities.

#### 4.5 CENTER-OF-GRAVITY CONTROL

Automatic center-of-gravity control can offer significant design advantages in the following ways.

- Reduction of the design center-of-gravity range at given flight conditions may allow further reduction in the horizontal tail volume coefficient (refer to the indication of "allowable center-of-gravity variation" on figure 7)
- Minimization of total drag with respect to center-of-gravity location can produce the optimum tradeoff of trim control parasite drag for wing- and tail-induced drag during cruising flight (refer to equation (C-19) and the explanation following that equation in Appendix C)

Automatic center-of-gravity control must be based upon a performance measure,  $P$ , which is sensitive to variations in center-of-gravity and aerodynamic-center locations. An example of a suitable performance measure is the square of the true airspeed. Then  $P = V_A^2$ . The drag equation can be solved for  $V_A^2$  and the resulting equation can be used (after further mathematical manipulations) as the basis for the center-of-gravity control law. Then:

$$P = V_A^2 = \frac{gT \cos(\xi + \theta - \gamma) - W[a_x \cos(\theta - \gamma) + a_z \sin(\theta - \gamma)]}{\frac{\rho S}{2} C_D} \quad (3)$$

where the symbol definitions are as follows:

T Power setting expressed as newtons of thrust.

- ξ Thrust line inclination angle with respect to fuselage waterline
- θ Pitch attitude of the fuselage waterline
- γ Aircraft flight path angle
- W Aircraft weight
- $a_x, a_z$  Respectively, longitudinal and normal measured aircraft acceleration
- ρ Density of atmosphere
- S Reference wing area for aircraft
- $C_D$  Total drag coefficient for aircraft which is a function of center of gravity location,  $x_{cg}$  (refer to equations (C-11), (C-12), and (C-13) of Appendix C)

If the equation for the rate of change of P:

$$\dot{P} = \frac{\partial P}{\partial x_{cg}} \dot{x}_{cg} + \left\{ \frac{\partial P}{\partial T} \dot{T} + \frac{\partial P}{\partial (\theta - \gamma)} (\dot{\theta} - \dot{\gamma}) + \frac{\partial P}{\partial a_x} \dot{a}_x + \frac{\partial P}{\partial a_z} \dot{a}_z + \frac{\partial P}{\partial \rho} \dot{\rho} + \frac{\partial P}{\partial W} \dot{W} \right\} \quad (4)$$

is solved for  $\partial P / \partial x_{cg}$ , the basis for the control law is obtained since  $\partial P / \partial x_{cg}$  is a monotone decreasing function of  $x_{cg}$  and is zero when P is a maximum for given values of T,  $(\theta - \gamma)$ ,  $a_x$ ,  $a_z$ ,  $\rho$  and W. However, special provisions must be made for the division by  $\dot{x}_{cg}$ , which may be zero.

The center-of-gravity control law may be mechanized which is functionally equivalent to that shown in figure 13. In the figure,  $f_c$  is the commanded fuel transfer flow rate and  $k_1$  is the ratio of the longitudinal distance over which fuel is transferred to the aircraft weight. The smoothing filter time constant,  $1/\omega_1$ , must be on the order of 30 seconds. The control system acts to maximize  $P = V_A^2$  with respect to  $x_{cg}$  only regardless of  $a_x$ ,  $a_z$ , T, W,  $\theta$ ,  $\gamma$  and  $\rho$ . The steady-state error in center-of-gravity control is approximately bounded by  $\pm a / [k_2 \partial^2 P / \partial x_{cg}^2]$ .

#### 4.6 RIDE QUALITY CONTROL

Ride quality is usually addressed only after the basic aircraft configuration, size, and strength design requirements are satisfied. This is because active ride quality control does not tend to impose design constraints which affect the key configuration parameters, wing loading and inherent directional stability, in any material way, while ride quality is almost completely determined by these parameters. (Ride quality is also determined to some extent by the low-frequency structural mode characteristics.)

Design practice for ride quality control is well established (refs, 58 to 62). The governing design principle is embodied in the "identical location of accelerometer and force" (ILAF) concept (ref. 31 and 61) which has received somewhat greater application in connection with structural mode control. The essential feature of the ILAF concept is that it assures that

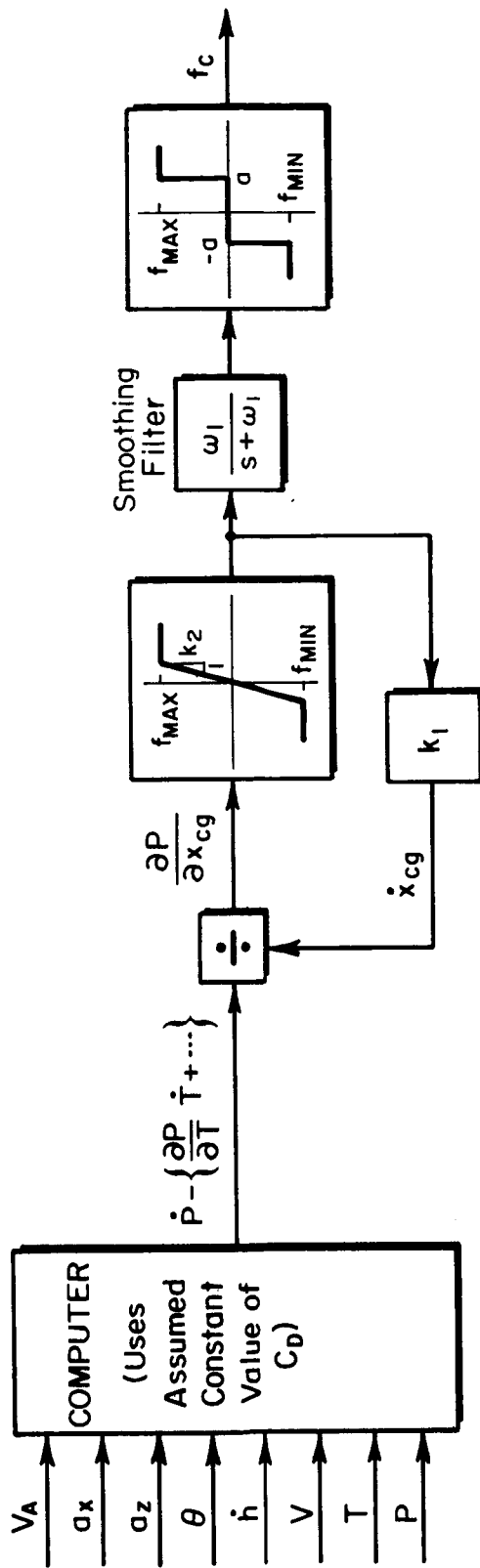


Figure 13. -- A Possible Mechanization for Center of Gravity Control

the generalized modal input\* to an acceleration sensor has the same sign as the generalized force applied to that mode (ref. 31). Since this is so for all modes, variations in phasing between applied force and sensed acceleration which can cause closed-loop stability problems are avoided. The effectiveness with which each mode can be controlled is dependent upon the magnitude of the generalized force available for that mode which in turn depends upon the magnitude of the mode shape at the force point location. If this magnitude is zero or very small at a particular force point for a particular mode, that mode must be controlled by means of another force point located elsewhere on the aircraft.

For longitudinal ride control, the most appropriate force point is direct lift control located on the wing since gust-induced change in wing lift is the main contribution to poor longitudinal ride. A secondary effect in poor longitudinal ride is the angular acceleration produced by the weathercock effect of the horizontal tail. The appropriate force point for controlling this contribution is the elevator. However, the angular acceleration can be only modestly modified because of potential interference with short period handling qualities characteristics. It should also be noted here that the angular acceleration response to gusts will tend to be greatly diminished in designs with nearly neutral inherent short-period stability if the stability augmentation is by means of pitch attitude and rate or inertial angle of attack and rate feedback to elevator in distinction to aerodynamic angle of attack and rate feedback to elevator. The direct lift control and elevator force points also offer some opportunity to control low-frequency structural modes contributing to poor ride. There are circumstances wherein adequate ride cannot be obtained at the critical location in the fuselage. In that case, an additional force point is required (e.g., the canards on the B-1).

For lateral ride quality control, the most appropriate force point is the rudder since gust-induced yawing moment from the rudder is the main contribution to poor lateral ride. The addition of lateral acceleration or angular acceleration feedbacks to the rudder can improve lateral ride considerably. However, these feedbacks can potentially interfere with the dutch roll handling qualities. It should be noted here that designs with reduced inherent directional stability will tend to have reduced angular acceleration response to gusts if the stability augmentation is by means of heading angle and rate feedback to rudder and not to aerodynamic sideslip or lateral acceleration (measured at the rudder center of percussion) feedback to rudder. The rudder is moderately effective for controlling low-frequency structural modes contributing to poor ride. This is because it is the rudder-plus-fin combination which is primarily responsible for forcing those modes in the first place. (The rudder-plus-fin combination is the primary yawing moment contributor, and is a major side force contributor.)

When acceleration feedbacks are used for ride control, they serve to increase slightly the effective mass or moment of inertia and to increase damping considerably. Consequently, the feedbacks are equalized with a pseudo-integration. The break frequency for the pseudo-integration must be well above the path mode frequencies, and, as mentioned previously, care must be taken in ride control system design to avoid affecting the attitude modes in ways unfavorable for handling qualities.

---

\*Applies for rigid and flexibility modes.

Ride quality control sometimes tends to affect loads in a favorable way. A simplified analysis of a yaw damper is given in Appendix D to illustrate this point.

#### 4.7 DYNAMIC LOAD ANALYSIS

Company practice in analyzing dynamic loads varies among commercial transport manufacturers. Furthermore, the practices of the manufacturers tend not to be extensively documented in literature which may be referenced in this report. (The complex, fluid, artful, and proprietary nature of these practices all contribute to this tendency.) For this reason, no recommended practices are presented for dynamic load analysis; instead the principal analysis techniques proposed in the literature are reviewed.

It has been common practice to predict the design gust loads on aircraft by assuming that atmospheric turbulence can be adequately represented by an isolated discrete gust velocity having a specified spatial or temporal gradient function, magnitude and wavelength. (See, for examples, ref. 63.) Whereas such a practice has been successful on relatively rigid low-speed aircraft, the practice is inadequate for application to contemporary flexible high-speed aircraft, because the flexibility may increase some loads and decrease others significantly (refs. 64 to 66). As a consequence, the prediction of gust loads on aircraft based upon the concept of continuous atmospheric turbulence velocity components characterized by power spectral densities has gradually gained wide acceptance since 1950 (refs 67 to 77).

Contemporary experience has served to emphasize the need for increased attention to retard structural fatigue. Coupled with this need is the requirement to predict the service life of a design. The first step in this prediction process is to obtain as accurate as possible a forecast of the dynamic loads involved. It has been established (ref. 78) that the significant fatigue loads on the airframe are caused by gusts, flight maneuvers, and ground rolling. Evidence suggests that up to 90 percent of the damage accumulated in a typical commercial transport can be related to the ground-air-ground (GAG) cycle. For a wing, which is fatigue critical on the lower surface, the maximum tension stress is the sum of lg flight stress and maneuver/gust increment, and the maximum compression is the sum of lg ground stress (inertia loads without airloads) and ground loads increment. In the once-per-flight GAG cycle, 75 percent of the stress range may be due to the lg ground and lg flight conditions on the wing. For the fuselage, the corresponding dominant loading is fuselage pressurization which may account for up to 80 percent of the GAG cycle stress range. Gust and maneuver loads are predominant loadings generating fatigue damage of the vertical tail and to a lesser degree the engine pylons and horizontal tail.

Since the mean-to-mean fluctuation of the GAG cycle is not amenable to control, active control offers potential reduction of longitudinal loads only for the incremental load fluctuation about the means level of the GAG cycle. Large potential for load reduction exists for lateral loads because there is no GAG cycle effect.

The complexities of treating more than the plunging motion of a rigid airframe with quasi-static aeroelastic corrections (refs. 67 to 71) inhibit acceptance of simplified aeroelastic dynamic analysis for load prediction in preliminary design. Some of the principal proposed analysis techniques which will be relevant when active load control technology is applied to subsonic-sonic CTOL transport aircraft are reviewed.

Two approaches to establishing gust loads based on power-spectral analysis are offered in reference 79 with a third recommendation for a combination of both approaches. One approach is called Mission Analysis, the other, Design Envelope Analysis. These analyses are conducted for each pertinent limit (or ultimate) load. A fourth approach, quite similar to the Mission Analysis approach, is the Rational Probability Analysis described in references 80 to 82.

These four approaches provide alternative ways for expressing aircraft exposure to loads while airborne. All approaches used the expected frequency of load exceedence per unit time as a function of load level in a given gust environment as the basis for evaluating an average expected frequency of load exceedence over the exposure scenario for the particular approach being used.

These four approaches are described in greater detail below.

Mission Analysis (ref. 79). The mission analysis predicts the average frequency of load exceedence per unit time as a function of load level for each pertinent load over each segment of the mission profile. The frequency of exceedence corresponding to limit (or ultimate) load is specified. A design value of each pertinent load is then determined from the appropriate exceedence frequency function. The design frequency of exceedence must be based on providing strength in new vehicles which is consistent with that strength demonstrated to be adequate in existing vehicles. The design limit loads, which exceed the limit loads by a factor of safety for understrength provision, can be defined in terms of a different appropriate frequency of occurrence.

Since it is anticipated that the aircraft will depend upon a stability augmentation system, the mission analysis must include appropriate fractions of flight time\* with the system degraded or even inoperative. In addition, if a specific emergency procedure, such as a conditional descent in altitude, involves a substantial increase in gust exposure, this must be included in the mission analysis.

Design Envelope Analysis (ref. 79). The design envelope analysis considers potentially critical combinations of speed, altitude, weight, and balance without regard for the operational mission profile. The gust power spectral density function and the product  $\sigma_w \eta_d$  are specified, where  $\sigma_w$  is the rms gust velocity and  $\eta_d$  is the ratio of design load to rms load. The product  $\sigma_w \eta_d$  is analogous to the discrete gust velocity  $U_{de}$  in Paragraph 25.341 of reference 2; it is specified as a function of altitude for each of one or more speeds, viz.,  $V_B$ , the design rough-air speed,  $V_C$ , the design cruise speed, and  $V_D$ , the design dive speed.

---

\*Conditioned on the reliability and failure mode analysis.

A pertinent design load is established by the product  $\sigma_w \eta_d \bar{A}$ , where  $\bar{A}$  is the predicted ratio of the rms value of load at the given point in the structure to the rms gust velocity.\* The selection of the values to be specified for  $\sigma_w \eta_d$  must be based on providing strength in the new aircraft which is consistent with that demonstrated to be adequate in existing aircraft. The appropriate values for  $\sigma_w \eta_d$  should correspond to the highest predicted value of the normalized load exceedence frequency ratio  $N_l/N_0$ , where  $N_l$  is the limit load exceedence frequency and  $2N_0$  is the frequency of (one-"g") trim load axis crossings. The values of  $\sigma_w \eta_d$  so estimated will then define lower bounds on the limit loads. The design limit loads, which exceed the limit loads by a factor of safety for understrength provision, can be defined by a different appropriate value of  $\sigma_w \eta_d$ ; and a reduced value of  $\sigma_w \eta_d$  can be established as a function of the time that stability augmentation is degraded or inoperative.

Combined Mission and Design Envelope Analysis (ref. 79). Only by means of a realistic mission analysis can the designer be assured that he is providing a safe yet not overly conservative level of strength to meet the gust loading. However, considerable judgment must be applied in the mission analysis, and the design loads so obtained are influenced accordingly. In particular, considerable care may be required to assure that a sufficient variety of off-nominal flight conditions is included. Consequently, a combined criterion is attractive in that it would retain the advantage of the mission analysis while at least partially overcoming its disadvantages.

$$*\bar{A} = \frac{\sigma_l}{\sigma_{wg}} = \frac{1}{\sigma_{wg}} \left\{ \int_0^\infty \left[ \Phi_{u_g u_g}^t(\omega) \cdot |T_{u_g}^l(\omega)|^2 + \Phi_{w_g w_g}^t(\omega) \cdot |T_{w_g}^l(\omega)|^2 \right] d\omega \right\}^{1/2}$$

where

- $\sigma_l$  is the rms load
- $\sigma_{wg}$  is the rms (normal) gust velocity
- $\Phi_{u_g u_g}^t(\omega)$  is the temporal power spectral density of longitudinal gust velocity, which is equal to  $\Phi_{u_g u_g}^s(\Omega)/U_0$
- $\Phi_{u_g u_g}^s(\Omega)$  is the spatial power spectral density of longitudinal gust velocity, where  $\Omega = \omega/U_0$
- $U_0$  is the true airspeed
- $\Phi_{w_g w_g}^t(\omega)$  is the temporal power spectral density of normal gust velocity, which is equal to  $\Phi_{w_g w_g}^s(\Omega)/U_0$
- $\Phi_{w_g w_g}^s(\Omega)$  is the spatial power spectral density of normal gust velocity
- $T_{u_g}^l(\omega)$  is the (closed-loop) load frequency response to longitudinal gust velocity, which can be obtained from the analogous transfer function by specializing the complex operator  $s$  to be purely imaginary; i.e., by  $s = j\omega$
- $T_{w_g}^l(\omega)$  is the (closed-loop) load frequency response to normal gust velocity, which can be obtained in the same way as  $T_{u_g}^l(\omega)$ . Methods for determining the transfer functions will be discussed subsequently at the end of the subtopic on design practices

For example, reference 79 suggests that conservative design values of  $\sigma_{wnd}$  could be used in lieu of an optional mission analysis. Or, even when a mission analysis is performed, a  $\sigma_{wnd}$  analysis might be required to provide a lower bound on mission analysis loads. In this way the  $\sigma_{wnd}$  analysis would provide a measure of insurance against the omission of critical and emergency operations from the mission analysis.

Rational Probability Analysis (refs. 80 to 82). The evolution of the probabilistic structural failure criterion proposed in reference 82 is based on U.S. Air Force experience with the B-52. Although the strength of the B-52 was adequate to meet its discrete gust design load level, the airplane was encountering turbulence severe enough to cause loss of the vertical fin. In modifying the aircraft to correct the problem, engineers evolved new gust load criteria based on the concept of continuous turbulence and probabilistic considerations. This approach came to be known as the rational probability analysis (RPA) and its application is discussed in reference 80. Reference 82 uses the practical flight experience reported in references 79 to establish an acceptable structural failure probability for an individual airplane and to present a design envelope analysis which may be used to supplement the RPA. However, references 80 to 82 offer no testing procedure for verifying or proving compliance with either the design ultimate load exceedence frequency or the structural failure probability. As a consequence RPA is quite unattractive for binding a contract when compared with the discrete gust criterion.

A thorough critique of present and proposed approaches to structural design criteria by statistical methods is presented in Volume I of reference 83. In spite of its shortcomings, the RPA (ref. 82) for defining the design ultimate load for aircraft is considered by reference 83 to be a significant contribution to the state-of-the-art of structural analysis. Accordingly, reference 83 adopts RPA as a first step in defining a goal for structural reliability in its procedural proposal in Volume II. The "new" procedure recommended in Volume II of reference 83 merely modifies the conventional "factor of safety" structural design procedures, which proceeds in terms of deterministic conditions which can be tested for compliance or noncompliance in advance of flight.

Rational Probability Analysis Joined With Deterministic Load Analysis. The procedure proposed in Volume II of reference 83 requires consideration of the statistical distribution of those parameters that affect structural reliability. However, all the statistical manipulations are performed at the beginning of the analytical procedure. Thus RPA contributes where it is best suited - in preliminary design. The statistical operations are used to help the preliminary designer decide upon deterministic values for limit conditions and for factors of safety applied to the limit loads associated with these limit conditions. In effect, the statistical calculations on which the choice of a limit condition is based help to quantify a prediction of the expected results in future operations from a knowledge of past results. The loads analyst, the strength analyst, the structural designer, and the structural test engineer will be working with discrete conditions, discrete loads, and discrete strength allowables just as they always have, yet the design conditions will already account for the reliability of nonstructural systems such as ACT systems.

The procedure proposed in Volume II of reference 83 recognizes explicitly that the structure should have the capability to survive designated overload and understrength situations. At present this capability is provided indirectly

and inconsistently by applying a factor of safety to limit loads to determine design ultimate loads.

To attempt to remedy the present inconsistency, a procedure establishing separate and distinct requirements for understrength and overload ( $\omega$ ) situations based on probabilities and statistics so as to be consistent with levels of structural and nonstructural reliability appropriate to the vehicle mission is indicated. The limit design load must include a provision to accommodate understrength structure so that "no failure" will occur at the limit load. The overload provision must accommodate abnormal operation caused by nonstructural systems, of which the active control system could be one source, and the crew another. The automatic envelope limiting feature of ACT can help bound overloads. Crew-induced overloads can be reduced by feel-system forces which the pilot can override only with deliberation.

Unfortunately, however, choosing the design bending, torsion, shear, and axial loads in the members of the wing, for example, from average predictions is easier said than done, because the various design loads are not necessarily perfectly correlated. Although relative measures of transverse shear and of torsional moment at a given wing station may be known, they may be quantified only as root-mean-square values, hence, without sign and without correlation coefficients. Whether maximum up-shear combines with maximum nose-up torsion or otherwise is not expressed. If maximum up-shear should correlate with maximum nose-up torsion, the shear flows would add in the forward wing spar and subtract in the aft spar; if instead, maximum up-shear should correlate with maximum nose-down torsion, the shear flows would add in the rear wing spar (ref. 79).

Reference 79 also points out that if the shear stresses cannot be integrated to give the correct bending moments, no single set of panel loads can be administered in either a static or fatigue test to duplicate the dynamic correlation. Dynamic load correlation, then, presents one of the problems in applying power spectral methods to practical detailed stress analysis.

One design technique for coping with dynamic load correlation is discussed in reference 79 and developed in reference 84. It is called the "joint probability technique," and we shall discuss it briefly in the following subtopic. Another design technique for circumventing the need to consider dynamic load correction is discussed and developed in reference 79. Although called the

"matching condition technique" in reference 79, it should be termed the "marginal probability technique," because it is an approximate simplification of the more precise "joint probability technique." We shall discuss the marginal probability technique subsequently.

Joint Probability Technique (refs. 79 and 84). Many structural elements experience simultaneous dynamic axial and shear stress with limit (or ultimate) strength defined by "interaction curves" or "strength envelopes." One way to solve the dynamic load correlation problem in such elements is to express a transfer function for each local axial and shear stress in terms of a linear combination of the applied shear force, torsion, and bending moment transfer functions at the same and other stations. In addition to estimating each  $\bar{A}$  as the square root of a local stress-to-gust velocity variance ratio, e.g.,  $\sigma_x/\sigma_w$  or  $\sigma_y/\sigma_w$ , one must predict the coefficient of correlation,  $\rho_{xy}$ , between local stresses x and y:

$$\rho_{xy} = \frac{\text{cov}(x, y)}{\sigma_x \sigma_y}$$

where  $\text{cov}(x, y)$  is the covariance of stresses x and y.

A design technique which incorporates  $\rho_{xy}$  as well as  $\sigma_x$  and  $\sigma_y$  is developed and applied in reference 84 under the name "joint probability technique." Under the design envelope form of criterion, it is necessary to identify local values of the design load-to-rms load ratio,  $\eta_d$ . The joint probability density of the local orthogonal axial and shear stresses must be estimated as a function of  $\sigma_w$ , the rms gust velocity. An illustration of a typical result from reference 79 for a particular value of  $\sigma_w$  is shown in figure 14. The volume under the joint probability density surface outside the strength envelope (i.e., the part now shown in figure 14) is then the probability that the design strength is exceeded. The design value of  $\eta_d$  is then established by selecting a strength envelope which is compatible with the probabilistic design goal. Under the mission analysis form of criterion the frequency of exceedence must be interpreted with respect to the joint strength envelope for loadings in two dimensions rather than with respect to a single dimension of loading.

Marginal Probability or "Matching Condition" Technique (ref. 79). The important simplifying characteristic of the marginal probability technique is that the load correlation coefficient is approximated either as zero or unity by rounding off. Hence the probability function for a load A may be expressed either with no regard for load B or by approximating perfect correlation with another load C.

By means of the power spectral analysis, one must obtain design values of shear, torsion, bending moment, and front and rear wing spar shear flows at several wing buttock lines, for example. If based on a design envelope analysis, these "design values" are root-sum-square values derived from the product  $\sigma_w \eta_d \bar{A}$ , where  $\bar{A}$  is the square root of a local stress-to-gust velocity variance ratio, e.g.,  $\sigma_x/\sigma_w$ .

For simplifying the technique in preliminary design, one may choose to establish elementary spanwise distributions of shear, torsion, and bending moment by superimposing various spanwise distributions such as:

- A. A "basic" lift and inertial force distribution caused by rigid-body plunging motion in turbulence.

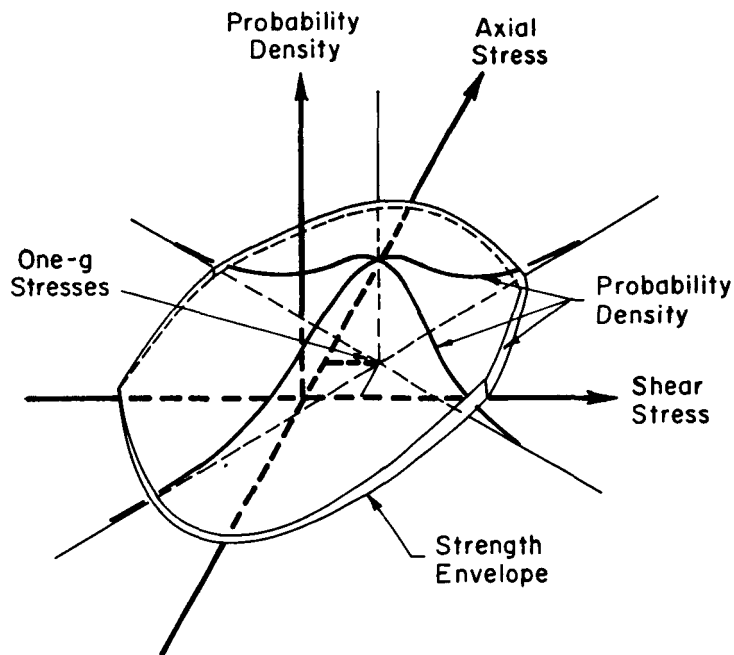


Figure 14. - Illustrative Joint Probability Density Function and Strength Envelope

- B. An "additional" lift and inertial load distribution caused by rigid body pitching motion in gusts or by the operation of load alleviation or load redistribution control surfaces such as flaps.
- C. Loads due to inertia forces and displacement-dependent aerodynamic forces in the first elastic mode.
- D. Loads due to inertia forces and displacement-dependent aerodynamic forces in the second elastic mode, etc.

At a subsequent design stage one may, by trial and error, find a linear combination of the various elementary modal spanwise load distributions to physically generate several design conditions which match or closely envelop the statistically defined shear flows obtained originally by power spectral methods. Ordinarily, no single combination can be found that will match all the statistically defined loads. Consequently, several combinations may be required. One, for example, may match the shears, bending moments, and shear flows, but embody lower torsions; another may match the torsions and shear flows, but embody lower shear forces and bending moments than required by the power spectral analysis. Together, however, the two combinations may envelop all of the statistically defined loads.

Approximations for the Rigid Airplane With Perfectly Correlated Loads (ref 79).  
 The classic single (plunging) degree-of-freedom model of a rigid airframe has been used in determining preliminary design gust loads on the wing for many

years (e.g., refs. 68, 69, 71, and 74). For this plunging model, all loads are presumed to be perfectly correlated with the normal acceleration of the center of gravity,  $a_{z_{cg}}$ . Where a design level of  $a_{z_{cg}}$  has been established for a given airplane, based on a design probability of exceedence, all loads and stresses are proportional to  $a_{z_{cg}}$ . Consequently, when  $a_{z_{cg}}$  reaches the value that corresponds to ultimate strength at some point in the structure, failure occurs. Only the weakest point in the structure is critical. No matter how many other points may be equally weak, there will be no reduction in the value of  $a_{z_{cg}}$  at which failure occurs, nor will there be any increase in the probability that the design strength will be exceeded.

The transfer functions developed in Appendix B show that the idealized plunging model of the rigid airframe gust response is also valid, if active control of the pitching degree of freedom is incorporated to augment the relaxed inherent stability. Furthermore, the transfer functions in Appendix B can be used to expand the scope of A to include the effect of longitudinal rms gust velocity,  $\sigma_u$ , as well as normal gust velocity,  $\sigma_w$ , on the idealized plunging model.\*

Methods for treating the coupled three-degree-of-freedom lateral motions of the rigid airframe in turbulence are developed in reference 73, and a simple rigid-body transfer function model for estimating the tail load associated with active control of the elevator is given in reference 67.

Approximations for the Large Flexible Airplane (ref. 79). In a large flexible airframe, the many diverse dynamic stresses will tend to be less than correlated with normal acceleration of the aircraft center of gravity ( $a_{z_{cg}}$ ). Suppose, nevertheless, that equal-marginal probability design values are established for each of these many loads or stresses. Then if the airframe be subjected to a sample of random atmospheric turbulence, the overall probability that some point or other will exceed its design load is greater than the marginal probability that any one given point will exceed its design load. For example, with two loads, A and B, the marginal probabilities of design load exceedence are designated as  $P(A)$  and  $P(B)$ . If  $P(A) = P(B)$  by hypothesis, it can be shown\*\* that:

$$P(A) \leq P(A \cup B) \leq 2P(A) \quad (5)$$

---

\*In this case  $\bar{A}$  becomes the ratio of the root-sum-square value of the load at a given point in the structure to either rms gust velocity, since  $\sigma_u$  can be expressed in terms of  $\sigma_w$  and vice versa.

\*\*In general, for two events A, B:

$$P(A \cup B) = P(A) + P(B) - P(A \cap B)$$

If A and B are completely dependent,  $P(A \cup B) = P(A) = P(B)$  by definition.

$$\therefore P(A \cup B) = P(A) = P(B)$$

which is the lower bound.

(footnote continued on following page)

The extension of this example to involve more than two loads is straightforward but tedious. Therefore, in the case of the large flexible airplane the overall structural unreliability depends not only upon the marginal probability of exceeding design load at the critical point, but also upon the degree of independence (or uncorrelation) among the various loads at other points in the structure.

In applying the marginal probability (or "matching condition") technique for utilizing statistically defined loads in stress analysis, the analyst treats a number of gust load conditions independently, e.g., wing root bending, nacelle shear, torsion or axial stress, tail load, fuselage bending, even as he treats ground-air-ground transition and taxiing loads or flight maneuvering loads independently of gust loads. Although each design load condition may be established at a level corresponding to a consistent marginal probability of exceedence, such an approach lacks rationality in that it fails to consider the contribution of relative independence (or uncorrelation) among loads to the overall probability of exceeding design strength. Of course, the joint probability technique begins to overcome this criticism, but even the joint technique treats only two stresses at a point. To extend the joint technique to take into account loads and stresses at many points would probably render the technique so complicated as to be of no value in preliminary design.

Instead, what would seem to be more desirable for the purposes of preliminary design are sound analytical approximations for correcting the short-period plunging-and-pitching model so as to account for the dynamic interactions among active (feedback) control, aeroelasticity, and unsteady aerodynamics. Such approximations were first offered over twenty years ago in reference 67 and subsequently developed in references 70 and 72 for the plunging model with unsteady lift and wing flexibility. More recently, reference 85 derives literal approximate factors for longitudinal short-period transfer functions with one or two coupled normal elastic modes (but without unsteady aerodynamics) for a variety of distinctive airframe configurations introduced in reference 7. Appendix F presents some of the control input transfer function forms and their literal approximate factors for "Configuration 3," which is a high-aspect-ratio swept-wing airplane having planform geometry and mass distribution similar to those of the B-47. Reference 8 shows that numerical values for the approximate and "exact" factors in three very different flight conditions compare favorably for "Configuration 3." Finally, equivalent stability derivatives are presented in Appendix F in order that the approximate factors may be used to investigate the effects of active control of short-period dynamics with pitch rate and either pitch-attitude or angle-of-attack feedback to the pitching-moment control in the presence of one or two coupled normal elastic modes.

---

(footnote continued from preceding page)

If A and B are mutually exclusive,  $P(A \cup B) = 0$

$$\therefore P(A \cup B) = P(A) + P(B)$$

If, in addition,  $P(A) = P(B)$  by hypothesis,

$$P(A \cup B) = 2P(A)$$

which is the upper bound. The upper bound occurs when the load exceedence events are mutually exclusive.

General methods for deriving approximate literal factors of transfer functions and for investigating active control sensor location effects in the presence of aeroelasticity are presented in reference 85. Reference 8 then discusses the sensitivity of the flexible airframe transfer functions to elastic mode shapes, and reference 86 discusses residual stiffness effects in truncated model analysis. The literal approximate factors for short-period transfer functions offer the preliminary loads analyst a valid tool by which he can expand the classic definition\* of  $\bar{A}$  to account for the dynamic interactions among active (feedback) control, aeroelasticity, and unsteady aerodynamics in response to longitudinal as well as normal stochastic gust velocity excitation.

#### 4.8 FLUTTER CONTROL

Active control of flutter has been previously identified in Section 2 as being a remote possibility for design application in the 1980's. However, certain design practices currently exist for assuring against unfavorable interaction between automatic flight control, stability augmentation and power actuation systems and flutter modes (ref. 87 and Chapters IX and X of ref. 88).

A substantial background of design practices for active structural mode control (refs. 89 to 98) provides some of the technological base required for active flutter control. Useful control concepts such as ILAF and DAA (differential angular acceleration) have been evolved (refs. 31, 61, and to 98 to 100) for structural mode control which also tend to provide limited favorable flutter suppression effects (ref. 32).

Active flutter control techniques per se have a very limited technological base, which is represented in the main by references 32 and 101 to 105. For this reason, a recommendation for design practice cannot be offered.

#### 4.9 ENVELOPE LIMITING

Methods for envelope limiting are through provision of artificial feel forces which inhibit excessive pilot demands upon airframe strength and through positive automatic limiting of commanded aircraft motion (Section 2).

Artificial Feel System (ref. 106). Artificial feel systems function to provide the pilot with a sense of the performance demands upon the aircraft that he is imposing by means of his control actions. The requirements for "stick-force per g" in the short-period frequency range, and for "stick-force per knot" statically have been mentioned previously. These requirements (in addition to requirements for the proper sense of cockpit control motions) also implicitly provide warnings as the aircraft limit load factor is approached, or as the stalling speed is approached. It is in this sense that the feel forces provide envelope limiting. The feel forces must be tailored so that pilots are unlikely to apply forces appropriate to the limiting levels of performance inadvertently, but at the same time it must be possible for the pilot to deliberately apply force in excess of those appropriate to the limiting levels of performance in emergency situations.

Artificial feel forces must also be tailored in an appropriate way to obtain good pilot-aircraft dynamic response characteristics. That is, the artificial feel forces result in force (in distinction to motion) stability augmentation.

---

\* $\bar{A}$  is the ratio of the rms value of load at a given point in the structure to the rms gust velocity.

This requirement arises because the artificial feel system is actually part of the closed-loop pilot-aircraft-stability augmentation system.

Automatic Envelope Limiting. Automatic envelope limiting is used to ensure that limiting levels of performance are not violated and to preserve control authority for inner loop control functions which are essential to stability of the pilot-flight control-aircraft system.

The recommended design practice is as follows:

- Enumerate all required envelope limits upon performance
- Divide the list according to limits which do and which do not take precedence over pilot control inputs. (That is, flight-critical stability augmentation demands upon control authority take precedence over pilot demands upon control authority. Load-factor demands upon control authority, etc.)
- Establish the precedence of the limiting functions in each division of the list (i.e., load-factor limits take precedence over pitch-attitude limits which in turn take precedence over flight-path-angle limits, etc.)
- Insert the automatic limiting feature shown in figure 15 at the appropriate points in the forward paths of the previously designed automatic control system loop structure.\* Each automatic limiting feature must be incorporated in such a way that its input signal does not contain output signal components from any precedent automatic limiting feature
- The automatic control system thus modified must be further modified by means of reconfiguring feedback paths and forward path equalization in order to obtain good dynamic response and performance properties for the complete system when one limiter is in its saturated state and all other limiters are in their unsaturated states. This must be repeated for each limiter. The reconfiguring of feedback paths and forward path equalization must be accomplished in a way that does not alter the small signal response, handling qualities, and performance of the complete system when all limiters are in the unsaturated state

The operation of the automatic limiting feature for a representative variable,  $x_n$ , in figure 15 is as follows

- In both the linear and nonlinear regions, the node implementing  $x_{ne} = x_{nCL} - x_n$  defines\*\* the  $x_{ne}$  error point in the loop structure. Therefore,  $x_{nCL}$  must be the  $x_n$  command. This quantity may be limited as indicated. The effective  $x_n$  command before limiting must then be  $x_{nCL}$

---

\*It is presumed here that the "previously designed automatic control system" is a small signal design for which the main considerations have been good dynamic response, handling qualities, and performance.

\*\*It is assumed that there are no inner loops with respect to the nth loop which feed back  $x_n$ .

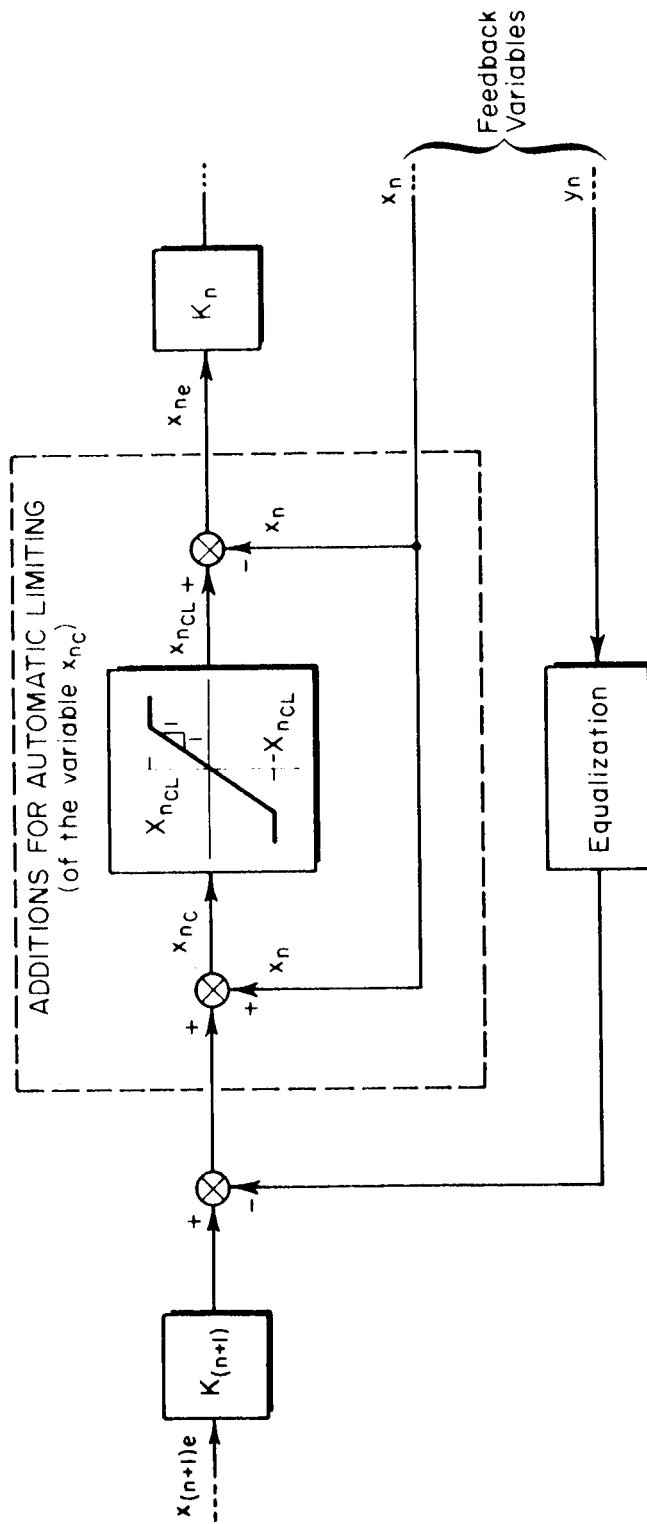


Figure 15. — Block Diagram Showing the Addition of an Automatic Limiting Feature to Basic Automatic Control System Loop Structure

- In the linear region, the two additional  $x_n$  feedback paths cancel. In effect, then, only the equalized feedback of  $y_n$  acts
- In the nonlinear region, the incremental gain on  $x_{nC}$  is zero. The commanded value of  $x_n$  is either  $+X_{nCL}$  or  $-X_{nCL}$

## Section 5

### CRITICAL TECHNICAL AREAS AND FUTURE RESEARCH AND DEVELOPMENT

This section of the report suggests the future research and development program needed to address the critical technical areas identified by the panel of aircraft industry experts. The several elements of this program are described in terms of their intended purpose and objectives in the subsections which follow.

#### 5.1 IMPROVEMENT OF MATHEMATICAL MODELS

Models having varying degrees of complexity and accuracy are used throughout the aircraft development cycle from preliminary design through flight test. Models currently in use, and especially those in use for the early stages of development, do not tend to incorporate adequate representations of structural flexibility, unsteady aerodynamics, and automatic and manual control functions for use in the ACT context. Research and development are needed to extend and refine those models. The following objectives are suggested:

##### Structural Dynamic Models

- Provide improved initial models of structural dynamic considerations at an earlier stage in design
- Examine alternatives to modal analysis techniques which are better suited for use in active control system design activity
- Develop structural weight factors and control system weight factors as a function of degree of commitment to active control of structural dynamic modes

##### Unsteady Aerodynamic Models

- Improve predictive accuracy throughout design development cycle, particularly in the transonic region
- Develop unsteady aerodynamic models which are appropriate for use with linearized structural dynamic and active control system models
- Develop unsteady aerodynamic control effectiveness models for key types of ACT control surfaces (i.e., wingtip vane, leading edge-trailing edge control surface pairs, spoilers, etc.) which will be used for high-frequency control of lift distribution

##### Steady Aerodynamic Models

- Develop improved transonic aerodynamic models
- Develop techniques for evaluating the root-mean-square component of drag
- Develop aerodynamic control effectiveness models for new types of ACT direct-lift control surfaces (flap configurations) which will be used for low-frequency control of lift distribution

## 5.2 DETAIL DESIGN OF ATT AIRCRAFT

The purpose of producing detail designs for one or more ATT aircraft is to obtain design experience in that portion of the aircraft development cycle wherein the cost-effectiveness impact of active controls can be evaluated with reasonable accuracy. A secondary purpose is to obtain estimates of the degree of commitment to active control functions which is cost effective. The following objectives are suggested:

### Preliminary Design

- Increase experience base for aircraft configuration cycling for design concepts including ACT
- Establish aircraft configuration scaling sensitivities for different degrees of commitment to active control functions
- Develop techniques for determining the required distribution of control authority over the aircraft
- Develop techniques for determining requirements for inherent stiffness and damping (aerodynamic and structural) and for required artificial stiffness and damping
- Develop techniques for evaluating the sensitivity of aircraft gross weight (at constant payload and range) to the degree of commitment to active control functions

### System Design of the Controlled Airframe

- Establish control system reliability requirements
- Establish control authority distribution and control rate requirements and hydraulic power requirements
- Confirm aircraft gross weight reduction advantages for the active control functions used
- Establish critical sources of airframe loading including those resulting from failures
- Estimate flutter boundaries
- Verify satisfaction of handling qualities criteria and ride quality criteria

### Reliability Analysis of Active Control System and Assessment of Failure Modes

- Determine level of failure protection (i.e., fail-operational, fail-safe, etc.) required for each active control function
- Develop control system architecture for flight-critical (fail-operational) and for non-flight-critical portions of the control system and a means for interfacing these portions of the control system
- Develop packaging concept for control system hardware
- Develop concepts for system self-test
- Identify reliability models for control system components

- Perform probability-tree analysis to identify failure modes which are not "extremely improbable." Iterate system architecture until all such failure modes can be safely detected and counteracted by the aircrew so that safe flight to landing is possible

#### Detail Design of Critical Components

- Reduce to practice the required component technology in power actuation, hydraulic power supplies, electronic power supplies, sensors, fault detection, fault isolation, hydraulic power distribution, and electronic power distribution, signal distribution, and component packaging

#### Cost-Effectiveness Evaluation

- Evaluate the impact of ACT application on direct operating costs
- Evaluate the impact of ACT application on maintenance costs. Consider system mean-time-between-maintenance actions, mean-time-to-repair, and the cost of out-of-service status
- Evaluate the impact of flight-critical active control function upon maintenance procedures
- Evaluate the impact of ACT application upon aircraft development schedule, development cost, and number of aircraft sales required to break even
- Evaluate the impact of ACT application upon the airworthiness certification procedure

### 5.3 IRON-BIRD SIMULATION PROGRAM

The purpose of the iron-bird simulation\* program would be to validate an active control system detail design. Emphasis would be placed particularly upon those aspects which have the greatest impact upon cost effectiveness. These are system and component reliability, false alarm rates, maintenance procedures, and system operability.

The objectives of the iron-bird simulation are to:

- Exercise the full hydraulic, electronic, and electromechanical portions of the ACT system
- Expose the ACT system to airline crews and realistic operational profiles to validate system operability
- Perform system checkout and maintenance actions according to airline practice
- Perform accelerated life test on critical subsystem components
- Assess the effects of system malfunctions and failures

---

\*An iron-bird simulation is an assembly of the actual electronic, hydraulic, and electromechanical components of an aircraft flight-control system in their final layout in the aircraft, but not within a flight-qualified airframe. The mounting, often an iron frame, gives rise to the name.

#### 5.4 CONTROL SYSTEM CRITERIA PANEL

A panel of experts in aircraft design and analysis should be convened for the purpose of reviewing the state of the art in control technology for implementing ACT functions and identifying active control system design criteria and recommended design practices.

The objectives of this panel should be as follows:

- Identify generic control laws for implementation of each active control function
- Present methodologies for designing control systems combining several ACT functions
- Present control system architecture for interfacing flight-critical and non-flight-critical control functions
- Develop control system architecture required to serve different reliability requirements. Sensing, computation, logic, actuation, power generation, and power distribution should be considered
- Present component reliability data
- Develop maintenance philosophy for flight-critical components of the control system
- Identify generic solutions to the failure-detection problem
- Develop the philosophy for annunciation of the status of the control system
- Present requirements for self-test architecture in the control system

#### 5.5 AEROELASTIC TECHNIQUES FOR ACT

The difficulties in confirming theoretical estimates of aeroelastic system behavior without a full-scale test aircraft are substantial. Small model tests present difficulties with respect to accurate motion and unsteady pressure distribution measurements. Larger subscale models or test aircraft might circumvent the need for these measurements at reasonable cost, but the techniques for correctly scaling models or test aircraft are presently undeveloped.

The purpose of the research below is to remove the above limitation.

- Evolve experimental techniques for the accurate measurement of elastic motion and unsteady aerodynamic pressure distributions for aeroelastic wind tunnel models
- Refine existing techniques for simulating turbulence fields in wind tunnel test sections

## Appendix A

### HORIZONTAL TAIL SIZING CRITERIA AND PRACTICES WITH ANGLE-OF-ATTACK STABILITY AUGMENTATION VIA ACTIVE CONTROL

The square of the longitudinal short-period undamped natural frequency for the free airframe can be expressed with good approximation as

$$\omega_{sp}^2 = \frac{C_{L\alpha}}{2\mu_c \left(\frac{k_y}{U_0}\right)^2} \left[ -\frac{C_{mq}}{4\mu_c} - C_{mC_L} \right] \quad (A-1)$$

by virtue of the fact that the drag coefficient  $C_D \ll C_L$  (ref. 107), and where

- $\mu_c = m/\rho S \bar{c}$  is the longitudinal relative density
- $k_y$  is the pitching radius of gyration
- $U_0$  is the trimmed true airspeed
- $C_{mq}$  is the nondimensional pitch damping stability derivative,  $[\partial C_m / \partial (q\bar{c} / 2U_0) \leq 0]$
- $-C_{mC_L}$  is the static margin expressed as a decimal fraction of the mean aerodynamic chord,  $\bar{c}$ .

The sum enclosed in brackets in equation (A-1) is referred to as the maneuver margin (ref. 55).<sup>\*</sup> The maneuver margin is seldom more than 2 to 5 percent of  $\bar{c}$  greater than the static margin. By using a primed notation to differentiate maneuver margin from static margin, the maneuver margin is

$$-C_{mC_L}' = -C_{mC_L} - \frac{C_{mq}}{4\mu_c} \quad (A-2)$$

and

$$\omega_{sp}^2 = -\frac{C_{L\alpha} C_{mC_L}'}{2\mu_c \left(\frac{k_y}{U_0}\right)^2} \quad (A-3)$$

<sup>\*</sup>When the static margin is zero, the gradient of elevator angle (and stick force) per "g" is a function only of the damping in pitch. As the static margin becomes negative, the gradient of elevator angle per "g" continues to reduce until at some aft c.g. station it will vanish. This c.g. station is termed the maneuver point.

Equation (A-3) connects  $\omega_{sp}$  with design parameters such as wing location, c.g. location, tail length, tail plane size, and feedback control effectiveness, all of which influence the maneuver margin. Equation (A-3) forms the basis for the approximate interpretation of ordinates in figures 8 and 9 in the text in terms of  $2\mu_c(k_y/U_0)^2\omega_{sp}^2/C_{L\alpha_{WB}}$  with the additional approximation that  $C_{L\alpha} = C_{L\alpha_{WB}}$ , where the subscripts "WB" refer to the wing-body combination without tail plane.

When the inherent maneuver margin is augmented by angle of attack feedback to the pitching moment control surface(s), the effective maneuver margin becomes

$$-C'_{mC_L} = \frac{x_{cg} - x_{acWB}}{\bar{c}} - \bar{V}\eta_H \frac{C_{L\alpha_H}}{C_{L\alpha_{WB}}} \left[ 1 - \frac{\partial\epsilon}{\partial\alpha} + \frac{\partial(\iota_H + \tau\delta_e)}{\partial\alpha} \right] - \frac{C_{mq}}{4\mu_c} \quad (A-4)$$

where

- $x_{cg}$  is the center of gravity station
- $x_{acWB}$  is the effective aerodynamic center station of the wing-body combination
- $\bar{c}$  is the mean aerodynamic chord of the wing
- $\bar{V} = S_H \ell_H / S \bar{c}$  is the horizontal tail volume coefficient
- $\eta_H = q_H / q$  is the dynamic pressure ratio at the horizontal tail
- $C_{L\alpha_H}$  is the partial derivative of the horizontal tail lift coefficient with angle of attack  $\alpha$
- $C_{L\alpha_{WB}}$  is the partial derivative of the wing body lift coefficient with angle of attack
- $\partial\epsilon/\partial\alpha$  is the partial derivative of downwash angle at the horizontal tail with angle of attack
- $C_{mq}/4\mu_c$  the pitch damping contribution, is usually negligible with respect to the angle of attack feedback contribution  $[\bar{V}\eta_H C_{L\alpha_H}/C_{L\alpha_{WB}}] [\partial(\iota_H + \tau\delta_e)/\partial\alpha]$ .

The effects of the nondimensional feedback control gain,  $\partial(\iota_H + \tau\delta_e)/\partial\alpha$  on the maneuver margin with stability augmentation is illustrated in figure A-1, where  $\iota_H$  refers to the incidence of the horizontal tail plane;  $\delta_e$  refers to the elevator deflection;  $\tau = \partial\alpha_H/\partial\delta_e$ , the elevator effectiveness in rotating the zero-lift axis of the tail plane, which is a nonlinear function of the ratio of the elevator area,  $\delta_e$ , to the horizontal tail plane area,  $\delta_H$ ; and  $\partial(\iota_H + \tau\delta_e)/\partial\alpha$  denotes the control surface gain on the feedback of angle of attack (or its more practical dynamical equivalent in reference 56 equalized normal acceleration). Increasing the nondimensional feedback control gain in figure A-1 as  $\bar{V}$  is reduced and/or as the wing-body aerodynamic center is moved forward of the center of gravity makes it possible to maintain the minimum

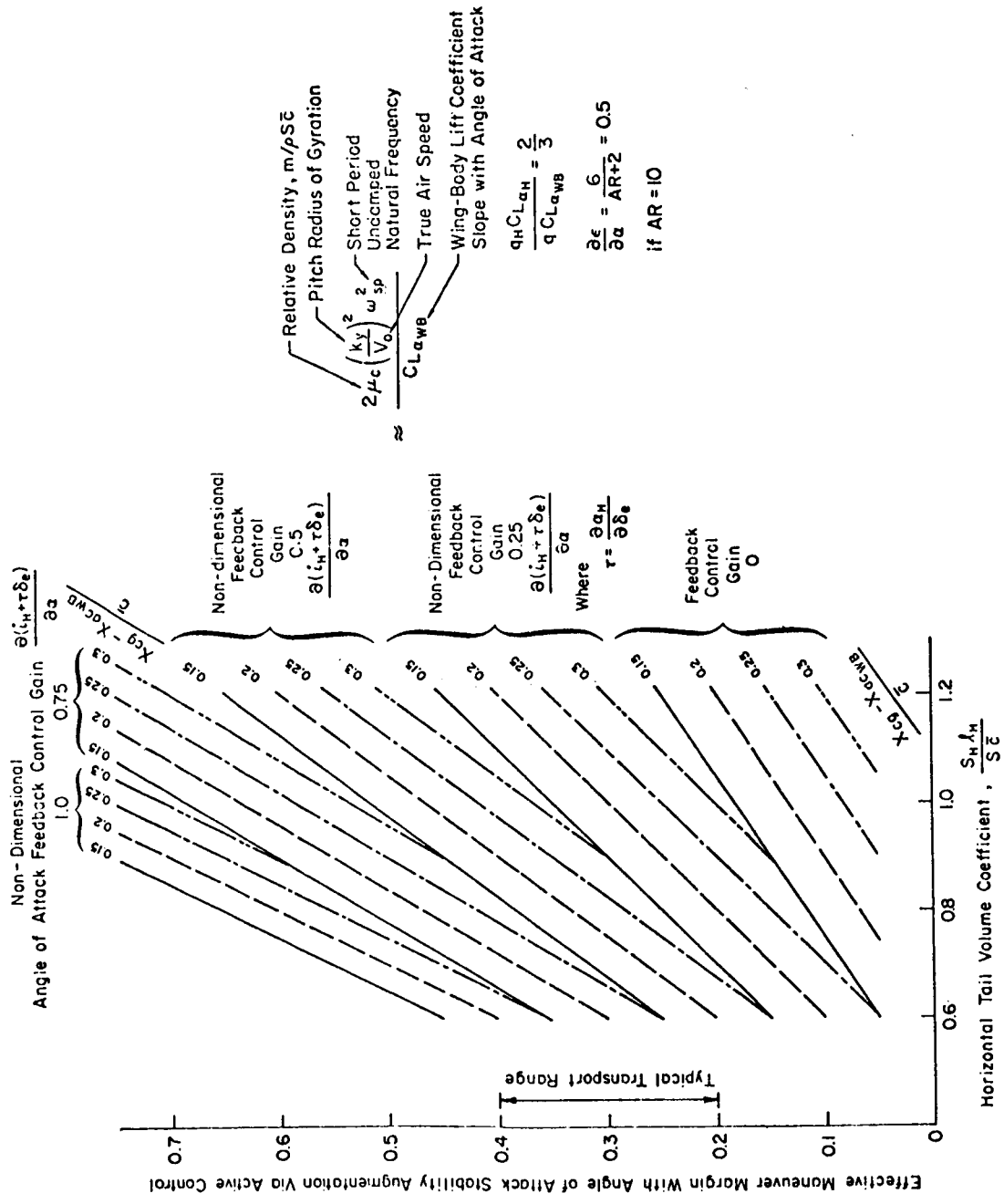


Figure A-1. — Effective Maneuver Margin With Angle-of-Attack Stability Augmentation Versus Horizontal Tail Volume Coefficient as a Function of Angle-of-Attack Feedback Control Gain

maneuver margin required by flying qualities criteria in each flight phase. The significance of these interrelationships is represented in figure 7 in the text by the two constraining lines labeled "Minimum Free Airframe Longitudinal Short Period Frequency" and "5% Stable Inherent Static Margin with Augmented Short Period Dynamic Stability." The implication is that the 5% stable inherent static margin is insufficient by itself to meet the minimum longitudinal short-period frequency requirement, which is, in turn, satisfied with increased feedback control gain as shown in figure A-1.

The feedback control gain  $\partial(\iota_H + \tau\delta_e)/\partial\alpha$  provides the preliminary designer with one connection between control surface authority required for gust regulation and the (closed-loop) variability in angle of attack (about its trimmed value) induced by a given level of variability in gust velocity with stability augmentation.

The other connection can be derived from the relationship for the short period damping coefficient with pitch rate ( $\dot{\theta}$ ) and/or angle-of-attack rate ( $\dot{\alpha}$ ) feedback augmentation. The short-period damping coefficient,  $2\zeta_{sp}\omega_{sp}$ , is given with good approximation by equation (A-5):

$$2\zeta_{sp}\omega_{sp} \doteq \frac{\rho S U_0}{2m}(C_{L\alpha} + C_D) - \frac{\left(\frac{\bar{c}}{2U_0}\right)}{2\mu_c\left(\frac{k_y}{U_0}\right)^2} \left(C_{m_q} + C_{m_{\dot{\alpha}\bar{c}}}\right) \quad (A-5)$$

Since  $1/T_{\theta 2} = \rho S U_0 C_{L\alpha}/2m$  and  $C_D \ll C_{L\alpha}$ , equation (A-5) can be rearranged as

$$2\zeta_{sp}\omega_{sp} - \frac{1}{T_{\theta 2}} \doteq - \frac{\left(\frac{\bar{c}}{2U_0}\right)}{2\mu_c\left(\frac{k_y}{U_0}\right)^2} \left(C_{m_q} + C_{m_{\dot{\alpha}\bar{c}}}\right) \quad (A-6)$$

where

$$C_{m_q} + C_{m_{\dot{\alpha}\bar{c}}}\frac{\bar{c}}{2U_0} = C_{m_{q_{WB}}} - \bar{V} \frac{\ell_H}{\bar{c}} \eta_H C_{L\alpha H} \left[ 2 \left( 1 + \frac{\partial \epsilon}{\partial \alpha} \right) + \frac{\partial(\iota_H + \tau\delta_e)}{\partial\left(\frac{\dot{\theta}\ell_H}{2U_0}\right)} + \frac{\partial(\iota_H + \tau\delta_e)}{\partial\left(\frac{\dot{\alpha}\ell_H}{2U_0}\right)} \right] \quad (A-7)$$

In equation (A-7),  $C_m(\dot{\alpha}\bar{c}/2U_0)$  represents the inherent damping caused by the downwash lag on the horizontal tail and the augmented damping by the angle of attack rate feedback gain  $\partial(\iota_H + \tau\delta_e)/\partial(\dot{\alpha}\ell_H/2U_0)$ . Similarly the damping-in-pitch,  $C_{m_q}$ , is augmented by the pitch rate feedback gain  $\partial(\iota_H + \tau\delta_e)/\partial(\dot{\theta}\ell_H/2U_0)$ .  $\ell_H/\bar{c}$  is the ratio of the horizontal tail length to the mean aerodynamic chord and  $\bar{V}\ell_H/\bar{c} = S_H\ell_H^2/S\bar{c}^2$  is the horizontal tail volumetric moment coefficient. Equation (A-6) shows that as long as  $-[C_{m_q} + C_m(\dot{\alpha}\bar{c}/2U_0)] > 0$ ,  $2\zeta_{sp}\omega_{sp} > 1/T_{\theta 2}$ , where  $1/T_{\theta 2}$  is the larger inverse time constant in the numerator of the pitch attitude response-to-control displacement transfer function. Figure A-2 portrays some of the conditions under which  $-[C_{m_q} + C_m(\dot{\alpha}\bar{c}/2U_0)] > 0$  as a function of the tail volumetric

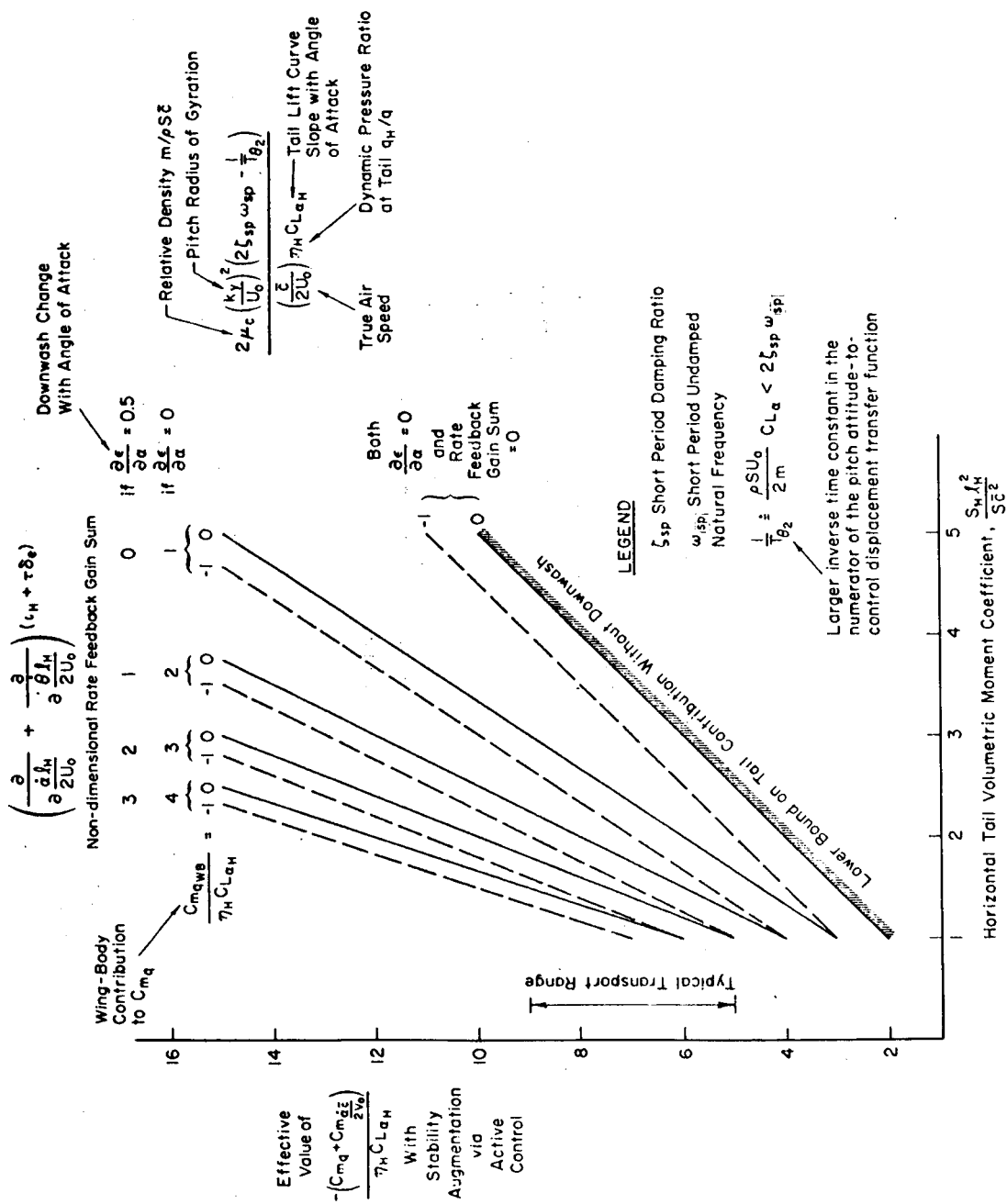


Figure A-2. — Effective Pitch Damping With Stability Augmentation Versus Horizontal Tail Volumetric Moment Coefficient as a Function of Rate Feedback Gain

moment coefficient and the sum of nondimensional feedback gains for  $\dot{\theta}$  and  $\dot{\alpha}$  which provide short period damping augmentation.

The ultimate effect of control authority limits on horizontal tail volume and wing location constraints in figure 7 of the text (with augmented short period dynamic stability) will depend on the trimmed flight condition and will require a stochastic dynamic analysis of gust-induced variability in control displacement and rate. For an example of this stochastic dynamic analysis, the reader may turn to Appendix B.

Appendix B  
 HORIZONTAL TAIL SIZING CRITERIA AND PRACTICES  
 WITH PITCH ATTITUDE STABILITY AUGMENTATION  
 VIA ACTIVE CONTROL

The short-period approximations for the Laplace-transformed linear differential equations of perturbed rigid airframe motion about a trimmed level flight condition are given below from reference 56, together with a third equation representing the feedback of a linear combination of pitch attitude and rate to the general control displacement variable,  $\delta$ . The independent disturbing variables are longitudinal and normal gust velocity,  $u_g$  and  $w_g$ , respectively.

$$(s - Z_w)w - U_0 s \theta = Z_\delta \delta - Z_u u_g - Z_w w_g \quad (B-1)$$

$$-(M_w^* s + M_w)w + (s - M_q) s \theta = M_\delta \delta - M_u u_g - [(M_w^* - M_q/U_0)s + M_w]w_g \quad (B-2)$$

$$-(K_\theta^* s + K_\theta)\theta = \delta - \delta_c \quad (B-3)$$

The dimensional stability derivatives are defined in reference 56:

- $U_0$  is the trimmed true airspeed in m/sec (ft/sec)
- $w$  is the perturbed inertial normal velocity in m/sec (ft/sec)
- $\theta$  is the perturbed pitch attitude in rad
- $K_\theta^*$  is the pitch rate feedback gain in sec
- $K_\theta$  is the dimensionless pitch attitude feedback gain
- $\delta_c$  is the pilot's control displacement command in rad

Three simplifying assumptions will be made in keeping with the purposes of relaxing inherent stability and reducing the horizontal tail volume coefficient:

Assumption 1. The normal force derivative  $Z_\delta$  is negligible, because it consists only of tail contributions.  $\therefore Z_\delta = 0$ .

Assumption 2. The inherent static margin is negligible.  
 $\therefore M_w^* = 0$ .

Assumption 3. The downwash lag effect on the horizontal tailplane is negligible.  $\therefore M_w = 0$ .

If equation (B-3) is substituted in equation (B-2) with these simplifying assumptions, the transformed short period characteristic equation becomes the cubic polynomial:

$$\Delta(s) = (s - Z_w)[s^2 + (K_\theta M_\delta - M_q)s + K_\theta M_\delta] \quad (B-4)$$

Equation (B-4) is the denominator of the transfer functions which can be formed from equations (B-1), (B-2), and (B-3). The transfer function numerators are listed below. Notice from equation (B-4), that since  $-M_q \geq -Z_w$  for transport aircraft, the inherent "short period" will be at least, and usually more than, critically damped without pitch attitude feedback.

Gust Input Numerators for Longitudinal Velocity,  $u_g$ :

$$N_{u_g}^\theta(s) = -M_u(s - Z_w) \quad (B-5)$$

$$N_{u_g}^\gamma(s) = \frac{Z_u}{U_0} [s^2 + (K_\theta M_\delta - M_q)s + K_\theta M_\delta + U_0 M_u Z_w] \quad (B-6)$$

Gust Input Numerators for Normal Velocity,  $w_g$ :

$$\frac{U_0 N_{w_g}^\theta(s)}{s} = M_q(s - Z_w) \quad (B-7)$$

$$U_0 N_{w_g}^\gamma(s) = Z_w [s^2 + (K_\theta M_\delta - 2M_q)s + K_\theta M_\delta] \quad (B-8)$$

Control Input Numerators:

$$N_{\delta_c}^\theta(s) = M_\delta(s - Z_w) \quad (B-9)$$

$$\frac{N_{\delta_c}^w(s)}{U_0} = M_\delta s \quad (B-10)$$

$$N_{\delta_c}^\gamma(s) = -M_\delta Z_w \quad (B-11)$$

The square of the short-period undamped natural frequency will be:

$$\omega_{sp}^2 = K_\theta M_\delta \quad (B-12)$$

from equation (B-4). By substituting the definition of  $M_\delta$  in terms of the non-dimensional control derivative,  $C_{m\delta} = -\bar{V}\eta_H C_{L\alpha_H}$ , where  $\delta = \iota_H + \tau\delta_e$ , and by defining  $K_\theta = -\partial(\iota_H + \tau\delta_e)/\partial\theta$  where  $\tau = \partial\alpha_H/\partial\delta_e$ , the elevator effectiveness,  $\iota_H$  is the horizontal tail incidence, and  $\delta_e$  is the elevator displacement, equation (B-12) can be expressed as:

$$\omega_{sp}^2 = \frac{\bar{V}\eta_H C_{L\alpha_H}}{2\mu_c \left(\frac{k_y}{U_0}\right)^2} \left[ \frac{\partial(\iota_H + \tau\delta_e)}{\partial\theta} \right] \quad (B-13)$$

where

$\bar{V} = S_H \ell_H / S \bar{c}$  is the horizontal tail volume coefficient

$\eta_H = q_H / q$  is the dynamic pressure ratio at the horizontal tail

$C_{L\alpha_H}$  is the the partial derivative of the horizontal tail lift coefficient with angle of attack

$\mu_c = m / \rho S \bar{c}$  is the longitudinal relative density

$k_y$  is the pitching radius of gyration

The effective maneuver margin with pitch attitude feedback can be derived from a rearrangement of equation (B-13) after dividing both sides of equation (B-13) by the partial derivative of the total lift coefficient with angle of attack,  $C_{L\alpha}$ , to preserve the equality. However, for this purpose we shall assume that the partial derivative of the wing-body lift coefficient with angle of attack,  $C_{L\alpha_{WB}} \doteq C_{L\alpha}$ , because the tail contribution to the lift coefficient is small and therefore negligible. The effective maneuver margin is:

$$2\mu_c \left(\frac{k_y}{U_0}\right)^2 \frac{\omega_{sp}^2}{C_{L\alpha_{WB}}} = \frac{\bar{V} \eta_H C_{L\alpha_H}}{C_{L\alpha_{WB}}} \left[ \frac{\partial(\iota_H + \tau \delta_e)}{\partial \theta} \right] \quad (B-14)$$

and is plotted in figure 10 in the text.

The short period damping coefficient,  $2\zeta_{sp} \omega_{sp}$

$$2\zeta_{sp} \omega_{sp} = K_{\dot{\theta}} M_{\delta} - M_q \quad (B-15)$$

from equation (B-4). By substituting the definition of  $M_{\delta}$  as before and by defining  $K_{\dot{\theta}} = -\partial(\iota_H + \tau \delta_e) / \partial \dot{\theta}$ , equation (B-15) can be expressed as:

$$2\zeta_{sp} \omega_{sp} = \frac{(\bar{c} / 2U_0)}{2\mu_c (k_y / U_0)^2} \left\{ -C_{m_{q_{WB}}} + \bar{V} \frac{\ell_H}{\bar{c}} \eta_H C_{L\alpha_H} \left[ 2 + \frac{\partial(\iota_H + \tau \delta_e)}{\partial(\dot{\theta} \ell_H / 2U_0)} \right] \right\} \quad (B-16)$$

where  $C_{m_{q_{WB}}}$  is the non-dimensional wing-body damping-in-pitch derivative.

Equations (B-13) or (B-14) and (B-16) provide a basis for relating augmented short period dynamic properties to design parameters such as tail length, tail-plane size and feedback control effectiveness. What remains now is to complete the connection between these design parameters and control displacement and rate authority. To complete this connection it is necessary to quantify the variability in control displacement and rate required to provide short period stability augmentation in the responses to stochastic gust disturbances and

deterministic, as well as stochastic, maneuvering commands. For commercial transport aircraft, the variability due to stochastic gust disturbances is the more crucial component, because, except for evasive maneuvers, the guidance, control, and maneuvering commands primarily determine trim control displacement and rate authorities. In what follows we shall illustrate the design practices using only the normal gust velocity. The procedure is analogous for the (independent) longitudinal gust velocity. The total variance can then be represented by the sum of the independent contributions.

The variability in normal gust velocity,  $w_g$ , can be characterized by the probability distribution of the standard deviation in  $w_g$ ,  $\sigma_{w_g}$ , in reference 74. Since the gust velocity amplitude distribution can be described by a Gaussian probability distribution, the use of a deterministic versine gust velocity model at a single wavelength is inappropriate for our purpose here. (See reference 56, however, for a discussion of the useful properties of a finite sum of sinusoids in representing a Gaussian random variable.) Nevertheless, because the gust velocity (amplitude) distribution is Gaussian, information about the probabilities of the gust velocity being within specific bounds is readily obtained from the tabulated properties (reference 108) of the Gaussian (normal) probability distribution once the standard deviation,  $\sigma_{w_g}$ , is known.

When a time-invariant linear system, such as our short-period perturbed model of the rigid airframe with pitch attitude and rate stability augmentation in equations (B-1), (B-2), and (B-3), is subjected to a Gaussian random disturbance in normal gust velocity,  $w_g$ , the distributions of control displacement and rate will also be Gaussian. Therefore, complete information about the (first) probability distributions of control displacement and rate can be obtained from their time-averaged squared values or, more compactly, their mean-squared values, which can be estimated readily for stationary linear systems of limited order by means of Phillips' integrals (reference 109).\*

The mean-squared value of the control variable,  $\delta$ , of interest (displacement or rate) can be expressed in terms of its power spectral density,  $\Phi_{\delta\delta}(\omega)$ , by the relationships (references 56 and 109):

$$\sigma_{\delta}^2 = \int_0^{\infty} \Phi_{\delta\delta}(f) df = \frac{1}{2\pi} \int_0^{\infty} \Phi_{\delta\delta}(\omega) d\omega = \frac{1}{2\pi} \int_{-\infty}^{\infty} \frac{\Phi_{\delta\delta}(\omega)}{2} d\omega \quad (\text{B-17})$$

because the power spectral density is an even function of frequency and the mean-squared value is defined as the integral power density over only positive frequencies.

The control power spectral density,  $\Phi_{\delta\delta}(\omega)$ , is related to the power spectral density of the normal gust velocity,  $\Phi_{w_g w_g}(\omega)$ , by the following relationship in the Fourier transform domain:

$$\Phi_{\delta\delta}(\omega) = \left[ \frac{\delta(j\omega)}{w_g(j\omega)} \right] \left[ \frac{\delta(-j\omega)}{w_g(-j\omega)} \right] \Phi_{w_g w_g}(\omega) = \left| \frac{\delta(j\omega)}{w_g(j\omega)} \right|^2 \Phi_{w_g w_g}(\omega) \quad (\text{B-18})$$

---

\* The tables have since been modified and extended through tenth-order systems including connections for  $I_7$  (ref. 110). The higher-order literal expressions for the integrals are lengthy, and the integrals can be expressed more compactly by means of Hurwitz determinants (ref. 111).

where  $\delta(j\omega)/w_g(j)$  is the Fourier transform of the control response weighting function for a unit impulse in  $w_g$ , and  $\delta(-j\omega)/w_g(-j\omega)$  is the conjugate of  $\delta(j\omega)/w_g(j\omega)$ .

The transfer function between  $w_g(s)$  and  $\delta(s)$  can be expressed from the ratio of equation (B-5) to equation (B-4) as:

$$\begin{aligned} \frac{\delta(s)}{w_g(s)} &= (K_{\dot{\theta}}s + K_{\theta}) \frac{N_{w_g}^{\theta}(s)}{\Delta(s)} \\ &= (K_{\dot{\theta}}s + K_{\theta}) \frac{(M_q/U_0)s}{[s^2 + 2\zeta_{sp} \omega_{sp} s + \omega_{sp}^2]} \end{aligned} \quad (B-19)$$

where  $\omega_{sp}^2$  is given by equation (B-13),  $2\zeta_{sp} \omega_{sp}$  by equation (B-16), and

$$\begin{aligned} K_{\theta} &= -\frac{\partial(\iota_H + \tau\delta_e)}{\partial\theta} \\ K_{\dot{\theta}} &= -\frac{\partial(\iota_H + \tau\delta_e)}{\partial\dot{\theta}} = -\left(\frac{\ell_H}{2U_0}\right) \frac{\partial(\iota_H + \tau\delta_e)}{\partial(\dot{\theta}\ell_H/2U_0)} \\ M_q &= \frac{(\bar{c}/2U_0)}{2\mu_c(k_y/U_0)^2} \left( C_{mqWB} - 2\bar{v} \frac{\ell_H}{\bar{c}} \eta_H C_{L\alpha_H} \right) \end{aligned} \quad (B-20)$$

Since the argument of the Laplace transform is complex,  $s = \sigma + j\omega$ , and the Fourier transform required in equation (B-18) can be derived from the transfer function in equation (B-19) by allowing  $\sigma$  to proceed to the limit zero.

The Dryden form of the normal gust power spectral density (reference 38 and 71) can also be expressed as the product of a Fourier transform and its conjugate. (Since the von Karman form of the gust power spectral density cannot be factorized in this way, the Dryden form is preferred for use in Phillips' integrals.) The gust power spectral density in references 38 and 71 is expressed in terms of a spatial frequency,  $\Omega$ , rad/in. (rad/ft) and must be transformed in terms of the temporal frequency,  $\omega = U_0 \Omega$ , rad/sec, so that the variance  $\sigma_{w_g}^2$  remains quantitatively and dimensionally invariant. Therefore:

$$\sigma^2 = \int_0^{\infty} \Phi^s(\Omega) d\Omega = \int_0^{\infty} \Phi^s\left(\frac{\omega}{U_0}\right) d\left(\frac{\omega}{U_0}\right) = \frac{1}{2\pi} \int_0^{\infty} \Phi(\omega) d\omega \quad (B-21)$$

where the superscript "s" denotes the spatial power spectral density defined in reference 38. Consequently, from equation (B-21), the temporal power spectral density for our purpose will be:

$$\Phi(\omega) = \frac{2\pi}{U_0} \Phi^s\left(\frac{\omega}{U_0}\right) \quad (B-22)$$

When particularized for normal gust velocity,  $w_g$ , equation (B-22) becomes:

$$\Phi_{w_g w_g}(\omega) = 2\sigma_{w_g}^2 \frac{L_w}{U_0} \frac{1 + 3\left(\frac{L_w \omega}{U_0}\right)^2}{\left[1 + \left(\frac{L_w \omega}{U_0}\right)^2\right]^2} \frac{(\text{m/sec})^2}{\text{rad/sec}} \quad (\text{B-23})$$

where a probability density function for  $\sigma_{w_g}$  is given in reference 74 and

$$L_w = \begin{cases} 543 \text{ m (1750 ft)}, & \text{if altitude} > 534 \text{ m (1750 ft)} \\ \text{altitude } h, & \text{if } 152 \text{ m (500 ft)} \leq h \leq 534 \text{ m (1750 ft)} \\ 152 \text{ m (500 ft)}, & \text{if altitude} < 152 \text{ m (500 ft)} \end{cases} \quad (\text{Ref. 38})$$

Equation (B-23) can be simplified with good approximation by:

$$\Phi_{w_g w_g}(\omega) \doteq \frac{4\sigma_{w_g}^2 L_w}{\sqrt{3} U_0} \frac{1}{\left[1 + \left(\frac{L_w \omega}{\sqrt{3} U_0}\right)^2\right]} \frac{(\text{m/sec})^2}{\text{rad/sec}} \quad (\text{B-24})$$

without altering the variance defined by equation (B-21). One of the conjugate spectral factors of equation B-24 is:

$$T_{w_g}(j\omega) = 2\sigma_{w_g} \sqrt{\frac{L_w}{\sqrt{3} U_0}} \frac{1}{\left[1 + \frac{L_w}{\sqrt{3} U_0} (j\omega)\right]} \quad (\text{B-25})$$

Equation (B-19) with  $s \rightarrow j\omega$  and equation (B-25) provide one set of conjugate spectral factors for equation (B-18) as:

$$T_{\delta}(j\omega) = 2\sigma_{w_g} \sqrt{\frac{L_w}{\sqrt{3} U_0}} \frac{(M_q/U_0)(j\omega)[K_{\theta}(j\omega) + K_{\theta}]}{\left[(j\omega)^2 + 2\zeta_{sp}\omega_{sp}(j\omega) + \omega_{sp}^2\right] \left[1 + \frac{L_w}{\sqrt{3} U_0} (j\omega)\right]} \quad (\text{B-26})$$

Phillips' integrals (ref. 109) are given in the form:

$$I_n = \frac{1}{2\pi j} \int_{-\infty}^{\infty} \frac{g_n(x) dx}{h_n(x)h_n(-x)} \quad (\text{B-27})$$

where

$$h_n(x) = a_0 x^n + a_1 x^{n-1} + \dots + a_n \quad (\text{B-28})$$

$$g_n(x) = b_0 x^{2n-2} + b_1 x^{2n-4} + \dots + b_{n-1} \quad (\text{B-29})$$

and the roots of  $h_n(x)$  all lie in the upper half plane. However, equation (B-17) requires that:

$$\sigma_{\delta}^2 = \frac{1}{2\pi} \int_{-\infty}^{\infty} \frac{\Phi_{\delta\delta}(\omega)}{2} d\omega = \frac{1}{2\pi j} \int_{-\infty}^{\infty} \frac{T_{\delta}(j\omega)T_{\delta}(-j\omega)}{2} d(j\omega) \quad (B-30)$$

If we identify  $x = j$  and  $T_{\delta}(x)T_{\delta}(-x) = g_n(x)/h_n(x)h_n(-x)$  between equations (B-27) and B-30), then equation (B-30) can be expressed in terms of a third-order Phillips' integral [equation (B-27) with  $n = 3$ ] as:

$$\sigma_{\delta}^2 = \frac{I_3}{2} = \frac{-a_2 b_0 + a_0 b_1 - \frac{a_0 a_1 a_2}{a_3}}{4 a_0 (a_0 a_3 - a_1 a_2)} \quad (B-31)$$

where

$$h_3(x) = \frac{L_w}{\sqrt{3} U_0} x^3 + \left(1 + 2\zeta_{sp} \omega_{sp} \frac{L_w}{\sqrt{3} U_0}\right) x^2 + \left(2\zeta_{sp} \omega_{sp} + \omega_{sp}^2 \frac{L_w}{\sqrt{3} U_0}\right) x + \omega_{sp}^2 \quad (B-32)$$

$$g_3(x) = 4\sigma_{wg}^2 \frac{L_w}{\sqrt{3} U_0} \left(\frac{M_q}{U_0}\right)^2 \left\{ \left[ \frac{l_H}{2U_0} \frac{\partial(\iota_H + \tau\delta_e)}{\partial(\partial l_H / 2U_0)} \right]^2 x^4 + \left[ \frac{\partial(\iota_H + \tau\delta_e)}{\partial\theta} \right]^2 x^2 \right\} \quad (B-33)$$

By comparing equation (B-28) with equation (B-32) and equation (B-29) with equation (B-33), we can identify:

$$a_0 = \frac{L_w}{\sqrt{3} U_0} \quad ; \quad a_1 = 1 + 2\zeta_{sp} \omega_{sp} \frac{L_w}{\sqrt{3} U_0}$$

$$a_2 = 2\zeta_{sp} \omega_{sp} + \omega_{sp} \frac{L_w}{\sqrt{3} U_0} \quad ; \quad a_3 = \omega_{sp}^2$$

$$b_0 = 4\sigma_{wg}^2 \frac{L_w}{\sqrt{3} U_0} \left[ \frac{l_H}{2U_0} \frac{\partial(\iota_H + \tau\delta_e)}{\partial(\partial l_H / 2U_0)} \right]^2 \left(\frac{M_q}{U_0}\right)^2$$

$$b_1 = 4\sigma_{wg}^2 \frac{L_w}{\sqrt{3} U_0} \left[ \frac{\partial(\iota_H + \tau\delta_e)}{\partial\theta} \right]^2 \left(\frac{M_q}{U_0}\right)^2 \quad ; \quad b_2 = 0$$

When these values are substituted in equation (B-31), the variance ratio becomes:

$$\left(\frac{\sigma_{\delta}}{\sigma_{wg}}\right)^2 = \frac{\left(\frac{M_q}{U_o}\right)^2 \left[\frac{\partial(\iota_H + \tau\delta_e)}{\partial\theta}\right]^2 - \left(\frac{M_q}{U_o}\right)^2 \left[\frac{\iota_H}{2U_o} \frac{\partial(\iota_H + \tau\delta_e)}{\partial(\dot{\theta}\iota_H/2U_o)}\right]^2 \left(2\zeta_{sp}\omega_{sp} + \omega_{sp}^2 \frac{L_w}{\sqrt{3} U_o}\right)}{\left[\frac{\omega_{sp}^2 L_w}{\sqrt{3} U_o} - \left(1 + \frac{2\zeta_{sp}\omega_{sp} L_w}{\sqrt{3} U_o}\right) \left(2\zeta_{sp}\omega_{sp} + \frac{\omega_{sp}^2 L_w}{\sqrt{3} U_o}\right)\right]} \quad (B-34)$$

where  $\delta = \iota_H + \tau\delta_e$ , the total horizontal tailplane control displacement. Equation (B-34) provides complete information about the (first) probability distribution of control displacement in terms of the probability distribution of normal gust velocity.

Computation of the variance of control rate,  $\sigma_{\dot{\delta}}^2$ , by means of Phillips' integrals requires the introduction of at least a first-order lag in equation (B-26) to represent the effective bandwidth in the closed-loop system of the control actuator. Otherwise the mean-squared control rate variance would be infinite. The approximate control rate power spectral density,  $\Phi_{\dot{\delta}\dot{\delta}}(\omega)$ , is then related to the control displacement power spectral density,  $\Phi_{\delta\delta}(\omega)$ , in equation (B-18) by equation (B-35).

$$\Phi_{\dot{\delta}\dot{\delta}}(\omega) = \left[\frac{j\omega}{1 + j\omega T_a}\right] \left[\frac{-j\omega}{1 - j\omega T_a}\right] \Phi_{\delta\delta}(\omega) = \frac{\omega^2}{1 + \omega^2 T_a^2} \Phi_{\delta\delta}(\omega) \quad (B-35)$$

where  $1/T_a$  is the effective (first-order) bandwidth of the control actuator in the closed-loop system in rad/sec, and  $[j\omega/(1 + j\omega T_a)]$  is the additional spectral factory by which equation (B-26) must be multiplied to express one conjugate spectral factor of  $\Phi_{\dot{\delta}\dot{\delta}}(\omega)$  as:

$$T_{\dot{\delta}}(j\omega) = 2\sigma_{wg} \sqrt{\frac{L_w}{\sqrt{3} U_o}} \frac{(M_q/U_o)(j\omega)^2 [K_{\dot{\theta}}(j\omega) + K_{\theta}]}{\left[(j\omega)^2 + 2\zeta_{sp}\omega_{sp}(j\omega) + \omega_{sp}^2\right] \left[1 + j\omega T_a\right] \left[1 + \frac{L_w}{\sqrt{3} U_o}(j\omega)\right]} \quad (B-36)$$

The control rate variance can be expressed by the relationships:

$$\sigma_{\dot{\delta}}^2 = \int_0^{\infty} \Phi_{\dot{\delta}\dot{\delta}}(f) df = \frac{1}{2\pi} \int_{-\infty}^{\infty} \frac{\Phi_{\dot{\delta}\dot{\delta}}(\omega)}{2} d\omega = \frac{1}{2\pi j} \int_{-\infty}^{\infty} \frac{T_{\dot{\delta}}(j\omega) T_{\dot{\delta}}(-j\omega)}{2} d(j\omega) \quad (B-37)$$

after the manner of equations (B-17) and (B-30) for control displacement. If we identify  $x = j\omega$  and  $T_{\dot{\delta}}(x)T_{\dot{\delta}}(-x) = g_n(x)/h_n(-x)$  between equations (B-27) and (B-37), then equation (B-37) can be expressed in terms of a fourth-order Phillips' integral [equation (B-27) with  $n = 4$ ] as:

$$\sigma_{\delta}^2 = \frac{I_4}{2} = \frac{b_0(-a_1 a_4 + a_2 a_3) - a_0 a_3 b_1 + a_0 a_1 b_2 + \frac{a_0 b_3}{a_4} (a_0 a_3 - a_1 a_2)}{4a_0(a_0 a_3^2 + a_1^2 a_4 - a_1 a_2 a_3)} \quad (\text{B-38})$$

where

$$\begin{aligned} h_4(x) &= (1 + T_a x) h_3(x) \\ &= \frac{L_w T_a}{\sqrt{3} U_0} x^4 + \left[ T_a \left( 1 + 2\zeta_{sp} \omega_{sp} \frac{L_w}{\sqrt{3} U_0} \right) + \frac{L_w}{\sqrt{3} U_0} \right] x^3 \\ &\quad + \left[ T_a \left( 2\zeta_{sp} \omega_{sp} + \omega_{sp}^2 \frac{L_w}{\sqrt{3} U_0} \right) + 1 + 2\zeta_{sp} \omega_{sp} \frac{L_w}{\sqrt{3} U_0} \right] x^2 \\ &\quad + \left[ T_a \omega_{sp}^2 + 2\zeta_{sp} \omega_{sp} + \omega_{sp}^2 \frac{L_w}{\sqrt{3} U_0} \right] x + \omega_{sp}^2 \end{aligned} \quad (\text{B-39})$$

$$\begin{aligned} g_4(x) &= x^2 g_3(x) \\ &= 4\sigma_{wg}^2 \frac{L_w}{\sqrt{3} U_0} \left( \frac{M_g}{U_0} \right)^2 \left\{ \left[ \frac{l_H}{2U_0} \frac{\partial(\iota_H + \tau \delta_e)}{\partial(\dot{\theta} l_H / 2U_0)} \right]^2 x^6 + \left[ \frac{\delta(\iota_H + \tau \delta_e)}{\partial \theta} \right]^2 x^4 \right\} \end{aligned} \quad (\text{B-40})$$

By comparing equation (B-28) with equation (B-39) and equation (B-29) with equation (B-40), we can identify:

$$\begin{aligned} a_0 &= \frac{L_w T_a}{\sqrt{3} U_0} & ; & \quad a_1 = T_a \left( 1 + 2\zeta_{sp} \omega_{sp} \frac{L_w}{\sqrt{3} U_0} + \frac{L_w}{\sqrt{3} U_0} \right) \\ a_2 &= T_a \left( 2\zeta_{sp} \omega_{sp} + \omega_{sp}^2 \frac{L_w}{\sqrt{3} U_0} \right) + 1 + 2\zeta_{sp} \omega_{sp} \frac{L_w}{\sqrt{3} U_0} \\ a_3 &= \omega_{sp}^2 \left( T_a + \frac{L_w}{\sqrt{3} U_0} \right) + 2\zeta_{sp} \omega_{sp} & ; & \quad a_4 = \omega_{sp}^2 \end{aligned}$$

$b_0$  and  $b_1$  remain exactly as defined previously following equation (B-33)

$$b_2 = b_3 = 0$$

When the values for  $b_0, \dots, b_3$  are substituted in equation (B-38), the variance ratio becomes:

$$\left(\frac{\sigma_{\dot{\delta}}}{\sigma_{wg}}\right)^2 = \frac{\frac{1}{T_a} \left(\frac{M_q}{U_o}\right)^2 \left[ \frac{l_H}{2U_o} \frac{\partial(\iota_H + \tau\delta_e)}{\partial(\dot{\delta}l_H/2U_o)} \right]^2 (-a_1 a_4 + a_2 a_3) - a_3 \frac{L_w}{\sqrt{3} U_o} \left(\frac{M_q}{U_o}\right)^2 \left[ \frac{\partial(\iota_H + \tau\delta_e)}{\partial\theta} \right]^2}{a_0 a_3^2 + a_1 (a_1 a_4 - a_2 a_3)} \quad (B-41)$$

where  $\dot{\delta} = (d/dt)(\iota_H + \tau\delta_e)$ , the total horizontal tailplane control rate and the values for  $a_0, \dots, a_4$  follow equation (B-40). Equation (B-41) provides complete information about the (first) probability distribution of control rate in terms of the probability distribution of normal gust velocity.

Rice (ref. 112) has determined several additional properties of Gaussian random processes besides the variance which are useful in characterizing the temporal properties of normally distributed control displacement and rate. Two useful properties are the expected (or average) number of null (i.e., trim) axis crossings per second and the expected number of exceedences per second with respect to a given level of displacement or rate. These additional properties are summarized in table B-1 in terms of the power spectral densities and variances of the control displacement and rate (ref. 56).

Table B-1. - SOME AVERAGE TEMPORAL PROPERTIES OF A GAUSSIAN RANDOM PROCESS COMPUTED FROM THE POWER SPECTRAL DENSITY  
[From ref. 56]

Mean Square Displacement	$\sigma_{\delta}^2 = \overline{\delta^2}(t) = \frac{1}{2\pi} \int_0^{\infty} \Phi_{\delta\delta}(\omega) d\omega$
Mean Square Rate	$\sigma_{\dot{\delta}}^2 = \overline{\dot{\delta}^2}(t) = \frac{1}{2\pi} \int_0^{\infty} \omega^2 \Phi_{\delta\delta}(\omega) d\omega$
Null Axis Crossings/Second	$N_0 = \frac{\sigma_{\dot{\delta}}}{\pi\sigma_{\delta}}$
Exceedences/Second (Positive crossing of level $x$ per sec. Also an approximation to the number of maxima per sec greater than $x$ for $x > 2\sigma$ )	$N_x = \frac{N_0}{2} e^{-(x^2/2\sigma^2)}$

The first probability distribution function of a random variable,  $x$ , having Gaussian amplitude statistics is:

$$F(x) = \frac{1}{2} \left[ 1 + \operatorname{erf} \frac{(x - \mu)}{\sigma \sqrt{2}} \right] \quad (\text{B-42})$$

where

$$\operatorname{erf} z = \frac{2}{\sqrt{\pi}} \int_0^z e^{-\xi^2} d\xi$$

$$\mu = E(x), \text{ the expected or mean value of } x$$

$$\sigma^2 = E(x - \mu)^2, \text{ the variance of } x$$

In our present application of the Gaussian amplitude distribution to the horizontal tailplane control displacement and rate, the mean value of control displacement is the trimmed value, and mean value of control rate is zero. We are interested in the probabilities of control displacement and rate remaining within or exceeding certain bounds so that we may design reasonable authority and rate limits for the anticipated gust environment. Such probabilities are readily estimated using equation (B-42) or tables of the Gaussian (normal) probability distribution (ref. 108), since the variance  $\sigma^2$  is known from multiplying the variance ratio in equations (B-34) and (B-41) by the variance of normal gust velocity,  $\sigma_{wg}^2$ .

When dealing with low probabilities of exceeding control authority and rate limits, we can approximate the error function by the first term in the asymptotic expansion:

$$\operatorname{erf} z \doteq 1 - \frac{e^{-z^2}}{z \sqrt{\pi}} ; \text{ if } z \gg 1 \quad (\text{B-43})$$

Equation (B-43) makes it possible to simplify the use of equation (B-42) to express the conditional (on  $\sigma$ ) probability of exceeding both a lower bound,  $X_L$ , and an upper bound,  $X_U$ , on control authority (or an absolute bound on rate) as follows:

$$\begin{aligned} 1 - \Pr \left[ X_L < x < X_U \mid \sigma \right] &= 1 - F\left(\frac{X_U - \mu}{\sigma}\right) + F\left(\frac{X_L - \mu}{\sigma}\right) \\ &= \frac{1}{2} \left[ 1 - \operatorname{erf} \frac{X_U - \mu}{\sigma \sqrt{2}} \right] + \frac{1}{2} \left[ 1 - \operatorname{erf} \frac{\mu - X_L}{\sigma \sqrt{2}} \right] \end{aligned} \quad (\text{B-44})$$

$$\doteq \frac{1}{\sqrt{2\pi}} \left\{ \frac{\sigma}{(X_U - \mu)} \exp \left[ -\frac{(X_U - \mu)^2}{2\sigma^2} \right] + \frac{\sigma}{(\mu - X_L)} \exp \left[ -\frac{(\mu - X_L)^2}{2\sigma^2} \right] \right\} \quad (\text{B-45})$$

if  $X_U - \mu \gg \sigma$  and  $\mu - X_L \gg \sigma$ .

If we identify  $(X_U - \mu)/\sigma = k_U \gg 1$  and  $(\mu - X_L)/\sigma = K_L \gg 1$ , equation (B-45) becomes:

$$1 - \Pr[X_L < x < X_U | \sigma] \doteq \frac{1}{\sqrt{2\pi}} \left\{ \frac{e^{-k_U^2/2}}{k_U} + \frac{e^{-k_L^2/2}}{k_L} \right\}; \quad \text{if } k_U \gg 1 \text{ and } k_L \gg 1 \quad (\text{B-46})$$

The factors  $k_U$  and  $k_L$  represent multiples of  $\sigma$  by which the upper and lower control authority (or rate) limits exceed the trimmed control displacement. In preliminary design calculations,  $k_U$  and  $k_L$  may be adjusted to establish an acceptably low value for the conditional probability of exceeding limits in a specific gust environment ( $\sigma_{wg}$ ) as the trim control displacement varies over the operating profile. (Usually the limits will be most critically restrictive in the power approach condition.) Repeated trial adjustments of  $k_U$  and  $k_L$  may be necessary in order to establish acceptable control authority (and rate) limits.

So far we have shown how to estimate only the conditional probability of exceeding limits in a specific gust environment characterized by a single value of  $\sigma_{wg}$ . In reality, however, we should not base preliminary design of limits on a single value of  $\sigma_{wg}$ , because a single value of the gust intensity is not representative over the operating profile. Instead,  $\sigma_{wg}$ , itself, should be treated as a stochastic variable. For example, the probability of occurrence of the gust intensity  $\sigma_{wg}$  in clear air turbulence (CAT) as a function of altitude can be represented by:

$$\Pr(\sigma_{wg} \geq \hat{\sigma}_{wg} ; h) = \Pr(\sigma_{wg} \geq \hat{\sigma}_{wg} | \text{CAT}) \Pr_{\text{CAT}}(h) \quad (\text{B-47})$$

where  $\Pr(\sigma_{wg} \geq \hat{\sigma}_{wg} | \text{CAT})$  is the conditional probability of equalling or exceeding the magnitude  $\hat{\sigma}_{wg}$ , if clear air turbulence is encountered and  $\Pr_{\text{CAT}}(h)$  is the probability of occurrence of clear air turbulence as a function of altitude. An expression analogous to equation (B-47) applies also to storm air turbulence (SAT).

The overall probability of exceeding control authority (or rate) limits as a function of altitude can be expressed as:

$$\begin{aligned} \Pr[X_L > x > X_U | h] &\doteq \Pr_{\text{SAT}}(h) \int_0^{\infty} \Pr[X_L > x > X_U | \sigma_{wg}] p(\sigma_{wg} | \text{SAT}) d\sigma_{wg} \\ &+ \Pr_{\text{CAT}}(h) \int_0^{\infty} \Pr[X_L > x > X_U | \sigma_{wg}] p(\sigma_{wg} | \text{CAT}) d\sigma_{wg} \end{aligned} \quad (\text{B-48})$$

where

- $p(\sigma_{wg} | \text{CAT})$  is the conditional probability density function of  $\sigma_{wg}$ , given that clear air turbulence is encountered and is obtained from reference 74 as  $(\sqrt{2/\pi}/b_1)\exp(-\sigma_{wg}^2/2b_1^2)$
- $\text{Pr}_{\text{CAT}}(h)$  is called  $P_1$  in reference 74
- $p(\sigma_{wg} | \text{SAT})$  is the conditional probability density function of  $\sigma_{wg}$ , given that storm air turbulence is encountered and is also obtained from reference 74 and  $(\sqrt{2/\pi}/b_2)\exp(-\sigma_{wg}^2/2b_2^2)$
- $\text{Pr}_{\text{SAT}}(h)$  is called  $P_2$  in reference 74, which provides numerical values for  $b_1$ ,  $P_1$ ,  $b_2$ , and  $P_2$  as functions of altitude
- $1 - \text{Pr}[X_L > x > X_U | \sigma_{wg}]$  is the conditional probability of exceeding both limits on control authority (or rate) as a function of  $\sigma_{wg}$  derived from equations (B-44) or (B-46) using the appropriate variance ratio from equations (B-34) or (B-41)

If one wishes to obtain a still broader probability estimate for exceeding the control authority or rate limits, a mission analysis approach may be applied to eliminate the conditional dependence upon altitude,  $h$ . The procedure is similar to that used to convert the conditional dependence upon  $\sigma_{wg}$  to a broader conditional dependence upon altitude in equation (B-48).

## Appendix C

### TRIM DRAG

#### C.1 AIRCRAFT WITH HORIZONTAL TAIL

The total drag coefficient,  $C_D = \text{Drag}/qS$ , can be partitioned into parasite and lift-induced components by equation (A-1) for an aircraft with a horizontal tail of area  $S_H$  and moment arm  $l_H$ , a wing of area  $S$  and mean aerodynamic chord  $\bar{c}$  and dynamic pressure  $q$ .

$$C_D = C_{D_0} + C_{D_0|\delta|} |\delta| + K_P (C_{L_0} + C_{L_{\alpha_{WB}}} \alpha)^2 + \eta_H (S_H/S) K_{PH} C_{LH}^2 + \eta_H (S_H/S) C_{LH} \epsilon \quad (C-1)$$

where

$K_P = 1/\pi AR e$  for the wing-body combination

$AR =$  Wing aspect ratio

$e =$  Oswald's efficiency factor for the wing-body combination

$K_{PH} = 1/\pi AR_H e_H$  for the horizontal tail

$AR_H =$  Tailplane aspect ratio

$e_H =$  Oswald's efficiency factor to the tailplane-body combination

$C_{D_0} = C_{D_{0WB}} + \eta_H (S_H/S) C_{D_{0H}}$  is the partition of zero lift drag coefficient between the wing-body combination and the horizontal tail of area  $S_H$

$C_{D_0|\delta|} = \eta_H (S_H/S) C_{D_{0H}|\delta|}$  is the partial derivative of zero lift drag coefficient with control surface displacement  $\delta$  for the horizontal tail

$\delta = \iota_H + \tau \delta_e$ , control displacement

$\iota_H =$  Incidence of the horizontal tail

$\delta_e =$  Elevator displacement

$\tau = \partial \alpha_H / \partial \delta_e$  is the elevator effectiveness in rotating the zero lift axis of the tailplane

- $\epsilon$  = Wing downwash angle at the horizontal tail
- $\epsilon_\alpha = \partial\epsilon/\partial\alpha = f(\ell_H/\bar{c})$  is the partial derivative of downwash at the horizontal tail with respect to the wing-body angle of attack and is a nonlinear function of the horizontal tail length to mean aerodynamic wing chord ratio,  $\ell_H/\bar{c}$
- $C_{L_0}$  = Lift coefficient at zero angle of attack and zero control displacement (defined in such a manner that the tail lift is zero)
- $C_{L_{\alpha_{WB}}}$  = Partial derivative of lift coefficient with angle of attack  $\alpha$  for the wing-body combination
- $C_{L_H}$  = The horizontal tail lift coefficient
- $C_{L_T} = \eta_H(S_H/S)C_{L_H}$  is the equivalent tail contribution to the total lift coefficient
- $C_{L_{T\alpha}} = \eta_H(S_H/S)C_{L_{\alpha_H}}(1-\epsilon_\alpha)$  is the equivalent tail contribution to the total partial derivative of lift coefficient with angle of attack  $\alpha$
- $\eta_H = q_H/q$  is the dynamic pressure ratio at the horizontal tail
- $C_{L_{\alpha_H}}$  = The partial derivative of the horizontal tail lift coefficient with respect to the angle of attack of the horizontal tail  $\alpha_H$
- $C_{L_\delta} = \eta_H(S_H/S)C_{L_{\delta_H}}$  is the partial derivative of the total lift coefficient with control displacement
- $C_{L_{\delta_H}}$  = The partial derivative of the horizontal tail lift coefficient with control displacement

The lift coefficient and pitching moment coefficient equations required to trim the aircraft can be solved for  $\alpha, \delta$  in terms of the gross weight,  $W$ , dynamic pressure,  $q$ , wing area,  $S$ , and  $C_{L_0}$ . Equations (C-2) and (C-3) represent the trim conditions.

$$\begin{bmatrix} C_{m_\alpha} & C_{m_\delta} \\ C_{L_\alpha} & C_{L_\delta} \end{bmatrix} \begin{Bmatrix} \alpha \\ \delta \end{Bmatrix} = \begin{Bmatrix} -C_{m_0} \\ W/qS - C_{L_0} \end{Bmatrix} \quad \begin{matrix} \text{(Trimmed } C_m = 0) \\ \text{(Trimmed } C_L = W/qS) \end{matrix} \quad \begin{matrix} \text{(C-2)} \\ \text{(C-3)} \end{matrix}$$

Horizontal tail drag contributions to the pitching moment are neglected in equation (C-2).

where

$$C_{L\alpha} = C_{L\alpha_{WB}} + C_{L\alpha_T}$$

$$C_{m\alpha} = C_{L\alpha_{WB}} \left( \frac{x_{cg} - x_{ac_{WB}}}{\bar{c}} \right) - \bar{V} \eta_H C_{L\alpha_H} (1 - \epsilon_\alpha)$$

$$C_{m\delta} = -\eta_H C_{L\delta_H} \bar{V}$$

$C_{m_0}$  = Pitching moment coefficient at zero angle of attack and zero control displacement

$\bar{V}$  =  $S_H l_H / S \bar{c}$  is the horizontal tail volume coefficient

$x_{cg}$  = The center of gravity station

$x_{ac_{WB}}$  = The wing-body aerodynamic center station

The angle of attack,  $\alpha$ , and the control displacement,  $\delta$ , required to trim the aircraft are given by equations (C-4) and (C-5) which represent the simultaneous solution of equations (C-2) and (C-3).

$$\alpha = \frac{-C_{m_0} C_{L\delta} + C_{L_0} C_{m\delta} - W C_{m\delta} / qS}{C_{m\alpha} C_{L\delta} - C_{L\alpha} C_{m\delta}} \quad (C-4)$$

$$\delta = \frac{C_{m_0} C_{L\alpha} - C_{L_0} C_{m\alpha} + W C_{m\alpha} / qS}{C_{m\alpha} C_{L\delta} - C_{L\alpha} C_{m\delta}} \quad (C-5)$$

The denominator of equations (C-4) and (C-5) can be expressed in simpler terms of tail geometry and partial derivatives of lift coefficient by the following substitutions:

$$\begin{aligned} \Delta &= C_{m\alpha} C_{L\delta} - C_{L\alpha} C_{m\delta} = \eta_H C_{L\delta_H} \left( \frac{S_H}{S} C_{m\alpha} + \bar{V} C_{L\alpha} \right) \\ &= \eta_H C_{L\delta_H} \left\{ \frac{S_H}{S} C_{L\alpha_{WB}} \left( \frac{x_{cg} - x_{ac_{WB}}}{\bar{c}} \right) - \frac{S_H}{S} \bar{V} \eta_H C_{L\alpha_H} (1 - \epsilon_\alpha) \right. \\ &\quad \left. + \bar{V} C_{L\alpha_{WB}} + \frac{S_H}{S} \bar{V} \eta_H C_{L\alpha_H} (1 - \epsilon_\alpha) \right\} \end{aligned} \quad (C-6)$$

$$= C_{L\alpha_{WB}} C_{L\delta_H} \eta_H \frac{S_H}{S} \left( \frac{x_H - x_{ac_{WB}}}{\bar{c}} \right) = C_{L\alpha_{WB}} C_{L\delta} \left( \frac{x_H - x_{ac_{WB}}}{\bar{c}} \right)$$

Similar substitutions in each expression for  $\alpha, \delta$  give:

$$\alpha = \frac{-C_{m_0} + \left(\frac{W}{qS} - C_{L_0}\right)\left(\frac{l_H}{\bar{c}}\right)}{C_{L_{\alpha_{WB}}}\left(\frac{x_H - x_{ac_{WB}}}{\bar{c}}\right)} \quad (C-7)$$

$$\delta = \frac{C_{m_0}C_{L_{\alpha}} + \left(\frac{W}{qS} - C_{L_0}\right)C_{m_{\alpha}}}{C_{L_{\alpha_{WB}}}C_{L_{\delta}}\left(\frac{x_H - x_{ac_{WB}}}{\bar{c}}\right)} \quad (C-8)$$

In equations (C-6) to (C-8) the horizontal tail length,  $l_H$ , is defined as  $x_H - x_{cg}$ , where  $x_H$  is the fuselage station for the center of tail lift. In turn,  $l_H = x_H - x_{cg} = x_H - x_{ac_{WB}} - (x_{cg} - x_{ac_{WB}})$  can be substituted in equation (C-7) to give:

$$C_{L_{\alpha_{WB}}}\alpha = -\frac{C_{m_0}}{\left(\frac{x_H - x_{ac_{WB}}}{\bar{c}}\right)} + \left(\frac{W}{qS} - C_{L_0}\right)\left[1 - \left(\frac{x_{cg} - x_{ac_{WB}}}{x_H - x_{ac_{WB}}}\right)\right] \quad (C-9)$$

Equation (C-10) represents the trimmed wing-body lift coefficient in terms of wing and tail moment arms with respect to the center of gravity:

$$C_{L_0} + C_{L_{\alpha_{WB}}}\alpha = \frac{W}{qS} - \frac{C_{m_0}}{\left(\frac{x_H - x_{ac_{WB}}}{\bar{c}}\right)} - \left(\frac{W}{qS} - C_{L_0}\right)\left(\frac{x_{cg} - x_{ac_{WB}}}{x_H - x_{ac_{WB}}}\right) \quad (C-10)$$

Further substitution and simplification of expressions for  $C_{L_{\alpha}}$  and  $C_{m_{\alpha}}$  in equation (C-8) give:

$$C_{L_{\delta}}\delta = \frac{C_{m_0}}{\left(\frac{x_H - x_{ac_{WB}}}{\bar{c}}\right)} + \left(\frac{W}{qS} - C_{L_0}\right)\left(\frac{x_{cg} - x_{ac_{WB}}}{x_H - x_{ac_{WB}}}\right) \quad (C-11)$$

$$+ \frac{S_H}{S} \eta_H \frac{C_{L_{\alpha_H}}}{C_{L_{\alpha_{WB}}}} (1 - \epsilon_{\alpha}) \left\{ \frac{C_{m_0}}{\frac{x_H - x_{ac_{WB}}}{\bar{c}}} - \left(\frac{W}{qS} - C_{L_0}\right) \left[ 1 - \left(\frac{x_{cg} - x_{ac_{WB}}}{x_H - x_{ac_{WB}}}\right) \right] \right\}$$

Equation (C-9) can be substituted in equation (C-11) to give the simpler form

$$C_{L\delta}^{\delta} = \frac{C_{m_0}}{\left(\frac{x_H - x_{acWB}}{\bar{c}}\right)} + \left(\frac{W}{qS} - C_{L_0}\right) \left(\frac{x_{cg} - x_{acWB}}{x_H - x_{acWB}}\right) - \frac{S_H}{S} \eta_H \frac{C_{L\alpha_H}}{C_{L\alpha_{WB}}} (1 - \epsilon_{\alpha}) (C_{L\alpha_{WB}} \alpha) \quad (C-11a)$$

in which we can recognize  $C_{L_T} \alpha = (S_H/S) \eta_H (C_{L\alpha_H}/C_{L\alpha_{WB}}) (1 - \epsilon_{\alpha}) (C_{L\alpha_{WB}} \alpha)$  so that equation (C-12) represents the trimmed tail contribution to the total lift coefficient in terms of wing and tail moment arms with respect to the center of gravity:

$$C_{L_T} = \eta_H \frac{S_H}{H} C_{L_H} = C_{L_T} \alpha + C_{L\delta}^{\delta} = \frac{C_{m_0}}{\left(\frac{x_H - x_{acWB}}{\bar{c}}\right)} + \left(\frac{W}{qS} - C_{L_0}\right) \left(\frac{x_{cg} - x_{acWB}}{x_H - x_{acWB}}\right) \quad (C-12)$$

Equation (C-12) can be substituted in equation (C-10) to confirm the obvious relationship from equation (C-3):

$$C_{L_0} + C_{L\alpha_{WB}} \alpha = \frac{W}{qS} - C_{L_T} \quad (C-3a)$$

where

$$C_{L_T} \geq 0, \text{ but } |C_{L_T}| = \left| \eta_H \frac{S_H}{H} C_{L_H} \right| \ll \frac{W}{qS}$$

Alternatively, equation (C-11) can be directly rearranged to give equation (C-11b):

$$C_{L\delta}^{\delta} = \left\{ \frac{C_{m_0}}{\left(\frac{x_H - x_{acWB}}{\bar{c}}\right)} + \left(\frac{W}{qS} - C_{L_0}\right) \left(\frac{x_{cg} - x_{acWB}}{x_H - x_{acWB}}\right) \right\} \left[ 1 + \frac{S_H}{S} \eta_H \frac{C_{L\alpha_H}}{C_{L\alpha_{WB}}} (1 - \epsilon_{\alpha}) \right] - \left(\frac{W}{qS} - C_{L_0}\right) \frac{S_H}{S} \eta_H \frac{C_{L\alpha_H}}{C_{L\alpha_{WB}}} (1 - \epsilon_{\alpha}) \quad (C-11b)$$

A reasonable approximation to the wing downwash angle at the horizontal tail is  $K_p e [(W/qS) - C_{L_T}]/2$ . If compressibility effects are neglected, the total drag coefficient in equation (C-1) can now be expressed as

$$C_D = C_{D_{OWB}} + \eta_H C_{D_{OH}} \left( \frac{S_H}{S} \right) + \frac{C_{D_{OH}} |\delta|}{C_{L\delta}} |C_{L\delta} \delta| + K_{PH} C_{LT} C_{LH} \quad (C-13)$$

$$+ K_P \left( \frac{W}{qS} - C_{LT} \right) \left( \frac{W}{qS} - C_{LT} \left[ 1 - \frac{e}{2} \right] \right)$$

where  $C_{L\delta} \delta$  is given by equation (C-11b),  $C_{L_{\alpha_{WB}}}$  by equation (C-9) and  $C_{LT}$  and  $C_{LH}$  by equation (C-12).

Observations and Conclusions about  $C_D$  for the aircraft with a tailplane.

1. The induced drag coefficient:

$$K_P \left( \frac{W}{qS} - C_{LT} \right) \left( \frac{W}{qS} - C_{LT} \left[ 1 - \frac{e}{2} \right] \right) + K_{PH} C_{LT} C_{LH} \geq K_P \left( \frac{W}{qS} \right)^2$$

if  $C_{LT} \leq 0$ , where  $K_P (W/qS)^2$  is the induced drag coefficient for a tailless aircraft.\* This is so because  $|C_{LT}| < W/qS$ ,  $[1 - e/2] > 0$ , and  $C_{LT} C_{LH} \geq 0$ .

2.  $C_{LT} \leq 0$ , if  $(x_{cg} - x_{ac_{WB}})/\bar{c} \leq -C_{m_0}/[W/qS - C_{L_0}]$ , which, in the special case  $C_{m_0} = 0$ , requires that the center of gravity be at or forward of the wing-body aerodynamic center. The dominant term involving tail contribution to induced drag is  $K_P (W/qS) (2 - e/2) C_{LT}$ .
3.  $C_{LT}$  is inversely proportional to  $[(x_H - x_{ac_{WB}})/\bar{c}]$ , which is on the order of 3 to 4.
4. The additional parasite drag of the horizontal tailplane is proportional to the tail area ratio,  $S_H/S$ .
5. The parasite drag of the tailplane control is proportional to:

$$|C_{L\delta} \delta| = \left| C_{LT} \left[ 1 + \frac{S_H}{H} \eta_H \frac{C_{L\alpha_H}}{C_{L\alpha_{WB}}} (1 - \epsilon_\alpha) \right] - \left( \frac{W}{qS} - C_{L_0} \right) \frac{S_H}{S} \eta_H \frac{C_{L\alpha_H}}{C_{L\alpha_{WB}}} (1 - \epsilon_\alpha) \right| \quad (C-14)$$

where  $C_{LT} \leq 0$  is inversely proportional to  $(x_H - x_{ac_{WB}})/\bar{c}$ , which is about 3 or 4, and independent of tail area, whereas the balance of the contribution is proportional to the tail area ratio,  $S_H/S$ . The parasite drag of the tailplane control will vanish if:

$$C_{LT} = \left( \frac{W}{qS} - C_{L_0} \right) \frac{\left[ \frac{S_H}{S} \eta_H \frac{C_{L\alpha_H}}{C_{L\alpha_{WB}}} (1 - \epsilon_\alpha) \right]}{\left[ 1 + \frac{S_H}{S} \eta_H \frac{C_{L\alpha_H}}{C_{L\alpha_{WB}}} (1 - \epsilon_\alpha) \right]} \quad (C-15)$$

\*See the first observation in the following topic, "Horizontal Tailless Aircraft."

Since  $C_{L_T}$  is given by equation (C-12), the parasite control drag will vanish if:

$$\frac{x_{cg} - x_{acWB}}{\bar{c}} = \frac{-C_{m_0}}{\left(\frac{W}{qS} - C_{L_0}\right)} + \left(\frac{x_H - x_{acWB}}{\bar{c}}\right) \frac{\left[\frac{S_H}{S} \eta_H \frac{C_{L\alpha_H}}{C_{L\alpha_{WB}}} (1 - \epsilon_\alpha)\right]}{\left[1 + \frac{S_H}{S} \eta_H \frac{C_{L\alpha_H}}{C_{L\alpha_{WB}}} (1 - \epsilon_\alpha)\right]} \quad (C-16)$$

which, in the special case,  $C_{m_0} = 0$ , requires that the center of gravity be aft of the wing-body aerodynamic center in the proportion:

$$0 < \frac{x_{cg} - x_{acWB}}{x_H - x_{acWB}} = \frac{\frac{S_H}{S} \eta_H \frac{C_{L\alpha_H}}{C_{L\alpha_{WB}}} (1 - \epsilon_\alpha)}{1 + \frac{S_H}{S} \eta_H \frac{C_{L\alpha_H}}{C_{L\alpha_{WB}}} (1 - \epsilon_\alpha)} \ll 1 \quad (C-17)$$

## C.2 HORIZONTAL TAILLESS AIRCRAFT

The total drag coefficient,  $C_D = \text{Drag}/qS$ , can be partitioned into parasite and lift-induced components by equation (C-18) for a horizontal tailless aircraft with wing area  $S$ , mean aerodynamic chord  $\bar{c}$ , effective elevon center of lift station  $x_e$ , center of gravity station  $x_{cg}$ , and dynamic pressure  $q$

$$C_D = C_{D_0} + C_{D_0|\delta|} |\delta| + K_P [C_{L_0} + C_{L\alpha} \alpha + C_{L\delta} \delta]^2 \quad (C-18)$$

where

$$K_P = 1/\pi A Re$$

AR = Wing aspect ratio

e = Oswald's efficiency factor

$$C_{D_0} = C_{D_{0WB}}$$

$$C_{D_0|\delta|} = C_{D_0|\delta|}$$

$$C_{L\delta} \equiv C_{L\delta}$$

$$C_{m\delta} = -C_{L\delta} \frac{x_e - x_{cg}}{\bar{c}}$$

$$C_{L\alpha} = C_{L\alpha_{WB}}$$

$$C_{m\alpha} = C_{L\alpha_{WB}} \left( \frac{x_{cg} - x_{ac_{WB}}}{\bar{c}} \right)$$

$$C_{L_0} + C_{L\alpha}\alpha + C_{L\delta}\delta = \frac{W}{qS} \quad \text{by equation (C-3)}$$

The denominator of the trim equations (C-2) and (C-3) for a tailless aircraft becomes:

$$\begin{aligned} \Delta &= C_{m\alpha}C_{L\delta} - C_{L\alpha}C_{m\delta} = C_{L\delta} \left[ C_{m\alpha} + C_{L\alpha} \left( \frac{x_e - x_{cg}}{\bar{c}} \right) \right] \\ &= C_{L\delta}C_{L\alpha_{WB}} \left[ \left( \frac{x_{cg} - x_{ac_{WB}}}{\bar{c}} \right) + \left( \frac{x_e - x_{cg}}{\bar{c}} \right) \right] \\ &= C_{L\delta}C_{L\alpha_{WB}} \left( \frac{x_e - x_{ac_{WB}}}{\bar{c}} \right) \end{aligned} \quad (C-19)$$

The  $\alpha$  and  $\delta$  required to trim the tailless aircraft are given by equations (C-20) and (C-21):

$$\alpha = \frac{-C_{m_0} + \left( \frac{W}{qS} - C_{L_0} \right) \left( \frac{x_e - x_{cg}}{\bar{c}} \right)}{C_{L\alpha_{WB}} \left( \frac{x_e - x_{ac_{WB}}}{\bar{c}} \right)} \quad (C-20)$$

$$\delta = \frac{C_{m_0}C_{L\alpha_{WB}} + \left( \frac{W}{qS} - C_{L_0} \right) \left[ C_{L\alpha_{WB}} \left( \frac{x_{cg} - x_{ac_{WB}}}{\bar{c}} \right) \right]}{C_{L\delta}C_{L\alpha_{WB}} \left( \frac{x_e - x_{ac_{WB}}}{\bar{c}} \right)} \quad (C-21)$$

$$C_{L\delta}\delta = \frac{C_{m_0} + \left( \frac{W}{qS} - C_{L_0} \right) \left( \frac{x_{cg} - x_{ac_{WB}}}{\bar{c}} \right)}{\left( \frac{x_e - x_{ac_{WB}}}{\bar{c}} \right)} \quad (C-21a)$$

The total drag coefficient in equation (C-18) can now be expressed as:

$$C_D = C_{D_{0WB}} + \frac{C_{D_0} |\delta|}{C_{L_\delta}} |C_{L_\delta} \delta| + K_P \left( \frac{W}{qS} \right)^2 \quad (C-22)$$

where  $C_{L_\delta} \delta$  is given by equation (C-21a).

Observations and Conclusions about  $C_D$  for the horizontal tailless aircraft.

1. The induced drag coefficient is  $K_P(W/qS)^2$ .
2. The parasite drag of the elevon displacement required to trim is inversely proportional to  $(x_e - x_{acWB})/\bar{c}$ , which is on the order of 0.5. Therefore, the parasite trim drag of the elevon is about six to eight times more sensitive to the inherent static margin of the wing-fuselage combination than the induced trim drag of a horizontal tail, which is inversely proportional to  $[(x_H - x_{acWB})/\bar{c}]$ , on the order of 3 to 4 [cf. equations (C-12), (C-14), and (C-21a); (C-13) and (C-22)]. The parasite drag of the elevon displacement will vanish if:

$$\frac{x_{cg} - x_{acWB}}{\bar{c}} = \frac{-C_{m_0}}{\left( \frac{W}{qS} - C_{L_0} \right)} \quad (C-23)$$

which, in the special case,  $C_{m_0} = 0$ , requires that the center of gravity be at the wing-body aerodynamic center.

Appendix D  
 COMPARISON OF RIDE AND TAIL LOAD RESPONSES  
 FOR A SIMPLIFIED CASE OF A YAW DAMPER

The purpose of this Appendix is to show that control of ride quality and control of lateral shear (and bending moment) load on the aft fuselage are similar objectives when viewed within the context of this simplified example. The results have more general instructive value, however. For example, effects of structural flexibility modes are similar in kind to the rigid-body mode considered in the example: the only difference being the conceptually unimportant difference in mode shapes. Furthermore, the conclusions for this simple example would seem to hold for all cases wherein ride is to be controlled in a portion of the aircraft which develops relatively little aerodynamic force (i.e., the fuselage), and the critical structural loading tends to occur at points where the main aerodynamic forces are carried into the portion of the aircraft in which ride is to be controlled (e.g., wing root, aft fuselage).

Consider the simplified yawing moment equation.

$$s^2\psi = N'_\beta(\beta - \beta_g) + N'_r(s\psi - s\beta_g) + N'_{\delta_r} \delta_r \quad (D-1)$$

If we neglect any change in flight path angle, then  $\beta = -\psi$  and the lateral acceleration input to a passenger located a distance  $l_x$  in front of the aircraft c.g. is  $a'_y$

$$a'_y = l_x s^2\psi \quad (D-2)$$

and to a lateral accelerometer located a distance  $l_a$  in front of the aircraft c.g. is  $a''_y$

$$a''_y = l_a s^2\psi \quad (D-3)$$

Let the yaw damper control law for the rudder be given by:

$$\delta_r = -K_a a''_y - K_r s\psi = -(K_a l_a s^2 + K_r s) \psi \quad (D-4)$$

The closed-loop transfer functions for responses to side gusts,  $\beta_g$ , are

$$\frac{\beta}{\beta_g} = \frac{-\psi}{\beta_g} = \frac{sN'_r + N'_\beta}{\Delta} \quad (D-5)$$

$$\frac{a'_y}{\beta_g} = \frac{-l_x s^2 (sN'_r + N'_\beta)}{\Delta} \quad (D-6)$$

where

$$\Delta = s^2 [1 + K_a l_a N'_{\delta_r}] + s [K_r - N'_r] + N'_\beta \quad (D-7)$$

The  $a'_y$  response is, of course, the main determinant of lateral ride quality. The lateral sharing tail load on the aft fuselage is the sum of aerodynamic forces on the tail and inertial reaction forces on the tail. If one assumes for the sake of simplicity that the stability derivatives,  $N'_\beta$  and  $N'_r$ , are due entirely to aerodynamic forces developed on the tail surfaces, then the tail load,  $T$ , on the aft fuselage in response to side gusts,  $\beta_g$ , is given approximately by the closed-loop transfer function

$$\frac{T}{\beta_g} = \frac{I_z - m_t l_t^2}{l_t} \frac{s^2 (sN'_r + N'_\beta)}{\Delta} \quad (D-8)$$

where  $I_z$  is the complete aircraft moment of inertia about the yaw axis with respect to its c.g.,  $m_t$  is the mass of the tail section, and  $l_t$  is the distance the tail section c.g. is behind the complete aircraft c.g.

The important point to appreciate is that the transfer functions for the ride response,  $a'_y$ , and the tail load response,  $T$ , to side gusts are the same except for a scale factor. Consequently, both responses are affected in precisely the same proportion by the yaw damper control law, and the control objective is to reduce the response in each case. The conclusion is that ride quality control and tail load control place similar, rather than conflicting, requirements for control.

In a more detailed treatment of the problem, the requirements would most likely be less similar than for this highly simplified treatment. Nevertheless, the basic trend revealed above would still be dominant.

## Appendix E

### APPROXIMATE TRANSFER FUNCTIONS FOR FLEXIBLE AIRFRAMES

The forms for the longitudinal transfer functions of a rigid airframe are well understood, and a summary of these forms may be found in reference 56. The addition of flexible degrees of freedom to a system has generally been treated to a lesser degree, but the forms for the transfer functions are nonetheless also well established (ref. 7). In general, the addition of each flexible mode will result in the addition of a pair of lightly damped roots to the numerator and denominator of each transfer function. Table E-1 summarizes the forms expected for control-input transfer functions where two, one, or no elastic degrees of freedom are included in the equations, and forward speed is assumed constant.

In reference 52, each of the transfer function factors shown in table E-1 was approximated by a limited number of terms involving directly the stability derivatives appearing in the equations of motion [Eq. (E-1), page E-2]. These direct relationships allow the effects of parameter changes to be predicted with a reasonable degree of confidence without actually recalculating the transfer function.

#### E.1 DISCUSSION OF METHODS OF DERIVATION

The approximate factors are based on the terms in the longitudinal equations of motion [eq. (E-1)]. Note that the mode shapes are normalized so that the generalized mass for each rigid and elastic mode is unity. Each term in equation (E-1) is, in turn, related to the airframe aerodynamic and elastic properties. Specifically, the terms in equation (E-1) are found from a knowledge of the structural mode shapes, airframe geometry, and lift and moment contributions as a function of local motions. Reference 52 derives the general form for the case of no downwash, and shows that the  $ij$ th element (row  $i$ , column  $j$ ) of equation (E-1) is given by

$$F_{\xi_{ij}} = -\frac{\rho U_0}{2} \sum_n \left\{ \left[ \left( SC_{L\alpha} \right)_n \varphi_{n, 1/4}^i \varphi_{n, 3/4}^j - \left( \frac{Sc^2 C_{mq}}{2} \right)_n \varphi_{ni}^i \varphi_{nj}^j \right] s + U_0 \left( SC_{L\alpha} \right)_n \varphi_{n, 1/4}^i \varphi_{n, 1/4}^j \right\} \quad (E-2)$$

where the subscript  $n_{1/4}^i$  denotes the quarter-chord point deflection of the  $n$ th surface caused by a load at point  $i$ , etc. This particular expression gives an indication of the importance of mode shape to each of the terms in equation (E-1). The contribution of each  $F_{\xi_{ij}}$  to the airframe transfer functions is given subsequently in tables E-2 and E-3. Equations (E-1) and (E-2) together, therefore, relate transfer function sensitivity to mode shape. Reference 52 also presents an analogous set of equations of motion for situations involving downwash contributions.

Basically, the derivation of approximate transfer function factors involves determining the terms which are important for each airframe configuration considered. This is done by substituting a typical set of numerical values



TABLE E-1. - SUMMARY OF TRANSFER FUNCTION FACTORED FORMS

	RIGID AIRFRAME	FIRST ELASTIC MODE	SECOND ELASTIC MODE	
DENOMINATOR	$\Delta$	$s \left[ s^2 + (2\zeta\omega)_{sp} s + \omega_{sp}^2 \right]$	$\left[ s^2 + (2\zeta\omega)_{1e} s + \omega_{1e}^2 \right]$	$\left[ s^2 + (2\zeta\omega)_{2e} s + \omega_{2e}^2 \right]$
CONTROL-INPUT NUMERATORS	$N_w$	$A_w s \left( s + \frac{1}{T_{w1}} \right)$	$\left[ s^2 + (2\zeta\omega)_{w1} s + \omega_{w1}^2 \right]$	$\left[ s^2 + (2\zeta\omega)_{w2} s + \omega_{w2}^2 \right]$
	$N_\theta$	$A_\theta \left( s + \frac{1}{T_{\theta 2}} \right)$	$\left[ s^2 + (2\zeta\omega)_{\theta 1} s + \omega_{\theta 1}^2 \right]$	$\left[ s^2 + (2\zeta\omega)_{\theta 2} s + \omega_{\theta 2}^2 \right]$
	$N_{\xi 3}$		$A_{\xi 3} s \left[ s^2 + (2\zeta\omega)_{\xi 3 1} s + \omega_{\xi 3 1}^2 \right]$	$\left[ s^2 + (2\zeta\omega)_{\xi 3 2} s + \omega_{\xi 3 2}^2 \right]$
	$N_{\xi 4}$			$A_{\xi 4} s \left[ s^2 + (2\zeta\omega)_{\xi 4 1} s + \omega_{\xi 4 1}^2 \right]$ $\times \left[ s^2 + (2\zeta\omega)_{\xi 4 2} s + \omega_{\xi 4 2}^2 \right]$

$$N_{azcg} = s(N_w - U_0 N_\theta)$$

TABLE E-2. - TRANSFER FUNCTION APPROXIMATE FACTORS;  
CONFIGURATION 3; 3 MODES

DENOMINATOR	$\Delta$ $\omega_{SP}^2 \doteq -U_0 M_w + Z_w M_q - \frac{U_0 M_{\xi_3} F_{\xi_3}}{(\omega_3^2 - F_{\xi_3}) + U_0 M_w}$ $(2\zeta\omega)_{SP} \doteq -Z_w - M_q - \frac{F_{\xi_3} (U_0 M_{\xi_3} + Z_{\xi_3})}{(\omega_3^2 - F_{\xi_3})}$ $\omega_{1e}^2 \doteq (\omega_3^2 - F_{\xi_3}) + \frac{U_0 M_{\xi_3} F_{\xi_3}}{(\omega_3^2 - F_{\xi_3}) + U_0 M_w}$ $(2\zeta\omega)_{1e} \doteq -F_{\xi_3} + \frac{F_{\xi_3} (U_0 M_{\xi_3} + Z_{\xi_3})}{(\omega_3^2 - F_{\xi_3})}$
CONTROL-INPUT NUMERATORS	$N_w$ $A_w = Z_\delta$ $\frac{1}{T_{w1}} \doteq \frac{U_0 M_\delta}{Z_\delta}$ $\omega_{w1}^2 \doteq (\omega_3^2 - F_{\xi_3}) + M_{\xi_3} \frac{F_{\xi_3}}{M_\delta}$ $(2\zeta\omega)_{w1} \doteq -F_{\xi_3} + \left( M_{\xi_3} + \frac{Z_{\xi_3}}{U_0} \right) \frac{F_{\xi_3}}{M_\delta}$
	$N_\theta$ $A_\theta = M_\delta$ $\frac{1}{T_{\theta 2}} \doteq -Z_w + M_w \frac{Z_\delta}{M_\delta} + \frac{F_{\xi_3} (M_{\xi_3} \frac{Z_\delta}{M_\delta} - Z_{\xi_3})}{(\omega_3^2 - F_{\xi_3})}$ $\omega_{\theta 1}^2 \doteq (\omega_3^2 - F_{\xi_3}) + M_{\xi_3} \frac{F_{\xi_3}}{M_\delta}$ $(2\zeta\omega)_{\theta 1} \doteq -F_{\xi_3} + M_{\xi_3} \frac{F_{\xi_3}}{M_\delta} + \frac{Z_{\xi_3} F_{\xi_3}}{(\omega_3^2 - F_{\xi_3})}$
	$N_{\xi_3}$ $A_{\xi_3} = F_{\xi_3}$ $\omega_{\xi_3 1}^2 \doteq U_0 F_{\xi_3} \frac{M_\delta}{F_{\xi_3}}$ $(2\zeta\omega)_{\xi_3 1} \doteq -Z_w - M_q + F_{\xi_3} \frac{M_\delta}{F_{\xi_3}} + F_{\xi_3} \frac{Z_\delta}{F_{\xi_3}}$

TABLE E-3. TRANSFER FUNCTION APPROXIMATE FACTORS;  
CONFIGURATION 3; 4 MODES

DENOMINATOR	$\omega_{sp}^2 \doteq -U_0 M_w + Z_w M_q - \frac{U_0 M_{\xi_3} F_{3w}}{(\omega_3^2 - F_{3\xi_3})}$ $(2\zeta\omega)_{sp} \doteq -Z_w - M_q - \frac{F_{3w}(U_0 M_{\xi_3} + Z_{\xi_3})}{(\omega_3^2 - F_{3\xi_3})} - \frac{M_{\xi_4} F_{4q}}{(\omega_4^2 - F_{4\xi_4})}$ $\omega_{1e}^2 \doteq (\omega_3^2 - F_{3\xi_3}) - \frac{M_{\xi_4}(U_0 F_{4w} + F_{4q} F_{3\xi_3})}{(\omega_4^2 - F_{4\xi_4}) - (\omega_3^2 - F_{3\xi_3})}$ $(2\zeta\omega)_{1e} \doteq -F_{3\xi_3} + \frac{F_{3w}(U_0 M_{\xi_3} + Z_{\xi_3})}{(\omega_3^2 - F_{3\xi_3})} + \frac{M_{\xi_4} F_{4q} + F_{3\xi_4} F_{4\xi_3}}{(\omega_4^2 - F_{4\xi_4})}$ $\omega_{2e}^2 \doteq (\omega_4^2 - F_{4\xi_4})$ $(2\zeta\omega)_{2e} \doteq -F_{4\xi_4}$
CONTROL-INPUT NUMERATOR	$A_w = Z_0$ $\frac{1}{T_{w1}} \doteq \frac{U_0 M_0}{Z_0}$ $\omega_{w1}^2 \doteq (\omega_3^2 - F_{3\xi_3}) - \frac{F_{3\xi_4}}{(\omega_4^2 - F_{4\xi_4})} \left[ F_{4\xi_3} - M_{\xi_3} \frac{F_{40}}{M_0} \right]$ $(2\zeta\omega)_{w1} \doteq -F_{3\xi_3} + \left[ \frac{Z_{\xi_4}(\omega_3^2 - F_{3\xi_3}) + U_0 M_{\xi_4} F_{3\xi_3}}{U_0(\omega_4^2 - F_{4\xi_4})} \right] \frac{F_{40}}{M_0}$ $\omega_{w2}^2 \doteq (\omega_4^2 - F_{4\xi_4}) + M_{\xi_4} \frac{F_{40}}{M_0}$ $(2\zeta\omega)_{w2} \doteq -F_{4\xi_4} + M_{\xi_4} \frac{F_{40}}{M_0} + F_{3\xi_4} \left[ \frac{M_{\xi_3} \frac{F_{40}}{M_0} - F_{4\xi_3}}{(\omega_3^2 - F_{3\xi_3}) - (\omega_4^2 - F_{4\xi_4})} \right]$

(continued on following page)

TABLE E-3. TRANSFER FUNCTION APPROXIMATE FACTORS;  
CONFIGURATION 3; 4 MODES (CONCLUDED)

$N_{\theta}$	$A_{\theta} = M_8$
	$\frac{1}{T_{\theta 2}} \doteq -Z_w + M_w \frac{Z_8}{M_8} - \frac{Z_{\xi 3} F_{3w}}{(\omega_3^2 - F_{3\xi 3})}$
	$\omega_{\theta 1}^2 \doteq (\omega_3^2 - F_{3\xi 3}) - \frac{F_{3\xi 4}}{(\omega_4^2 - F_{4\xi 4})} \left[ F_{4\xi 3} - M_{\xi 3} \frac{F_{4\delta}}{M_8} \right]$
	$(2\zeta\omega)_{\theta 1} \doteq -F_{3\xi 3} + \left[ \frac{Z_{\xi 4} (\omega_3^2 - F_{3\xi 3}) + U_0 M_{\xi 4} F_{3\xi 3}}{U_0 (\omega_4^2 - F_{4\xi 4})} \right] \frac{F_{4\delta}}{M_8}$
	$\omega_{\theta 2}^2 \doteq (\omega_4^2 - F_{4\xi 4}) + M_{\xi 4} \frac{F_{4\delta}}{M_8}$
	$(2\zeta\omega)_{\theta 2} \doteq -F_{4\xi 4} + M_{\xi 4} \frac{F_{4\delta}}{M_8} + F_{3\xi 4} \left[ \frac{M_{\xi 3} \frac{F_{4\delta}}{M_8} - F_{4\xi 3}}{(\omega_3^2 - F_{3\xi 3}) - (\omega_4^2 - F_{4\xi 4})} \right]$
$N_{\xi 3}$	$A_{\xi 3} = F_{3\delta}$
	$\omega_{\xi 3 1}^2 \doteq \left[ \frac{U_0 F_{3w} (\omega_4^2 - F_{4\xi 4})}{(\omega_4^2 - F_{4\xi 4}) \frac{F_{3\delta}}{M_8} + U_0 F_{3w} + F_{3\xi 4} \frac{F_{4\delta}}{M_8}} \right]$
	$(2\zeta\omega)_{\xi 3 1} \doteq -F_{4\xi 4} - M_q$
	$\omega_{\xi 3 2}^2 \doteq (\omega_4^2 - F_{4\xi 4}) + \left[ U_0 F_{3w} \frac{M_8}{F_{3\delta}} + F_{3\xi 4} \frac{F_{4\delta}}{F_{3\delta}} \right]$
	$(2\zeta\omega)_{\xi 3 2} \doteq -M_q + \left[ F_{3q} + F_{3w} \frac{Z_8}{M_8} \right] \frac{M_8}{F_{3\delta}}$
$N_{\xi 4}$	$A_{\xi 4} = F_{4\delta}$
	$\omega_{\xi 4 1}^2 \doteq -U_0 M_w + \left[ U_0 F_{4w} + \frac{U_0 F_{3w} F_{4\xi 3}}{(\omega_3^2 - F_{3\xi 3})} - Z_w F_{4q} \right] \frac{M_8}{F_{4\delta}}$
	$(2\zeta\omega)_{\xi 4 1} \doteq -Z_w - M_q - \frac{U_0 M_w F_{3\xi 3}}{(\omega_3^2 - F_{3\xi 3})} + F_{4q} \frac{M_8}{F_{4\delta}}$
	$\omega_{\xi 4 2}^2 \doteq (\omega_3^2 - F_{3\xi 3}) - \left[ \frac{U_0 F_{3w} F_{4\xi 3}}{(\omega_3^2 - F_{3\xi 3})} \right] \frac{M_8}{F_{4\delta}}$
	$(2\zeta\omega)_{\xi 4 2} \doteq \frac{-(\omega_3^2 - F_{3\xi 3}) F_{3\xi 3}}{(\omega_3^2 - F_{3\xi 3}) + U_0 M_w} + F_{4w} \frac{Z_8}{F_{4\delta}}$

CONTROL - INPUT NUMERATORS

for speed, altitude, etc., into the equations, and then neglecting the small terms. In doing this, it is assumed implicitly that moderate changes in the parameters will not affect the segregation of small and large terms; that is, small terms remain small over a reasonable range of parameter variation.

Appendix B in reference 52 describes two methods which were used to determine literal approximate factors for each of the airframe configurations considered. Here we shall present approximate factors only for "Configuration 3," which is a high aspect ratio swept wing airplane having planform geometry and mass distribution similar to the B-47. Numerical values for the normal elastic mode model of "Configuration 3" are given in Section 5 of reference 51, and numerical values for the approximate and "exact" factors are shown to compare favorably at three very different flight conditions in reference 53. An illustration of two elastic modes for "Configuration 3" is reproduced from reference 52 in figure E-1.

## E.2 APPROXIMATE FACTORS

The approximate factors for the denominator and numerators for each of the control-input transfer functions for "Configuration 3" are presented in tables E-2 and E-3. Inspection of these tables reveals that the transfer function factors for flexible airframes contain the rigid airframe factors derived in reference 56 (with aeroelastic corrections) along with the elastic-mode factors.

Rather than include a list of validity conditions for each set of factors, it is suggested that the applicability of the approximations be determined by finding the exact numerical factors for a nominal case, and comparing them with the numbers obtained by using the approximate formulas. Reference 53 has done this for three diverse flight conditions with favorable results. The reason for suggesting this approach is quite simple: the alternative of calculating the required validity conditions (see Appendix B in reference 52) would be unreasonably lengthy and complicated. It is therefore impractical and unnecessary to present a list of validity conditions. The justification for the method suggested lies in the assumption that moderate changes in parameters from the nominal values will not affect the segregation of large and small terms.

## E.3 ADEQUACY OF ONE- AND TWO-ELASTIC-MODE REPRESENTATIONS

Regardless of the validity of the approximations, there is still a basic question as to the number of modes required to adequately represent the system(s) under study. This subject is investigated in reference 51, and "Configuration 3" is shown to be accurately represented with only one or two flexible modes, the frequency response curve being accurate (as determined by comparison with a five-elastic-mode case) up to the characteristic frequency of the last flexible mode included.

## E.4 REPRESENTATION OF PITCH RATE AND ATTITUDE FEEDBACK TO THE PITCHING MOMENT CONTROL

According to normal mode theory, the deflection of a point  $i$  on the fuselage can be expressed as

$$-Z_i = \varphi_{i1}h + \varphi_{i2}\theta + \sum_{k>2} \varphi_{ik}\xi_k \quad (E-3)$$

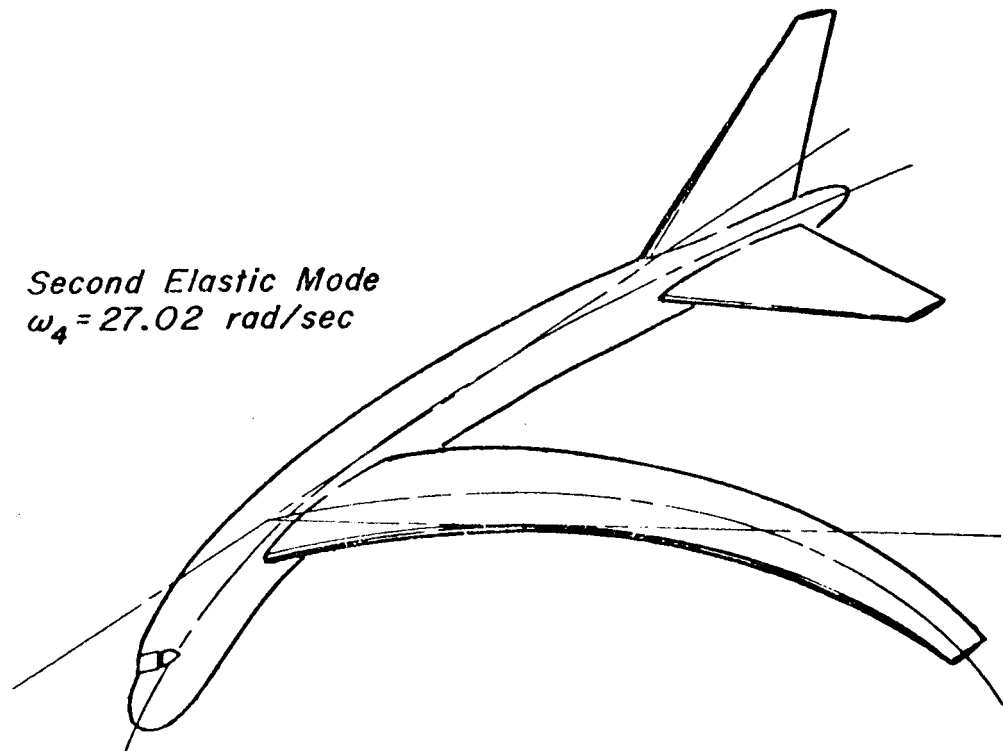
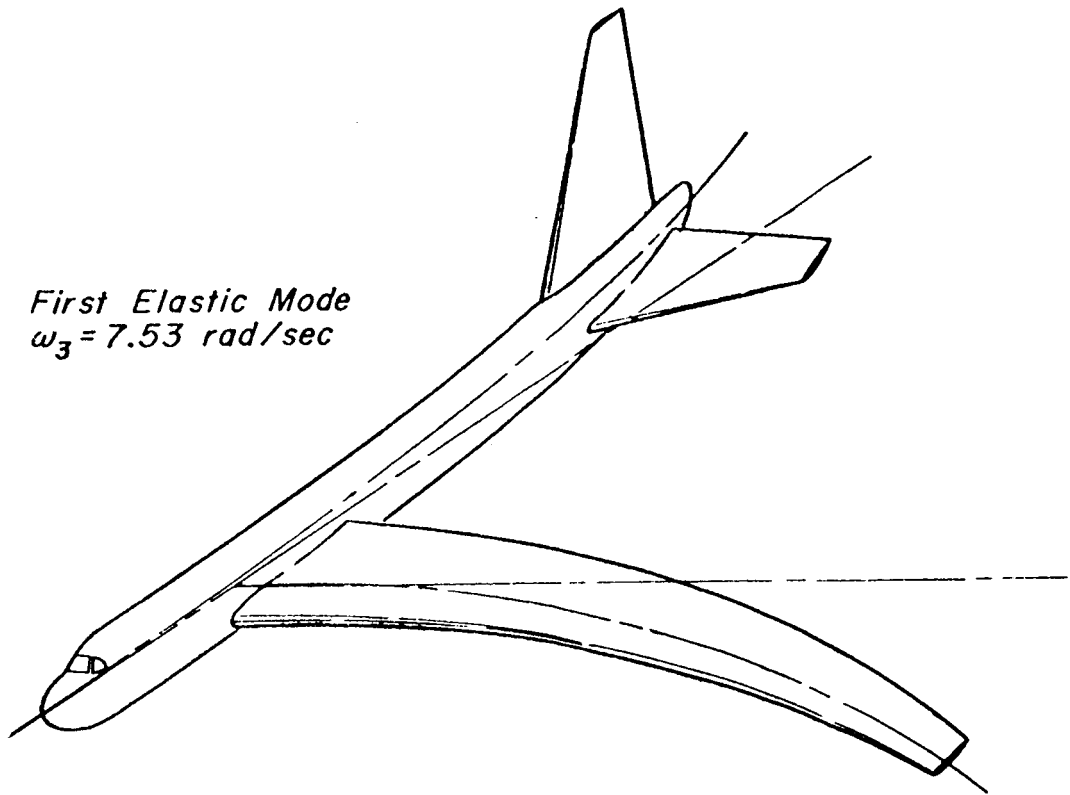


Figure E-1. – Elastic Modes for Configuration 3

where the vertical displacement  $h$  can be expressed as the linear combination

$$h = \frac{U_0\theta - w}{s}, \text{ if the initial condition } h(0) = 0 \quad (\text{E-4})$$

Any transfer function involving  $h$  can thus be expressed as a linear combination of transfer functions for  $\theta$  and  $w$  from table E-1.

If a vertical gyro is used as a sensor, the gyro will measure the local inclination of the fuselage,  $\theta_i \equiv -dz_i/dx$ :

$$\theta_i = \varphi'_{i1}h + \varphi'_{i2}\theta + \sum_{k>2} \varphi'_{ik}\xi_k \quad (\text{E-5})$$

where the prime superscript denotes differentiation with respect to  $x$ . For the rigid-body modes

$$\varphi'_{i1} = 0 \quad (\text{E-6})$$

and

$$\varphi'_{i2} = 1 \quad (\text{E-7})$$

Therefore,

$$\theta_i = \theta + \sum_{k>2} \varphi'_{ik}\xi_k \quad (\text{E-8})$$

A rate gyro located at the same point will measure  $s\theta_i$ , if the initial condition  $\theta_i(0) = 0$ .

Since we wish to apply a linear combination of pitch rate and pitch attitude feedback to the pitching moment control  $\delta$ , we can express the feedback equation as

$$\delta = \delta_c - \left(K_{\dot{\theta}} + \frac{K_{\theta}}{s}\right)\dot{\theta} - (K_{\theta}s + K_{\theta}) \sum_{k>2} \varphi'_{ik}\xi_k \quad (\text{E-9})$$

which is compatible with the dependent variables in equation (E-1). The feedback equation [eq. (E-9)] expresses the complete physical motion detected by the pitch rate and attitude sensors without any filtering.\*

If we substitute equation (E-9) in equation (E-1), we can express the result in the form of equation (E-10). In equation (E-10) feedback control equation (E-9) is embodied within the airframe equations of motion by adding terms involving  $K_{\theta}/s$  products to the  $\dot{\theta}$  column and by defining the new (primed) equivalent

---

\*This representation of the physical motion is based on the derivation in Section IV of reference 24. The effect of filtering can be approximated by setting  $\varphi'_{ik} = 0$  in equation (E-9) for the normal modes above the filter bandwidth.



stability derivatives listed below. The primed derivatives in equation (E-10) incorporate the effective pitch rate and attitude feedback and are defined as follows:

Definitions for equation (E-10)

$$\begin{array}{lll}
 Z'_q = Z_q - K_{\theta} Z_{\delta} & Z'_{\xi_k} = Z_{\xi_k} - K_{\theta} \phi'_{ik} Z_{\delta} & Z'_{\xi_k} = Z_{\xi_k} - K_{\theta} \phi'_{ik} Z_{\delta} \\
 M'_q = M_q - K_{\theta} M_{\delta} & M'_{\xi_k} = M_{\xi_k} - K_{\theta} \phi'_{ik} M_{\delta} & M'_{\xi_k} = M_{\xi_k} - K_{\theta} \phi'_{ik} M_{\delta} \\
 F'_{kq} = F_{kq} - K_{\theta} F_{k\delta} & F'_{j\xi_k} = F_{j\xi_k} - K_{\theta} \phi'_{ik} F_{j\delta} & F'_{j\xi_k} = F_{j\xi_k} - K_{\theta} \phi'_{ik} F_{j\delta}
 \end{array}$$

Already implied by the equations of motion is the following assumption:

Assumption: The unsteady aerodynamic derivatives  $Z_w, M_w, F_{kw}, F_{kq}$  are negligible.

Also shown in equation (E-10) on the right side of the equality are the linearly independent gust velocity components which disturb the airframe. By considering only the first elastic mode in addition to the rigid-body equations, equation (E-10) can be partitioned as follows:

$$\left[ \begin{array}{c|c} \text{Rigid-body} & \text{Coupling} \\ \text{characteristic} & \text{terms} \\ \text{determinant} & \\ \hline \text{Coupling} & \text{Elastic mode} \\ \text{terms} & \text{characteristic} \\ & \text{equation} \end{array} \right] \begin{Bmatrix} w \\ \theta \\ \xi_3 \end{Bmatrix} = \left\{ \begin{array}{c} \text{Independent rigid-body} \\ \text{forcing functions} \\ \hline \text{Independent elastic mode} \\ \text{forcing functions} \end{array} \right\} \quad (\text{E-11})$$

Reference 55 presents a method for expanding the characteristic determinant (transfer function denominator) of equation (E-11) about the indicated rigid-body partition to find the changes in the factors of the rigid-body characteristic determinant caused by aeroelastic coupling as functions of the feedback control gains. The method is equally applicable to finding the changes in the factors of each rigid body transfer function numerator caused by aeroelastic coupling as functions of the feedback control gains. Furthermore, the partitioning method can be progressively applied to each successive elastic mode, albeit one at a time.

The rigid-body short-period transfer functions with pitch rate and pitch attitude feedback to the pitching moment control have been derived here in Appendix B. Three rigid-body transfer functions for  $az_{cg}$ , the normal acceleration at the center of gravity are repeated below for the case of relaxed inherent stability ( $M_w = 0$ ) negligible downwash lag effect ( $M_w = 0$ ) and negligible normal control force ( $Z_{\delta} = 0$ ).

1. Control command displacement input,  $\delta_c$

$$\frac{az_{cg}}{\delta_c} = \frac{U_0 M_{\delta} Z_w s}{(s - Z_w) [s^2 + (K_{\theta} M_{\delta} - M_q) s + K_{\theta} M_{\delta}]} \quad (\text{E-12})$$

2. Longitudinal gust velocity input,  $u_g$

$$\frac{a_{z_{cg}}}{u_g} \doteq \frac{-Z_{us}}{s - Z_w}, \text{ if } |U_o M_u Z_w| \ll K_\theta M_\delta \quad (\text{E-13})$$

3. Normal gust velocity input,  $w_g$

$$\frac{a_{z_{cg}}}{w_g} \doteq \frac{-Z_{ws}}{s - Z_w}, \text{ if } -2M_q \ll K_\theta M_\delta \quad (\text{E-14})$$

The wing root bending moment (WRBM) is defined as

$$\text{WRBM} = \left[ EI \left( - \frac{d^2 z_i}{dy^2} \right) \right]_{y=0} \quad (\text{E-15})$$

where  $-Z_i$  is given by equation (E-3) with the auxiliary equation (E-4). Therefore,

$$- \frac{d^2 z_i}{dy^2} = \frac{d^2 \phi_{i1}}{dy^2} h + \frac{d^2 \phi_{i2}}{dy^2} \theta + \frac{d^2 \phi_{i3}}{dy^2} \xi_3 + \frac{d^2 \phi_{i4}}{dy^2} \xi_4 \quad (\text{E-16})$$

However, for the rigid-body modes

$$\frac{d^2 \phi_{i1}}{dy^2} = \frac{d^2 \phi_{i2}}{dy^2} = 0 \quad (\text{E-17})$$

Therefore

$$\text{WRBM} = (EI)_o \left\{ \left[ \frac{d^2 \phi_{i3}}{dy^2} \right]_o \xi_3 + \left[ \frac{d^2 \phi_{i4}}{dy^2} \right]_o \xi_4 \right\} \quad (\text{E-18})$$

where the subscript "o" refers to evaluation at buttock line 0, and transfer functions for  $\xi_3$  and  $\xi_4$  can be computed by the methods of reference 113 using the partitioning of equation (E-10) shown in equation (E-11).

#### E.5 REPRESENTATION OF PITCH RATE AND ANGLE OF ATTACK FEEDBACK TO THE PITCHING MOMENT CONTROL $\delta$

According to normal mode theory, the local angle of attack of a point  $i$  on the fuselage,  $\alpha_i$ , is

$$\alpha_i \equiv \frac{w_i}{U_o} = \theta_i + \frac{s Z_i}{U_o} \quad (\text{E-19})$$

where  $\theta_i$  is given by equation (E-5), and  $-Z_i$  is given by equation (E-3).

The angle of attack at the center of gravity,  $\alpha_{cg}$ , is

$$\alpha_{cg} \equiv \frac{w}{U_o} = \theta - \frac{sh}{U_o} \quad (\text{E-20})$$

If equations (E-3) and (E-5) are substituted in equation (E-19), and equation (E-20) is used to simplify the result,  $\alpha_i$  becomes

$$\alpha_i = \frac{w}{U_0} + \sum_{k>2} \left( \frac{\varphi_{ik}}{U_0} s + \varphi'_{ik} \right) \xi_k - \frac{l_{xi}}{U_0} s \theta \quad (E-21)$$

where the substitutions

$$\varphi_{i1} = 1 \quad (E-22)$$

$$\varphi_{i2} = l_{xi} \quad (E-23)$$

have been made for the rigid-body modes.

If the active control system incorporates a linear combination of pitch rate and angle of attack (or its dynamical equivalent) feedback to the pitching moment control  $\delta$ , we can express the feedback equation as

$$\delta = \delta_c - \frac{K_\alpha}{U_0} w + \left( \frac{K_\alpha l_{xi}}{U_0} - K_\theta \right) \dot{\theta} - \sum_{k>2} \left[ \left( K_\theta \varphi'_{ik} + \frac{K_\alpha \varphi_{ik}}{U_0} \right) s + K_\alpha \varphi'_{ik} \right] \xi_k \quad (E-24)$$

which is compatible with the dependent variables in equation (E-1). As before in the case of equation (E-9), the effect of filtering can be approximated by setting  $\varphi_{ik} = 0$  and  $\varphi'_{ik} = 0$  in equation (E-24) for the normal modes above the filter bandwidth.

If we substitute equation (E-24) in equation (E-1), we can express the result in the form of equation (E-25). In equation (E-25) feedback control equation (E-24) is embodied within the airframe equations of motion by defining the new (double primed) equivalent stability derivatives listed below.

Definitions for equation (E-25)

$Z''_q = Z_q + \left( \frac{K_\alpha l_{xi}}{U_0} - K_\theta \right) Z_\delta$	$Z''_{\xi_k} = Z_{\xi_k} - \left( K_\theta \varphi'_{ik} + \frac{K_\alpha \varphi_{ik}}{U_0} \right) Z_\delta$
$M''_q = M_q + \left( \frac{K_\alpha l_{xi}}{U_0} - K_\theta \right) M_\delta$	$M''_{\xi_k} = M_{\xi_k} - \left( K_\theta \varphi'_{ik} + \frac{K_\alpha \varphi_{ik}}{U_0} \right) M_\delta$
$F''_{kq} = F_{kq} + \left( \frac{K_\alpha l_{xi}}{U_0} - K_\theta \right) F_{k\delta}$	$F''_{j\xi_k} = F_{j\xi_k} - \left( K_\theta \varphi'_{ik} + \frac{K_\alpha \varphi_{ik}}{U_0} \right) F_{j\delta}$
$Z''_w = Z_w - \frac{K_\alpha}{U_0} Z_\delta$	$Z''_{\xi_k} = Z_{\xi_k} - K_\alpha \varphi'_{ik} Z_\delta$
$M''_w = M_w - \frac{K_\alpha}{U_0} M_\delta$	$M''_{\xi_k} = M_{\xi_k} - K_\alpha \varphi'_{ik} M_\delta$
$F''_{kw} = F_{kw} - \frac{K_\alpha}{U_0} F_{k\delta}$	$F''_{j\xi_k} = F_{j\xi_k} - K_\alpha \varphi'_{ik} F_{j\delta}$



Also shown on the right side of the equality are the linearly independent gust velocity components which disturb the airframe. Notice also that except for the new definitions of the double-primed stability derivatives, the left side of equation (E-25) is identical in form to the left side of equation (E-1). Therefore, the approximate factors in tables E-2 and E-3 will remain valid for the characteristic denominator and the control-input numerators with pitch rate and angle-of-attack feedback control as long as the numerical values of the double-primed derivatives remain compatible with the assumptions on which the approximate factors are based.

By considering only the first elastic mode in addition to the rigid-body equations, equation (E-25) can be partitioned as in equation (E-11). Then the method in reference 55 can be used to establish the changes in the factors of each rigid-body gust-input transfer function numerator caused by aeroelastic coupling as functions of the feedback control gains. Furthermore, the partitioning method can be progressively applied to each successive elastic mode, albeit one at a time.

The rigid-body short-period transfer functions with pitch-rate and angle-of-attack feedback to the pitching moment control are presented in reference 56. Three rigid-body transfer functions for  $\alpha_{zcg}$ , the normal acceleration at the center of gravity, are repeated below for the case with negligible normal control force ( $Z_\delta = 0$ ).

1. Control command displacement input,  $\delta_c$

$$\frac{\alpha_{zcg}}{\delta_c} = \frac{U_o M_\delta Z_w s}{\Delta''} \quad (E-26)$$

2. Longitudinal gust velocity input,  $u_g$

$$\frac{\alpha_{zcg}}{u_g} = \frac{-Z_u s^3 + (Z_u M_q'' - U_o M_u) s^2 + U_o (Z_u M_w'' + M_u) s + U_o (Z_u M_w'' - M_u Z_w)}{\Delta''} \quad (E-27)$$

3. Normal gust velocity input,  $w_g$

$$\frac{\alpha_{zcg}}{w_g} = \frac{-Z_w}{\Delta''} \quad (E-28)$$

where  $\Delta'' = s[s^2 - (U_o M_w + Z_w + M_q'')s - (U_o M_w'' - M_q' Z_w)]$

The wing root bending moment can be estimated from equation (E-18) as discussed previously.

In summary, valid approximate factors for the flexible airframe transfer functions offer the preliminary loads analyst a practical design aid for predicting the interactions among aeroelasticity, unsteady aerodynamics, and active feedback control technology when applying power spectral methods for gust load analysis.

Appendix F  
LONGITUDINAL STABILITY DERIVATIVE DEFINITIONS

Table F-1. LONGITUDINAL NONDIMENSIONAL STABILITY DERIVATIVES  
(STABILITY AXIS SYSTEM) [From ref. 56]

BASIC NONDIMENSIONAL STABILITY DERIVATIVES		THEORETICAL AFT HORIZONTAL TAIL CONTRIBUTION	NONDIMENSIONAL STABILITY DERIVATIVE PARAMETERS
TOTAL AIRFRAME			
DEFINITIONS	UNIT		
$C_D = \frac{\text{DRAG}}{qS}$	$\frac{1}{1}$		
$C_{D_u} = \frac{U}{2} \frac{\partial C_D}{\partial U}$	$\frac{1}{1}$		$x_u = (-C_D - C_{D_u})$
$C_{D_\alpha} = \frac{\partial C_D}{\partial \alpha}$	$\frac{1}{\text{rad}}$		$x_w = \frac{1}{2}(C_L - C_{D_\alpha})$
$C_{D_\delta} = \frac{\partial C_D}{\partial \delta}$	$\frac{1}{\text{rad}}$		$x_\delta = \frac{-1}{2} C_{D_\delta}$
$C_L = \frac{\text{LIFT}}{qS}$	$\frac{1}{1}$		
$C_{L_u} = \frac{U}{2} \frac{\partial C_L}{\partial U}$	$\frac{1}{1}$		$z_u = (-C_L - C_{L_u})$
$C_{L_\alpha} = \frac{\partial C_L}{\partial \alpha}$	$\frac{1}{\text{rad}}$	$C_{L_{\alpha h}} \frac{q_h}{q} \frac{S_h}{S} \left(1 - \frac{\partial \epsilon}{\partial \alpha}\right)$	$z_w = \frac{1}{2} (-C_{L_\alpha} - C_D)$
$C_{L_{\dot{\alpha}}} = \frac{\partial C_L}{\partial \left(\frac{d\alpha}{2U}\right)}$	$\frac{1}{\text{rad}}$	$2C_{L_{\dot{\alpha} h}} \frac{q_h}{q} \frac{S_h}{S} \frac{l_h}{c} \frac{\partial \epsilon}{\partial \alpha}$	$z_{\dot{w}} = \frac{-1}{4} C_{L_{\dot{\alpha}}}$
$C_{L_q} = \frac{\partial C_L}{\partial \left(\frac{qc}{2U}\right)}$	$\frac{1}{\text{rad}}$	$2C_{L_{qh}} \frac{q_h}{q} \frac{S_h}{S} \frac{l_h}{c}$	$z_q = \frac{-1}{4} C_{L_q}$
$C_{L_\delta} = \frac{\partial C_L}{\partial \delta}$	$\frac{1}{\text{rad}}$	$C_{L_{\delta h}} \frac{q_h}{q} \frac{S_h}{S} \frac{\partial \alpha_h}{\partial \delta}$	$z_\delta = -\frac{1}{2} C_{L_\delta}$
$C_M = \frac{M}{qSc}$	$\frac{1}{1}$		
$C_{M_u} = \frac{U}{2} \frac{\partial C_M}{\partial U}$	$\frac{1}{1}$		$m_u = \frac{1}{2} \left(\frac{c}{k_y}\right)^2 (C_M + C_{M_u})$
$C_{M_\alpha} = \frac{\partial C_M}{\partial \alpha}$	$\frac{1}{\text{rad}}$	$-\frac{l_h}{c} [C_{L_\alpha}]_h$	$m_w = \frac{1}{2} \left(\frac{c}{k_y}\right)^2 C_{M_\alpha}$
$C_{M_{\dot{\alpha}}} = \frac{\partial C_M}{\partial \left(\frac{d\alpha}{2U}\right)}$	$\frac{1}{\text{rad}}$	$-\frac{l_h}{c} [C_{L_{\dot{\alpha}}}]_h$	$m_{\dot{w}} = \frac{1}{4} \left(\frac{c}{k_y}\right)^2 C_{M_{\dot{\alpha}}}$
$C_{M_q} = \frac{\partial C_M}{\partial \left(\frac{qc}{2U}\right)}$	$\frac{1}{\text{rad}}$	$-\frac{l_h}{c} [C_{L_q}]_h$	$m_q = \frac{1}{4} \left(\frac{c}{k_y}\right)^2 C_{M_q}$
$C_{M_\delta} = \frac{\partial C_M}{\partial \delta}$	$\frac{1}{\text{rad}}$	$-\frac{l_\delta}{c} C_{L_\delta}$	$m_\delta = \frac{1}{2} \left(\frac{c}{k_y}\right)^2 C_{M_\delta}$

\*The symbol "q", in addition to its normal use to designate pitching velocity, is used in these tables to also denote the dynamic pressure,  $\rho U^2/2$ , in accordance with long-established aeronautical practice. When particularized by the subscript "h" (or "v") it signifies the local dynamic pressure at the horizontal (or vertical) tail. The local flow angles relative to free stream conditions are denoted by  $-\epsilon$  (xz plane) and  $-\sigma$  (xy plane).

Table F-2. LONGITUDINAL DIMENSIONAL STABILITY DERIVATIVES  
(STABILITY AXIS SYSTEM) [From ref. 56]

QUANTITY	IN TERMS OF BASIC STABILITY DERIVATIVES			IN TERMS OF NONDIMENSIONAL STABILITY DERIVATIVE PARAMETERS
	DIMENSIONAL		NONDIMENSIONAL see Table F-V	
	DEFINITIONS	UNIT		
$X_u$	$\frac{1}{m} \frac{\partial X}{\partial u}$	$\frac{1}{\text{sec}}$	$\frac{\rho S U}{m} (-C_D - C_{D_u})^{\dagger}$	$\frac{1}{\tau} x_u^{\dagger}$
$X_w$	$\frac{1}{m} \frac{\partial X}{\partial w}$	$\frac{1}{\text{sec}}$	$\frac{\rho S U}{2m} (C_L - C_{D_w})$	$\frac{1}{\tau} x_w$
$X_\delta$	$\frac{1}{m} \frac{\partial X}{\partial \delta}$	$\frac{\text{ft}}{\text{sec}^2 \text{rad}}$	$\frac{\rho S U^2}{2m} (-C_{D_\delta})$	$\frac{U}{\tau} x_\delta$
$Z_u$	$\frac{1}{m} \frac{\partial Z}{\partial u}$	$\frac{1}{\text{sec}}$	$\frac{\rho S U}{m} (-C_L - C_{L_u})^{\dagger}$	$\frac{1}{\tau} z_u$
$Z_w$	$\frac{1}{m} \frac{\partial Z}{\partial w}$	$\frac{1}{\text{sec}}$	$\frac{\rho S U}{2m} (-C_{L_w} - C_D)$	$\frac{1}{\tau} z_w$
$Z_{\dot{w}}$	$\frac{1}{m} \frac{\partial Z}{\partial \dot{w}}$	$\frac{1}{\text{ft}}$	$\frac{\rho S c}{4m} (-C_{L_d})$	$\frac{c}{\tau U} z_{\dot{w}}$
$Z_q$	$\frac{1}{m} \frac{\partial Z}{\partial q}$	$\frac{\text{ft}}{\text{sec-rad}}$	$\frac{\rho S U c}{4m} (-C_{L_q})$	$\frac{c}{\tau} z_q$
$Z_\delta$	$\frac{1}{m} \frac{\partial Z}{\partial \delta}$	$\frac{\text{ft}}{\text{sec}^2 \text{rad}}$	$\frac{\rho S U^2}{2m} (-C_{L_\delta})$	$\frac{U}{\tau} z_\delta$
$M_u$	$\frac{1}{I_y} \frac{\partial M}{\partial u}$	$\frac{1}{\text{sec-ft}}$	$\frac{\rho S U c}{I_y} (C_M + C_{M_u})$	$\frac{2}{\tau c} m_u$
$M_w$	$\frac{1}{I_y} \frac{\partial M}{\partial w}$	$\frac{1}{\text{sec-ft}}$	$\frac{\rho S U c}{2I_y} C_{M_w}$	$\frac{1}{\tau c} m_w$
$M_{\dot{w}}$	$\frac{1}{I_y} \frac{\partial M}{\partial \dot{w}}$	$\frac{1}{\text{ft}}$	$\frac{\rho S c^2}{4I_y} C_{M_d}$	$\frac{1}{\tau U} m_{\dot{w}}$
$M_q$	$\frac{1}{I_y} \frac{\partial M}{\partial q}$	$\frac{1}{\text{sec}}$	$\frac{\rho S U c^2}{4I_y} C_{M_q}$	$\frac{1}{\tau} m_q$
$M_\delta$	$\frac{1}{I_y} \frac{\partial M}{\partial \delta}$	$\frac{1}{\text{sec}^2 \text{rad}}$	$\frac{\rho S U^2 c}{2I_y} C_{M_\delta}$	$\frac{U}{\tau c} m_\delta$

<sup>†</sup>The thrust-gradient terms are neglected here in the interests of symmetry and consistency.

<sup>†</sup> $\tau = m/\rho U S$  in the dimensionless time first proposed by H. Glauert, A Nondimensional Form of the Stability Equations of an Aeroplane, Br ARC R and M 1093, 1927.

<sup>\*</sup>For  $C_{L_u} = 0$ , as in subsonic flight, and  $C_L = W/(\rho U^2 S/2)$ , as in trimmed flight for  $\gamma_0 = 0$ ,  $Z_u = -2g/U_0$ .

## REFERENCES

1. Braslow, A. L.; and Alford, W. J.: Overview: Keeping Air Leadership. *Astronautics and Aeronautics*, vol. 10, no. 8, Aug. 1972, pp. 26-31.
2. Anon.: Airworthiness Standards: Transport Category Airplanes. FAR, vol. III, part 25, 1965, 1970.
3. Anon.: Tentative Airworthiness Standards for Supersonic Transports. FAA, 1965, 1971.
4. Anon.: Special Conditions for the Societe Nationale Industrielle Aerospatiale/British Aircraft Corporation Concorde Model Airplane. Special Conditions No. 25-43-EU-12, FS-72-266-S, FAA, Dept. of Transportation, June 21, 1972.
5. Hood, Ray V.: Active Controls Changing the Rules of Structural Design. *Astronautics and Aeronautics*, vol. 10, no. 8, Aug. 1972, pp. 50-54.
6. Pearce, B. F.; Ashkenas, I. L.; and Johnson, W. A.: Development and Implications of Literal Approximate Longitudinal Transfer Functions for Flexible Airframes. IAS Paper No. 62-92, June 1962.
7. Schwendler, R. G.; and Mac Neal, R. H.: Optimum Structural Representation in Aeroelastic Analyses. ASD TR-61-680, Mar. 1962.
8. Pearce, B. F.; and Siskind, R. K.: Topics on Flexible Airplane Dynamics, Part II: The Application of Flexible Airframe Transfer Function Approximations and the Sensitivity of Airframe Transfer Functions to Elastic Mode Shapes. ASD TDR-63-334, Part II, July 1963.
9. Tomlinson, L. R.: Problems and Solutions Related to the Design of a Control Augmentation System for a Longitudinally Unstable Supersonic Transport. NASA TM X-2620, 1972.
10. Stapleford, R. L., et al: Development of Satisfactory Lateral-Directional Handling Qualities in the Landing Approach, Appendix F, Redundancy in Stability Augmenters, NASA CR-239, July 1965.
11. Holloway, R. B.; Thompson, G. O.; and Rohling, W. J.: Prospects for Low Wing-Loading STOL Transports with Ride Smoothing. AIAA Paper No. 72-64, Jan., 1972.
12. Anon.: Softride - B-1 Performance Enhancer. North American Rockwell, Combat Crew, Jan. 1971, pp. 8-11.
13. Anon.: Military Specification, Airplane Strength and Rigidity Flight Loads. MIL-A-008861A (USAF), Mar. 31, 1971.
14. Notess, C. B.: Some Statistical Analyses Relevant to Establishing Structural Design Criteria for Aircraft in Maneuvering Flight. Cornell Aero. Lab., Inc., AC-1578-F-1, Mar. 1962.
15. Rainey, A. G.; and Abel, I.: Wind-Tunnel Techniques for the Study of Aeroelastic Effects on Aircraft Stability, Control, and Loads. AGARD Conf. Proc., No. 46, Apr. 1969.
16. Gilman, J., Jr.; and Bennett, R. M.: A Wind-Tunnel Technique for Measuring Frequency-Response Functions for Gust Load Analyses. AIAA Paper No. 65-787, Nov. 1965.

17. Ingram, C. T.; and Eichenbaum, F. D.: A Comparison of C-141A Flight Test Measured and Theoretical Vertical Gust Responses. J. Aircraft, vol. 6, no. 6, Nov.-Dec. 1969, pp. 532-536.
18. Newberry, C. F.; Arnold, J. I.; and Kass, G. J.: The Effect of Active Controls on Structural Responses. 31st AGARD Symposium, Nov. 1970.
19. Newberry, C. F.: Consideration of Stability Augmentation Systems for Large Elastic Aircraft. AGARD Conf. Proc., No. 46, Apr. 1969.
20. Oehman, W. I.: Analytical Study of the Performance of a Gust Alleviation System for a STOL Airplane. NASA TN D-7201, Apr. 1973.
21. Wykes, J. H.: Structural Dynamic Stability Augmentation and Gust Alleviation of Flexible Aircraft. AIAA Paper No. 68-1067, Oct. 1968.
22. Jackson, C. E.; Thorson, K. R.; Wherry, J. E.; and Dempster, J. B.: The Influence of Dynamic Loads on Aircraft Fatigue. Proc. of the Symposium on Fatigue of Aircraft Structures, WADC-TR-59-507, Aug. 1959, pp. 449-478.
23. Corsetti, C. D.; and Dillow, J. D.: A Study of the Practibility of Active Vibration Isolation Applied to Aircraft During the Taxi Condition. AFFDL-TR-71-159, July 1972.
24. Ashkenas, I. L.: Summary and Review of Aeromechanical Devices and Possible Applications. WADC Technical Note 58-159, June 1958 (Report originally CONFIDENTIAL, now downgraded to unclassified).
25. Dempster, J. B.; and Roger, K. L.: Evaluation of B-52 Structural Response to Random Turbulence with Stability Augmentation Systems. J. Aircraft, vol. 4, no. 6, Nov.-Dec. 1967, pp. 507-512.
26. Burris, P. M.; and Bender, M. A.: Aircraft Load Alleviation and Mode Stabilization (LAMS), B-52 System Analysis, Synthesis, and Design. AFFDL-TR-68-161, Nov. 1969.
27. Burris, P. M.; and Bender, M. A.: Aircraft Load Alleviation and Mode Stabilization (LAMS), C-5A System Analysis, and Synthesis. AFFDL-TR-68-162, Nov. 1969.
28. Fischler, J. E.: Supercritical Flow Effects on Some Unsteady Aerodynamic Coefficients Used for Flutter Analysis. J. Aircraft, vol. 5, no. 6, Nov.-Dec. 1968, pp. 555-563.
29. Polve, J. H.: The State of Ignorance of Flutter-Flight Testing. AIAA Paper No. 66-883, Nov. 1966.
30. Reed, W. H., III; and Abbott, F. T., Jr.: A New "Free-Flight" Mount System for High-Speed Wind-Tunnel Flutter Models. Presented at Symposium on Aeroelastic and Dynamic Modeling Technology, Dayton, Ohio, Sept. 23 to 25, 1963.
31. Wykes, J. H.; Nardi, L. U.; and Mori, A. S.: XB-70 Structural Mode Control System Design and Performance Analyses. NASA CR-1577, July 1970.
32. Nissim, E.: Flutter Suppression Using Active Controls Based on the Concept of Aerodynamic Energy. NASA TN D-6199, Mar. 1971.

33. McRuer, D.; Graham, D.; Krendel, E.; and Reisener, W., Jr.: Human Pilot Dynamics in Compensatory Systems: Theory, Models, and Experiments with Controlled Element and Forcing Function Variations. AFFDL-TR-65-15, July 1965.
34. Ashkenas, I. L.; and McRuer, D. T.: A Theory of Handling Qualities Derived from Pilot-Vehicle System Considerations. Aerospace Eng., vol. 21, no. 2, Feb. 1962, pp. 60, 61, and 83-102.
35. McRuer, D. T.; and Jex, H. R.: A Review of Quasi-Linear Pilot Models. IEEE Trans., vol. HFE-8, no. 3, Sept. 1967, pp. 231-249.
36. Kleinman, D. L.; and Baron, S.: Manned Vehicle Systems Analysis by Means of Modern Control Theory. NASA CR-1753, June 1971.
37. Weir, D. H.; and Phatak, A. V.: Model of Human Operator Response to Step Transitions in Controlled Element Dynamics. NASA SP-128, 1966, pp. 65-83.
38. Anon.: Military Specification, Flying Qualities of Piloted Airplanes. MIL-F-8785B (ASG), Aug. 7, 1969.
39. Allen, R. W.; Jex, H. R.; and Magdaleno, R. E.: Manual Control Performance and Dynamic Response under Vertical and Lateral Sinusoidal Vibration. AMRL TR-73-78, Oct. 1973.
40. Rustenburg, J. W.: Ride Quality Design Criteria for Aircraft with Active Mode Control Systems. ASD TR-72-64, Oct. 1972.
41. Holloway, R. G.; and Brumaghim, S. H.: Tests and Analyses Applicable to Passenger Ride Quality of Large Transport Aircraft. NASA TM X-2620, 1972.
42. Broderson, A. B.; von Gierke, H. E.; and Guignard, J. C.: Ride Evaluation in Aerospace and Surface Vehicles. NASA TM X-2620, 1972.
43. Gornstein, R. J.; Shultz, W. M.; and Stair, L. D.: Marine Vehicle Ride Quality. NASA TM X-2620, 1972.
44. Graybiel, A.: Some of the Mechanisms Underlying Motion Sickness. NASA TM X-2620, 1972.
45. Anon.: Military Specification, Airplane Strength and Rigidity; Flutter, Divergence, and Other Aeroelastic Instabilities. MIL-A-008870A (USAF), Mar. 31, 1971.
46. Strahota, R. A.; and Jenny, R. B.: Combat Maneuver Enhancement with CCV. AFFDL Rept. 609348, 1972.
47. Ullman, D.; Rohling, W. J.; Pasley, L. H.; and Wattman, W. J.: Compatibility of Maneuver Load Control and Relaxed Static Stability for B-52E and TFX Model 818. AFFDL-TR-71-183, Jan. 1972.
48. Kujawski, B. T.; Jenkins, J. E.; and Eckholdt, D. C.: Longitudinal Analysis of Two CCV Design Concepts. AIAA Paper No. 71-786, July 1971.
49. Thompson, G. O.; and Arnold, J. I.: B-52 Controls Configured Vehicle System Design. NASA TM X-2620, 1972.

50. Anderson, D. C.; Berger, R. L.; and Hess, J. R.; Jr.: Maneuver Load Control and Relaxed Static Stability Applied to a Contemporary Fighter Aircraft. *J. Aircraft*, vol. 10, no. 2, Feb. 1973, pp. 112-120.
51. Holloway, R. B.; Burris, P. M.; and Johannes, R. P.: Aircraft Performance Benefits from Modern Control Systems Technology. *J. Aircraft*, vol. 7, no. 6, Nov.-Dec. 1970, pp. 550-553.
52. Rohling, W. J.; Pasley, L. H.; and Wattman, W. J.: Compatibility of Maneuver Load Control and Relaxed Static Stability. AFFDL-TR-71-183, Jan. 1972.
53. Rynaski, E. G.; and Weingarten, N. C.: Flight Control Principles for Control Configured Vehicles. AFFDL-TR-71-154, Jan. 1972. pp. 44-46.
54. Watson, J. H.: Control Requirements for Control Configured Vehicles. Paper presented at AIAA 2nd Atmos. Flight Mech. Conf., Palo Alto, Calif., September 1972.
55. Perkins, C. D.; and Hage, R. E.: *Airplane Performance, Stability and Control*, John Wiley and Sons, 1949.
56. McRuer, D.; Ashkenas, I.; and Graham, D.: *Aircraft Dynamics and Automatic Control*, Princeton Univ. Press (Princeton, N.J.), 1973
57. Hofmann, L. G., et al: Analysis of Limited Authority Manual Control Systems, AFFDL-TR-71-6, July 1971.
58. Davis, H. M.; and Swaim, R. L.: Controlling Dynamic Response in Rough Air. AIAA Paper No. 66-997, Dec. 1966.
59. Holloway, R. B.; Thompson, G. O., and Rohling, W. J.: Prospects for Low Wing-Loading STOL Transports with Ride Smoothing. *J. Aircraft*, vol. 9, no. 8, Aug. 1972, pp. 525-530.
60. Edinger, L. D.: Design of Elastic Mode Suppression Systems for Ride Quality Improvement and Application to an SST. AIAA Paper No. 67-571, Aug. 1967.
61. Smith, R. E.; Lum, E. L.; and Yamamoto, T. G.: Application of Linear Optimal Theory to Control of Flexible Aircraft Ride Qualities. AFFDL-TR-67-136, Jan. 1968.
62. O'Massey, R. C.; Leve, H.; and Gaume, J. G.: An Aircraft Manufacturer's Approach to Rideability Criteria, NASA TM X-2620, 1972.
63. Bisplinghoff, R. L.; Ashley, H.; and Halfman, R. L.: *Aeroelasticity*. Addison-Wesley (Cambridge, Mass.), 1955, pp. 673-685.
64. Press, H.; Houbolt, J. C.; and Diederich, F. W.: Some Applications of Generalized Harmonic Analysis to Problems in Airplane Dynamics. Vol. I, Aircraft Structures and Materials, NACA-University Conference on Aerodynamics, Construction and Propulsion, 20-22 Oct. 1954, pp. 1-1 to 1-13.
65. Press, H.; and Houbolt, J. C.: Some Applications of Generalized Harmonic Analysis to Gust Loads on Airplanes. *J. Aero. Sci.*, vol. 22, no. 1, Jan. 1955, pp. 17-26.

66. Bisplinghoff, R. L.; Ashley, H.; and Halfman, R. L.: Aeroelasticity. Addison, Wesley (Cambridge, Mass.), 1955, pp. 685-694.
67. Rea, J. B.: Dynamic Analysis of Aeroelastic Aircraft by the Transfer Function-Fourier Method. J. Aero. Sci., vol. 18, no. 6, June 1951, pp. 375-397.
68. Fung, Y. C.: Statistical Aspects of Dynamic Loads. J. Aero. Sci., vol. 20, no. 5, May 1953, pp. 317-330.
69. Press, H.; and Mazelsky, B.: A Study of the Application of Power Spectral Methods of Generalized Harmonic Analysis to Gust Loads on Airplanes. NACA Rep. 1172, 1954.
70. Houbolt, J. C.; and Kordes, E. E.: Structural Response to Discrete and Continuous Gusts of an Airplane Having Wing-Bending Flexibility and a Correlation of Calculated and Flight Results. NACA Rep. 1181, 1954.
71. Press, H.; Meadows, M. T.; and Hadlock, I.: A Re-evaluation of Data on Atmospheric Turbulence and Airplane Gust Loads for Application in Spectral Calculations. NACA Rep. 1272. 1954.
72. Diederich, F. W.: The Response of an Airplane to Random Atmospheric Disturbances. NACA TN 3910, 1957.
73. Eggleston, J. M.: A Theory for the Lateral Response of Airplanes to Random Atmospheric Turbulence. NACA TN 3954, 1957.
74. Press, H.; and Steiner, R.; An Approach to the Problem of Estimating Severe and Repeated Gust Loads for Missile Operations. NACA TN 4332, 1958.
75. Funk, J.; and Cooney, T. V.: Some Effects of Yaw Damping on Airplane Motions and Vertical Tail Loads in Turbulent Air. NASA Memo 2-17-59L, 1959.
76. Therson, K. R.; and Bohne, Q. R.: Application of Power Spectral Methods in Airplane and Missile Design. J. Aero. Sci., vol. 27, no. 2, Feb. 1960, pp. 107-116.
77. Houbolt, J. C.; Steiner, R.; and Pratt, K. G.: Dynamic Response of Airplanes to Atmospheric Turbulence Including Flight Data on Input and Response. NASA TR R-199, 1964.
78. Jackson, C. E., et al: The Influence of Dynamic Loads on Aircraft Fatigue. Proceedings of the Symposium on Fatigue of Aircraft Structures, WADC Tech. Rept. No. 59-207, pp. 449-478, Aug. 1959.
79. Hoblit, F. M., et al: Development of a Power-Spectral Gust Design Procedure for Civil Aircraft. FAA Tech. Rept. ADS-53, Jan. 1966.
80. Austin, W. H., Jr.: Application of a Rational-Probability Analysis for Determination of Ultimate Design Loads on Large, Flexible, Military Aircraft. SEG-TDR-64-24, May 1964.
81. Austin, W. H., Jr.: Environmental Conditions to be Considered in the Structural Design of Aircraft Required to Operate at Low Levels. SEG TDR-65-4, Jan. 1965.

82. Austin, W.H., Jr.: Development of Improved Gust Load Criteria for United States Air Force Aircraft. SEG-TR-67-28, Sept. 1967.
83. Bouton, I., et al: Quantitative Structural Design Criteria by Statistical Methods, Vol. I: A Critique of Present and Proposed Approaches to Structural Design Criteria; Vol. II: The Philosophy and Implementation of the New Procedure; Vol. III: Computer Programs and User's Guide. AFFDL-TR-67-107 (3 Vols.), June 1968.
84. Fuller, J.R., et al: Contributions to the Development of a Power-Spectral Gust Design Procedure for Civil Aircraft. FAA Tech. Rept. ADS-54, 1966.
85. Pearce, B.F.; Johnson, W.A.; and Siskind, R.K.: Analytical Study of Approximate Longitudinal Transfer Functions for a Flexible Airframe. ASD TR-62-279, Apr. 1962.
86. Pearce, B.F.: Topics on Flexible Airplane Dynamics, Part I: Residual Stiffness Effects in Truncated Modal Analysis. ASD TR-63-334, Part I, July 1963.
87. Hinds, W.E.: Theoretical Studies and Computations on the Influence of Servomechanisms on the Flutter of Servo-controlled Aircraft. WADC-TR-56-432, Nov. 1958.
88. Anon.: The Hydraulic System. Bureau of Aeronautics, Navy Dept., Rep. AE-61-4-IV, Mar. 1953.
89. Swaim, R.I.: Aircraft Elastic Mode Control. J. Aircraft, vol. 8, no. 2, Feb. 1973, pp. 65-71.
90. Edinger, L.D.; Schenk, F.L.; and Curtis, A.R.: Study of Load Alleviation and Mode Suppression (LAMS) on the YF-12A Airplane. NASA CR-2158, Dec. 1972.
91. Johannes, R.P., et al: LAMS, A Technology to Control Aircraft Structural Modes. Presented at 1970 Case Studies in System Control; sponsored by the IEEE Professional Group on Automatic Control, Georgia Inst. of Tech., June 23, 1970.
92. Johannes, R.P.; and Burris, P.M.: Flight Controls Damp Big Aircraft Bending — Smoother Rides Result. Control Eng., vol. 14, no. 9, Sept. 1967, pp. 81-85.
93. Burris, P.M.; Dempster, J.B.; and Johannes, R.P.: Flight Testing Structural Performance of the LAMS Flight Control System. AIAA Paper No. 68-244, Mar. 1968.
94. Smith, R.E.; and Lum, E.L.S.: Linear Optimal Theory Applied to Active Structural Bending Control. AIAA Paper No. 66-970, Dec. 1966.
95. Arnold, J.I.: Automatic Control for Damping Large Aircraft Elastic Vibrations. NAECON, (Dayton, Ohio) May 6-8, 1968, pp. 49-55.
96. Andrew, G.M.; and Johnson, J.M., Jr.: Automatic Control of Aeroelastic Modes. IAS Paper No. 62-86, June 1962.
97. Burris, P.M.; and Bender, M.A.: Aircraft Load Alleviation and Mode Stabilization (LAMS). AFFDL-TR-68-158, Apr. 1969.

98. Wykes, J.H.; and Knight, R.J.: Progress Report on a Gust Alleviation and Structural Dynamic Stability Augmentation System (GASDSAS) Design Study. AIAA Paper No. 66-999, Dec. 1966.
99. Wykes, J.H.; and Mori, A.S.: An Analysis of Flexible Aircraft Structural Mode Control. (Part 1, Unclassified Data), AFFDL-TR-65-190, June 1966.
100. Smith, R.E.; and Lum, E.L.S.: Linear Optimal Control Theory and Angular Acceleration Sensing Applied to Active Structural Bending Control on the XB-70. AFFDL-TR-66-88, May 1967.
101. Done, G.T.S.: The Effect of Linear Damping on Flutter Speed. R. & M. No. 3396, British A.R.C., 1965.
102. Nissim, E.: Effect of Linear Damping on Flutter Speed, Part I: Binary Systems. Aeron. Quart., vol. XVI, pt. 2, May 1965, pp. 159-178.
103. Moon, F.C.; and Dowell, E.H.: The Control of Flutter Instability in a Continuous Elastic System Using Feedback. AIAA/ASME 11th Structures, Structural Dynamics, and Materials Conference, Denver, Colo., Apr. 1970, pp. 48-65.
104. Theisen, J.G.; and Robinette, W.C.: Servo Control of Flutter. AIAA Structural Dynamics and Aeroelastic Specialist Conf. Proc., New Orleans, Apr. 16-17, 1969 pp. 228-239.
105. Thompson, G.O.: Active Flutter Suppression — An Emerging Technology. JAAC Paper No. 7-B2, pp. 608-615.
106. Anon: The Artificial Feel System. Bur. of Aeron., Navy Dept., Rep. AE-6-4-V, (prepared by Northrup Aircraft, Inc.) May 1953.
107. Ashkenas, I.L.; and McRuer, D.T.: Approximated Airframe Transfer Functions and Application to Single Sensor Control Systems. WADC TR 58-82, June 1958, p. 72.
108. Abramowitz, M.M.; and Stegun, I., eds.: Handbook of Mathematical Functions. NBS, Applied Math. Series 55, U.S. Government Printing Office (Washington, D.C.), 1964.
109. James, H.M.; Nichols, N.B.; and Phillips, R.S.: Theory of Servomechanisms. McGraw-Hill Book Co., 1947, pp. 369-370.
110. Booton, R.C., Jr.; et al: Nonlinear Servomechanisms with Random Inputs, Rept. 70, Dynamic Analysis and Control Lab., MIT (Cambridge, Mass.) Aug. 20, 1953, pp. 38-42.
111. Newton, G.C., Jr.; Gould, L.A.; and Kaiser, J.F.: Analytical Design of Linear Feedback Controls, John Wiley and Sons, 1957, pp. 366-381.
112. Rice, S.O.: Mathematical Analysis of Random Noise. in N. Wax, ed., Selected Papers on Noise and Stochastic Processes, Dover (New York), 1954, pp. 133-294.
113. Pass, H.R.; Pearce, B.F.; and Wolkovitch, J.: Topics on Flexible Airplane Dynamics, Part III: Coupling of the Rigid and Elastic Degrees of Freedom of an Airframe. ASD IR-63-334, Part III, July 1963.